JIMMA UNIVERSITY

SCHOOL OF GRADUATE STUDIES

JIMMA INSTITUTE OF TECHNOLOGY

FACULTY OF MECHANICAL ENGINEERING

POST GRADUATE PROGRAM

(MSc IN MANUFACTURING SYSTEM ENGINEERING)

THESIS TITLE: NUMERICAL MODELING OF SAND-CASTING PROCESS PARAMETERS THAT MINIMIZE SHRINKAGE DEFECT IN CASE FOR ALUMINUM ALLOY (AL-242 GRADE)

BY: YONAS OFKELA SASSIGA

DECEMBER 2019

JIMMA, ETHIOPIA

JIMMA UNIVERSITY

SCHOOL OF GRADUATE STUDIES

JIMMA INSTITUTE OF TECHNOLOGY

FACULTY OF MECHANICAL ENGINEERING

POST GRADUATE PROGRAM

(MSc IN MANUFACTURING SYSTEM ENGINEERING)

THESIS TITLE: NUMERICAL MODELING OF SAND-CASTING PROCESS PARAMETERS THAT MINIMIZE SHRINKAGE DEFECT IN CASE FOR ALUMINUM ALLOY (AL-242 GRADE)

By: Yonas Ofkela Sassiga

Main Advisor: Dr. Mesay Alemu (Asst. Prof)

DECEMBER 2019

JIMMA, ETHIOPIA

DECLARATION

I hereby declare that the work, which is being presented in this thesis, entitled "**numerical modeling of sand-casting process parameters that minimize shrinkage defect in case for aluminum alloy (al-242 grade)"** my original work, carried out under the supervisions of **Dr. Mesay Alemu.** It has not been presented for a degree of any other university and all source of materials used for this thesis are duly acknowledged.

Yonas Ofkela	_____	_____
Student	Signature	Date

This is to certify that the above declaration made by the candidate is correct to the best of my knowledge.

Dr. Mesay Alemu	_____	_____
Advisor	Signature	Date

JIMMA UNIVERSITY

SCHOOL OF GRADUATE STUDIES

JIMMA INSTITUTE OF TECHNOLOGY

FACULTY OF MECHANICAL ENGINEERING

NUMERICAL MODELING OF SAND-CASTING PROCESS PARAMETERS THAT MINIMIZE SHRINKAGE DEFECT IN CASE FOR ALUMINUM ALLOY (AL-242 GRADE)

By**:** Yonas Ofkela Sassiga

Approved by board of Examiners

	Signature	Date
.....	_____	_____
Stream of Chair		
Dr. Mesay Alemu (Assistance Professor.)	_____	_____
Advisor		
----------	_____	_____
Internal examiner		
----------	_____	_____
External examiner		

DECEMBER 2019

JIMMA ETHIOPIA

ACKNOWLEDGEMENT

First, I would like to express my heartfelt gratitude to my advisor **Dr. Mesay Alemu** for his guidance, supervision and willingness despite his very busy schedule; without which this study would not come to this phase. I gratefully acknowledge **Mr. Faid Shirab** for his contribution throughout the duration, which has a vital role for the achievement of this study. I also would like to thank Mr. Mitiku soboka for his assistance during the Laboratory experiment. His guidance and motivation help me to perform the experiments in good manner. Last but not least, I would like to thank others whose name are not mentioned here, but contributed for the completion of this thesis. Finally, I wish to express my heartfelt regards to my family for their patience and endless support during of this thesis.

.

ABSTRACT

In today's world a casting production without any defect is almost impossible as well as the foundry manufacturing in developing countries have a major problem of quality and productivity because of involvement of the number of process parameters in casting process which are difficult to control. In this study, the casting product is faced shrinkage defects which is causing one of chronic problems. Though the process is completely uncontrolled, defects in casting are observed and hence casting process is identified as process of uncertainty which challenges explanation about the cause of casting defects. The main objective of this study is to analyze the effects of casting process parameters and reduce the shrinkage defect in Aluminium alloy product. To overcome the process of analysis 3-D model is done by Solid work, by ProCAST the temperature distribution and shrinkage porosity defect indication are performed, ANSYS for casting simulation is helpful to visualize solidification, cooling and to predict the location of external defects on product such as shrinkage porosity defect and hot spot, by Taguchi method the three important input parameters such as pouring temperature, pouring riser size and pouring time are selected and compared which causes shrinkage defect on cast product separated. The real-time application of the study reflects from the fact that experimentation is performed on nine different casting practical data obtained from experimentation is used for simulation. Shrinkage defects has also been quantified through experimental validation studies and compared well with casting process simulation. The simulation of ANSYS result is validated with experimental result. The results indicate that the selected process parameters significantly cause shrinkage defects in the workshop. It is observed from experimental trials in a workshop that the average value of minimum casting defect is 3.01% for aluminium production. Improvement excreted new gating and feeding system design to reducing shrinkage defect to improve in casting yield 88.9% observed.

KEYWARDS*: Casting, porosity, pouring temperature, shrinkage defect*

TABLE OF CONTENT **page**

LIST OF FIGURES

LIST OF TABLE

NOMENCLATURE

AC surface area of casting

ANOVA Analysis of Variance

OA Orthogonal array

V/A Casting modulus

Ar Surface area of riser

AL Lateral area of riser,

A Total surface area of riser,

At Top cross-sectional area of riser

Ae Exit area of riser

AX Mold face areas in the x- direction

Ay Mold face areas in the y - direction

AZ Mold face areas in the z- direction

b Contraction ratio from liquid to solid

C Constant of material properties

Cmm Specific heat of the mould material

Cm Specific heat capacity metal

Cs Specific heat for the solid

Cl Specific heat of the liquid metal

Qx Heat flow rate in x- direction of mold

Qy Heat flow rate in y - direction of mold

IHTC interfacial heat transfer confident

Qz Heat flow rate in z -direction of mold

R cooling rate (°C/s)

F_S Solid fraction

H Heat transfer coefficient at mold-metal

S fluidity factor

T_n the sand mold temperature

Ta the metal temperature

T wall thickness of the casting

T_{mi} initial temperature of the mould

To initial temperature of mould

Tm metal melting temperature

T_{st} starting metal temperature

Tp Pouring liquid temperature

Ts Surface temperature

T∞ Free stream fluid temperature

W_{sb} weight of sand before washing

W_{sa} weight of sand after washing

Wg gross weight of castings

Wi Mass of the metal in the ingate area

Tc solidification time of casting

Δt solidification time or time step size

Hc Convection heat transfer coefficient

μ dynamic viscosity, kg/m/s

F_L liquid fractions

H_f heat of fusion of metal

V linear velocity of metal flow

Xi individual trials of each experiment

1 CHAPTER

1. INTRODUCTION

The metals casting process is one of the oldest manufacturing methods which started in Mesopotamia around 3600BC. Bronze age, which is estimated at 2000 BC brought more refinement into the casting process. Moulds which were made of baked clay and the cire Perdue or lost wax process, was used for making ornaments etc. The technology was greatly improved by the Chinese around 1500 BC. The Indus valley civilization has the evidence of cast product too. It is the conventional process from several centuries and even today in the 21st century. Its applications include automotive parts, spacecraft components and many of the industrial and domestic parts. The principle of casting process involves creating a hollow shape of the metallic component to be made in which liquefied metal is poured into the previously prepared mould cavity and allowed to solidify (A. Reis, Z et al, 2012, Gajbhiye et al., 2014; Vanara and Shalediya, 2018). Start anew paragraph the mould is usually made of sand, an object similar in shape and size to the casting required, which is a pattern is embedded in the sand (Jain, 2003). Casting product can have defects as a result of shrinkage and gas evolution. The major fundamental effects which contribute to the formation of shrinkage defects in solidifying metal are: (i) shrinkage defect resulting from the volume reducing, control parameter and thermal problem, and (ii) gas evolution resulting from the reduced insolubility in solid metal compared to the liquid (Katz, 2012; Prajapati and Sutaria, 2013).

Casting defects are the result of improper pattern and gating system and riser design, improper mould and core construction, improper melting and pouring practices, because of moulding and core making materials, improper metal composition and inadequate melting temperature, rate of pouring and improper care of the cooling system (Choudhari et al., 2014a; Gajbhiye et al., 2014; Prajapati and Sutaria, 2013).

Shrinkage is a phenomenon concerning the reduction in the size of a casting product during its transition from a liquid to a solid state. The volume in both the liquid and solid phases changes under the influence of temperature. The phenomenon of metal shrinkage has a substantial impact on the quality of castings (Kadhim, 2010 and Ingle and Sorte, 2017; Jabur).

The process of casting solidification is uncontrollable and complex; hence simulation of such a process is needed in industries. The commonly observed defects like shrinkage cavity, porosity, shrinkage defect and sink can be reduced by designing an appropriate feeding and gating system to obtain directional solidification in the casting which leading to feeders. Major parameters of a feeding system include the location of feeder, shape of feeder, size and feed aids of feeder (Ahmad, 2015; Vasava and Joshi, 2013). The phenomenon of casting shrinkage cannot be avoided. However, it is possible to minimize the occurrence of its negative effects on the casting. To achieve this, computer simulation is inevitably necessary. Various simulation software such as finite element method (FEM), ProCAST (Quick cast) etc. are available to find these defects and minimize them (Heine et al., 1976; John et al., 2013). The aim of this thesis focused to analysis the effect of casting process parameters and reducing the effect of shrinkage defect in case of aluminum alloy (Al-242).

1.1 Motivation

Manufacturing of defect-free components at low cost and high productivity is important for the casting industry today. The major challenges that the industry faces are large number of shop floor trials, high rate of rejection and low casting yield. Figure 1.1 shows that among the foundry casting defects, the many related sand casting process shrinkage defect hold a majority.

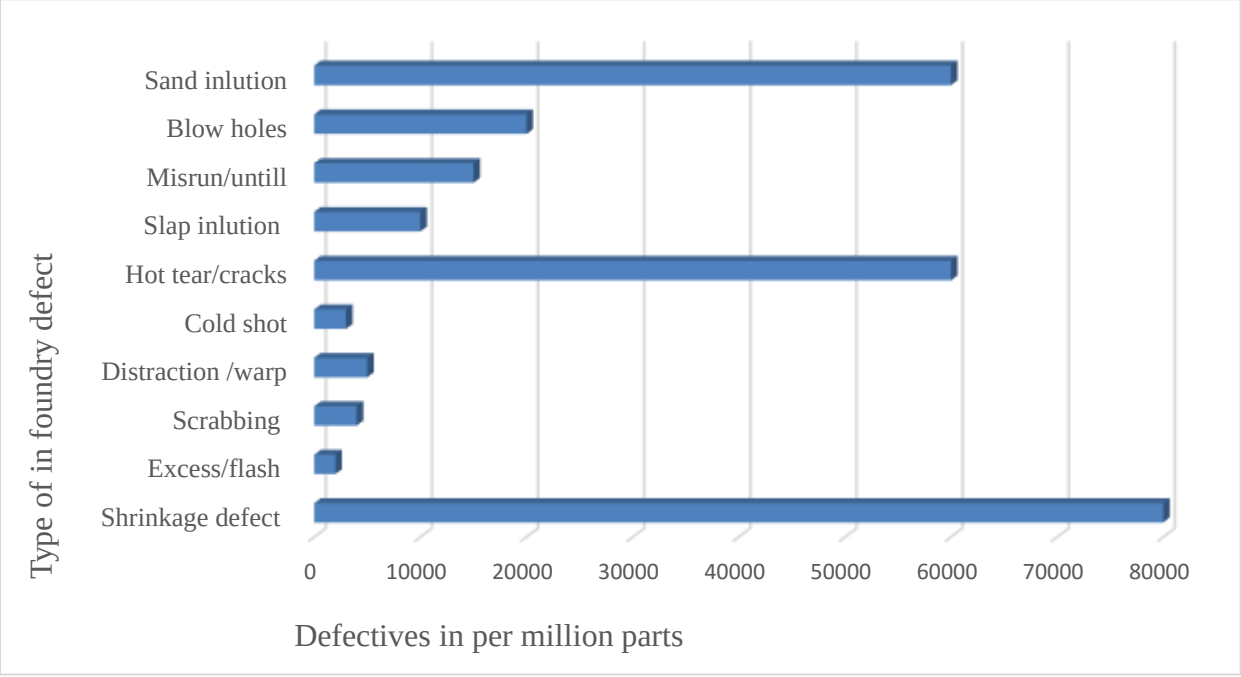

Figure 1.1 Defectives millions parts affect in foundry casting (Behera et al., 2010)

Solidification of the molten metal after being poured is an important phase in the casting process, which greatly affects the casting quality and its yield. The last freezing regions are the most probable locations of shrinkage defect, which need feeders appended at suitable location on the casting. Optimizing the casting parameters, which cause shrinkage defect, can improve casting yield and productivity. Therefore, it is important to study and optimizing the effect of shrinkage defect on casting product. The simulation software such as sold work, ANSYS, and ProCAST are used to predict the location of the defect, and as well as Tanguchi method.

1.2 Statement of the Problem

Nowadays, a lot of casting defects like shrinkage defects, sand inclusions, poor surface finish, porosity, flash and cold shut are facing the casting industries as a serious problem. The foundries are suffering from poor quality and productivities. Among these defects, shrinkage defect is one which can be counted as the most challenging problems in castings and needs a great consideration. Due to this defect, a lot of casting products are being rejected and the casting industries are losing a huge amount of resources spent starting from the product and casting design up to the final production.

The control of the sand-casting process parameters like pouring rate, pouring temperature, gating system (feeder, riser, runner), melting temperature, pouring time and fettling should be improved in order to minimize the casting imperfections. Even though many researchers have investigated the cause and effects of these defects, the problems are still occurring in all foundries. Hence, it is important to conduct a research on casting process parameters of shrinkage defects particularly of Aluminum. In recent years, with advances in computer technology, casting simulation is being increasingly applied to casting manufacturing and the application of this simulation has been most beneficial, for avoiding shrinkage defect, by predict of shrinkage defects without having to discover them in the foundry through the usual trial and error process, which can be very tedious, time consuming, and expensive. In this study, the experimental investigation and numerical simulation will be carried out in order to get more information about the shrinkage defects on Aluminum casting. So, the objective of this study is to minimize the shrinkage defects and improve the quality of the aluminum casting by using Tanguchi method and simulation with its experimental validation.

1.3 Objective of the Research

1.4.1 General Objective

To analysis, the effects of casting process parameters and reduce the effect of shrinkage defect in case of Aluminium alloy on produce part.

1.4.2 Specific Objectives

- To analyze shrinkage defects process parameters;
- To analysis gating system that maximize quality value of flywheel casting product
- To identify parameters that have significant impacts on flywheel casting defects.
- To validate empirical result with and experimental results.

1.4 Significance of the Study

The study is useful write in correct way the casting quality. The effectives of shrinkage parameters cause defect on casting process. The foundry industries will be benefited from the minimization of the casting losses, reduction of risk, enhancement of their productivity. Therefore, it earns industrial profit and economic growth. It gives customers' satisfaction due to the fact that high quality and defects free castings can be produced and hence served to the expected purpose and service life effectively. It is also best input for the factory workers and researchers who are working on the foundry industries.

1.5 Limitations of the study

- Lack of thermo-physical measuring apparatus of the mold channels and an assumption has made for the completion of the study
- Limitation number of software unlicensed (AutoCAST, Megma cast and click2 CAST).
- Macro shrinkage is a concentrated zone of shrinkage holes or single shrinkage porosity defect in cast products that can be detected through non-destructive tests such as radiography, ultrasound, and magnetic particle method.

1.6 Structure of the Thesis

After this introduction chapter, the thesis is divided into seven chapters. The contents of each chapter is briefly outlined as follows.

Chapter 2 contains a review of relevant literature on Aluminum alloy sand casting process parameters. This review highlights recent research and discovery on a design; analysis and

simulation of Al alloy sand casting process and provides a theory and approaches of modelling Al-alloy sand casting process.

The materials and methods used in this thesis are presented in Chapter 3, where the approaches and procedures used for this thesis are briefly described.

Chapter 4 provides the general formulation of casting process parameter and mathematical modelling for Al-alloy sand casting process.

Design of the gating system, metal flow conditions, metal melting, pour parameters and solidification conditions, and modes of heat transfer from casting to mold are discussed in Chapter 5. The simulation of the Al-alloy sand casting process is also discussed in this Chapter.

Chapter 6 provides the results and discussion of the thesis. Finally, the conclusion and recommendation are presented in Chapter 7.

2 CHAPTER

2. LITERATURE REVIEW

In this section, the basic concept of sand casting and shrinkage defects with their possible causes and parameters, basics of gating system, metal flow, pour time and thermal history, possible design of experiment and software applications were discussed. Since the main agenda of the research us to find free defects cast product and qualification of the shrinkage defect minimizing, the research and literature work is done to serve that purpose. Previously trial and error method was used to reduce the defects occurred during solidification process. Modern scenario analysis software's are used to predict the defects during solidification process. Shrinkage defect is a common defect which is shown after solidification. In sand casting process many parameters have to be considered to tray reduce shrinkage defect (Jabur and Kadhim, 2010; Katz, 2012).

Around 90 % of all the casting defects are because of improper design of gating, risering and feeding system, the rest is due to production faults and human errors (Rajput, 2008). For simulating such defects the author used FEM and VEM based methods are widely used (Behera et al., 2010) and also the authors used ProCAST to simulated the 3D model of fasting finally, simulation result is validated experimental result. According to this study the yield is improved by 8% and shrinkage defect is reduced by 1%.

(Ravi and Joshi, 2007) used the simulation software for assuming quality and yield optimization without trial and error on shop floor. In their study present, the numerical method was used to determine the modeling process parameters for the sand casting process, which cause shrinkage defect. The authors observed that the process parameters (i.e., green strength, moisture content, pouring temperature, pouring time, gating/riser feeding, mold hardness vertical and mold hardness horizontal) significantly affect the casting defects.

In modern manufacturing, it is difficult to produce defect free casting product and also it is great challenge for reducing the percentage of scrap and shrinkage porosity defect. The formation of various casting defects is not only related with sand casting process parameters but also highly related to nature of fluid flow during the mold filling stage and type of solidification. Any improper

designing of gating and feeding system results in mold erosion, hot spot, non-uniform solidification, shrinkage porosities, lower casting yield (%) etc. Therefore, it is significant to take special care in designing gating and feeding system to obtain defect free casting. The main function of gating system is to carry clean molten metal from ladle to the casting cavity ensuring complete filling (Masoumi et al., 2005).

(Tomar and Dwivedi, 2015) presented that casting solidification embodies a huge deal with several profiles like metal flow, temperature gradient and heat transfer. These stages are complex and takes place between the casting and mould. Casting quality is influenced by the thermo physical properties of the molten metal and mould cavity. Heat transfer from metal cast to atmosphere through mould walls play vital role. (Das and Himte, 2013) predicted and analyzed a casting defect using FE approaches. They used ANSYS software to predict temperature and thermal stress distribution, which are the key element of casting, after casting solidification.

One of the critical elements that has to be considered for producing a high-quality sand-casting product is the gating and Risering system design as well pour temperature and pour time of solidification (Masoumi et al., 2005). Improper design of gating and Risering system results in shrinkage defect (cold shut) and shrinkage porosities. These defects negatively affect mechanical properties. Therefore, adequate care is necessary in designing gating and Risering systems for improved yield of defect free castings and the assistant good gating and riser/feeding could reduce the turbulence in the melt flow, air entrapment, sand inclusion, oxide film and dross (Shafiee et al., 2009). Melt flow influences solidification time, which is an important parameter that could alter the microstructure and mechanical properties of the cast part. This parameter is influenced by design and dimension of gating components and also impart on the cooling rate of the casting (Tomar and Dwivedi, 2015). Hot spot from casting can be removed through optimum positioning and designing of riser and author has designed riser with higher value of modulus for increasing the solidification time compared to casting (Ingle and Sorte, 2017). Computer-aided casting design and simulation is a faster tool for optimizing the feeder design of castings (Choudhari et al., 2014b). This problem feeder shift solution, the feeder profits it improvement yield casting and as well as eliminated shrinkage defect problem (Farrokhnejad, 2013).

In 2013, Choudhari and co-workers (Choudhari et al., 2013) studied how to minimize critical defects in casting process considering various parameters. The authors applied the process

parameters optimization for reducing the defects like cold shut, blowhole, run, porosity and sand inclusion. They performed an experimental based on DoE by varying the main three factors which are pouring temperature, handling time and pouring time. The results give the optimum range of temperature which is 1420-1450℃, handling time is 9-11 second and pouring time is 4-5 seconds.

Again in 2014, Choudhari and co-workers (Choudhari et al., 2014b) investigated casting defect reduction process and the way to improve casting productivity in automotive component. The author used the design of experiments technique to analyze the sand related defects in shell mould casting. The most influencing parameters were selected for the experimental purpose. The experiments were conducted and the responses were measured. ANOVA analysis was done which defined that which casting process parameters significantly affect the percentage of rejection in casting. The defect was reduced from 2.3 % to a maximum up to 2.8%.

("Rajesh Rajkolhe, J. G. Khan, 2014.) conclude that various defect is generated in casting process while manufacturing, defects may like as shape related, filling related, thermal related and other defects by appearance. While performing various number of process parameters as trial and error basis they find out various challenges and uncertainty in casting process. Such types of defects are developed poor quality and productivity. To obtain high quality they were found their remedies to minimize those challenges and uncertainty also rejections. This action may help to improve quality as well as productivity in manufacturing industry.

Most models for predicting and minimized shrinkage porosity defect formation originate from the one-dimensional (1D) model of (K. Kubo and R.D. Pehlke:, 1966) and the two-dimensional (2D) model of (K. Kubo and R.D. Pehlke:, 1985). Over the past two decades, several advances in the development of porosity models for castings have been made (C. Pequet, et al 2016), developed a three-dimensional (3D) model that applies a dynamic mesh refinement algorithm for the semi-solid mushy zone. The 3D multi-phase model developed by predicts the feeding velocity, liquid pressure, and porosity distributions during alloy solidification (A. Reis, Z et al,2012,and A. Reis, Y et al, 2002). However, it does not consider the formation of surface sinks. The model by predicts the formation of surface sinks and internal porosity (A. Reis, Z et al,2012). In this model, a volume-of-fluid (VOF) approach is used to track the liquid surface movement during solidification. Their results showed that in alloys with a long freezing range, shrinkage defects tend to form on the

exterior surface of a casting, while in the short freezing range alloys, such defects tend to appear in the form of internal porosities.

Despite some success of modeling to predict shrinkage porosity in castings, a comprehensive model that predicts surface sinks, internal porosity, mass feeding and centerline shrinkage porosity in castings is lacking.

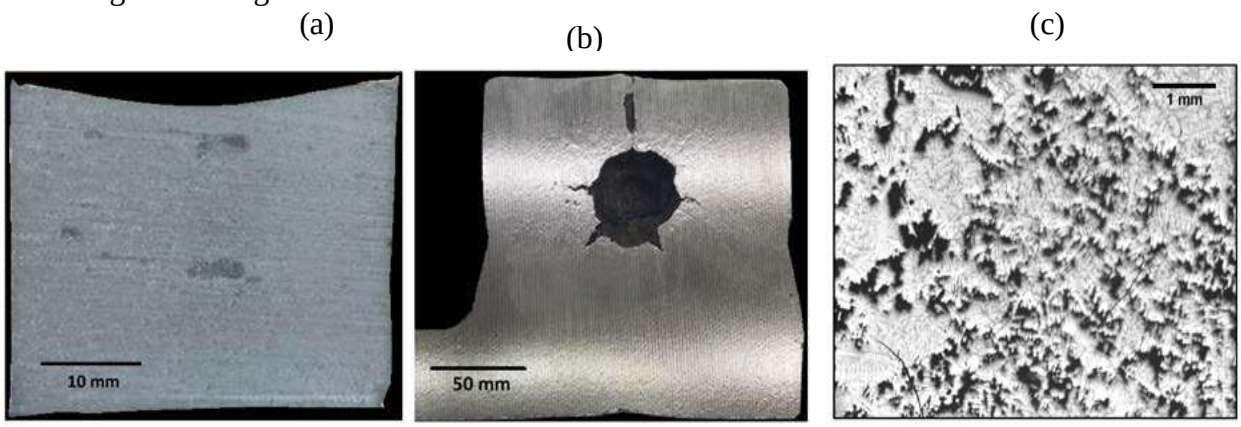

Figure 2.1 Surface sink and porosity defects caused by shrinkage:(A. Reis, Z et al,2012): (a) surface depression or surface sink, (b) external shrinkage porosity defect, (c) internal shrinkage porosity.

Here a computational model for the prediction of surface sinks and external shrinkage defects in castings is presented. Transient temperature, solidification temperature and fractional solidification are obtained from casting is process parameter optimization that consists of following stages: Analysis an orthogonal array using selected process parameters, performing experimental trials according to this array, finding out the influential factors using mean effect, S/N ratio plot and ANOVA analysis, forming regression equation and finally confirmation test in the selected level through castings product in workshop. Lastly simulation technique consists of following stages, analyzing the various design of multi-cavity mold with feeder, gating system and predict defect location, based on simulation results using ProCAST and ANSYS simulation software, finding out the optimum gating and feeding system from simulation results, experimental validation with simulation results through work shop trials and as well details study the influence of pouring temperature, pouring gating system element and pouring time causes shrinkage defect of Aluminium alloy using sand casting process.

2.2 Cause and effect diagram helps in following ways

Once a defect has been identified, potential causes of this undesirable effect has to be analyzed. Cause Effect Diagram is a useful tool in finding potential causes. By using this fishbone diagram, all contributing factors of defects and their relationship are displayed in a place. It identifies areas of problem where data can be collected and analyzed. The fish bone diagram for shrinkages is shown in Figure 2.2.

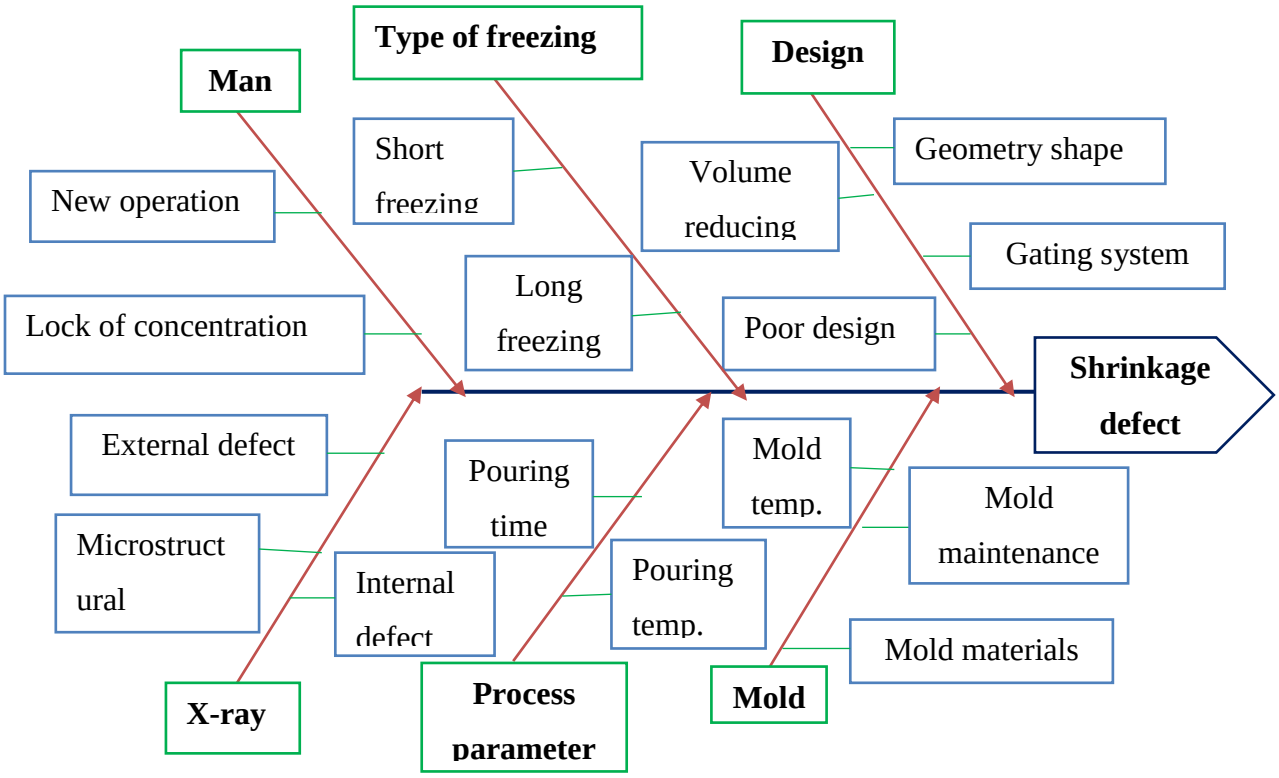

Figure 2.2. Cause and effect diagram for shrinkages (Çetinel, M., 2001)

2.1 Research Gap and Contribution of the Study

A number of researchers studies the caused and the effect of shrinkage defect as well as shrinkage defect reducing trails by using volume casting reducing under solidification state. They identified that the main causes of shrinkage defect are poor gating system, poor pouring system and condition of solidification. In case of Aluminum alloy, these casting process parameters play a huge role for the formation of shrinkage defect. However, the way of reducing the formation of this shrinkage defect and its effect are not properly addressed so far. The shrinkage defect parameters should be optimized, simulated and experimentally validated to get more accurate results. Therefore, in this study the parameters that cause shrinkage defect are optimized by Tanguchi methods, simulated by ProCAST and Experiment are used to validate the results.

3 CHAPTER

3. MATERIAL AND METHODS

In this Chapter, the methods and materials used for the study are briefly described. The equipment used included moulding box, rammer, runner, riser, shovel, furnace, and crucible, draw screw, vent wire, etc. Different methods used were used together data such as books, journal, articles and as well as used computer tool (ANSYS, ProCAST and Minitab).

3.1 Experimental Procedure in Casting

This section explains the casting procedure of making aluminum casting product part (flywheel). Producing process consists of pattern making analysis, mold box preparation, pouring metal, solidification, shake out and cleaning. A mould box of size standard compare was used 250 x 200 x 120. The mould cavity was to be proposed in two parts, cope, the upper part and drag, the lower part. To prevent entrapment of hot gases during pouring, vent holes were made by using a vent wire. Cope and drag were joined and mold box was prepared. Figure 3.4 and figure 3.1 represents the necessary tools for mold making with casting process. Standard procedures and equipment were used to evaluate the pouring temperature, pouring riser size (ingate system) and poring times (solidification times) as well as sand sample. All experimental tests were carried out at Jimma University institute of Technology mechanical engineering foundry shop. Molten aluminum at a temperature of 750^0C from the furnace was poured into the pouring basin of the mold box until the mold was filled completely.

Aluminium was melted input in an electrical furnace. The pouring temperatures of the melting Aluminum alloy castings were measured by a thermocouple /digital furnace. Molten metal was poured and allowed to solidify. In this present experimental casting used pouring temperature between range (630^oc-750^oc). The pouring temperature measured readings obtained from the furnace as shown in Figure. 3.3. After pouring the molten metal into cavity the casting was allowed to solidify for 44 minutes. After solidification, metal component was removed from its mold by shaking using a draw screw. Next cleaning process was performed for the removal of sand, scale and excess metal from the casting. The following is used material experiment procedure and used pattern as shown figure 3.1 to 3.4. The final casting along with the wooden pattern used, are shown in Figure.3.1.

Figure 3-1 wooden pattern and material used for experimental cast

The thermocouples digital furnace final casting obtained complete liquid melting metal is shown Figure. 3.3. It is setup for temperature measurement time to time and by used electrical energy melting metal industry change any shape form of easy.

Figure 3-2 Setup for Temperature Measurement and used melting metal machine

Molten aluminium at a temperature of 750^{o}C from the furnace was poured into the pouring basin of the mould box until the mould was filled. After solidification, a metal component was removed into mould show as figure 3.4.

Figure 3-3 Determination of Pouring Temperatures

The following show that raw material used aluminum alloy melting forusing experimental casting testing.

Figure 3-4 Raw material used produced casting part

3.2 Chemical Composites in Aluminum Alloy

Al-242 is a cast aluminum alloy consisting of element 0.7% silicon, 1% iron, 3.5 to 4.5% copper, 1.7 to 2.3% nickel, 1.2 to 1.8% magnesium, 0.35% zinc, 0.25% titanium, and 0.35% manganese. Aluminum alloy (Al-242) is commonly used to make aluminum parts where higher temperature strength and reduced thermal expansion are required (Katz, S., 2012).

Table 5.1 Aluminum grade (Al-242) composition

Si %	Fe%	Cu%	Mn%	Mg%	Cr%	Zn%	Ni%	Ti%	Pb%	Other%
0.7	1	3.5-4.5	0.35	1.2-1.8	0.25	0.35	1.7-2.3	0.25	0.15	0.15

3.3 Determination of Pouring Temperatures

Pouring temperature is a vital tool in the foundry industry in the manufacture of quality castings. The pouring temperatures of the Aluminum alloy castings were measured by a thermocouple (digital furnace machine). In the pouring ladle, the tip of the instrument was allowed to make contact with the base of the molten metal contained in it. For each casting, two temperature readings were noted and recorded accordingly. The first being the temperature reading at the beginning of pouring of the molten metal into the mould and the second being the temperature reading immediately the mould is filled up. The average of these two temperatures calculated were the temperatures for the particular casting. This method was used done nine (9) castings. The poured molten metal was allowed to solidify and cool, then removed from the sand. The optimum pouring temperature range is 630°c to 750^{o}c. At temperatures higher than this range, the casting results in large crystals, low strength and gases are entrapped in the castings, leading to defects known as shrinkage defect, blowholes etc. Additional pouring temperature or superheat increases the fluidity and considers the allowance for heat losses before they are in their final position in the mould. Increase in pouring temperature results in a lower rate of heat extraction by the mould. Higher pouring temperature leads to decreased shrinkage porosity defect.

3.4 Methods for Minimizing Defects

In this, the proposed method of eliminating rate due to casting defect analysis, the Taguchi method and simulation is used for analysis in sand casting shrinkage defects. Whereas computer tool casting simulation technique is used for, filling and solidification defects such as shrinkage defect and with related. Flow the chart analysis/proposed method of reducing shrinkage defect in sand casting as shown in Figure 3.5.

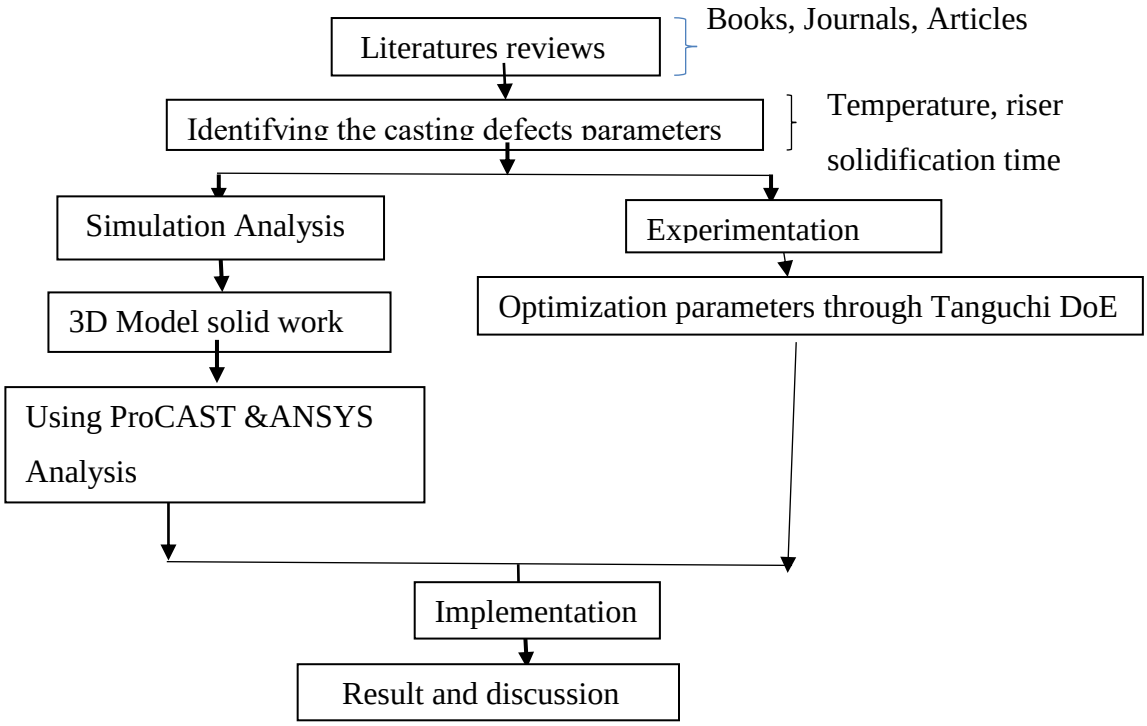

Figure 3-5 Steps involved in the methodology

3.5 Taguchi method

The methodology used to achieve analysis process parameters using Taguchi is as given below:

i) To select the influencing process parameters with their levels and perform the trial casting as per Taguchi method, then observed experimental data. **ii)** To analyze the experimental data using statistical tools. An Analysis of variance (ANOVA) can be obtained to determine the statistical significance of the parameters. Means plots and SN ratio plots can be plotted to determine the preferred levels of parameters considered for experimentation. Regression analysis is performed to determine the relationship between dependent and independent variables. **iii)** Select optimum levels of control parameters, perform confirmation experiments and implement the process.

4 CHAPTER

4. FORMULATION OF CASTING PROCESS PARAMETER

A casting system is good if it satisfies the objective function and free from the pouring related defects like cold shut, misrun, shrinkage porosity defect, higher turbulence, sand inclusion and gaseous entrapments (Heine et al., 1976). These can be achieved, if the following six constraints are satisfied: (1) clay contents, (2) pouring time, (3) mould erosion, (4) gating system with elements (riser size, feeder, runner, sprue, etc.), (5) Reynolds number (6) pouring temperature. These constraints are described in detail in the following sections.

4.1 Clay Contents

Clay in moulding sand can be particles which fill to restore on a provided period when suspended in water. These particles are generally less than 20 microns in diameter. The percentage of clay water content for a weight of using moulding sand can be calculate using the following Equation (Gajbhiye et al., 2014),

$$Clay\ Content(\%) = \frac{Wsb - Wsa}{Wsb} * 100 \qquad (4.1)$$

Where, W_{sa} -Weight of sand after washing, W_{sb} -Weight of sand before washing,

4.2 Pouring Time

Pouring time is the time taken in pouring the molten metal in sprue for casting. Slow pouring of metal leads to freeze fast before filling out the mould and mould result from cold shuts in the castings whereas rapid pouring (filling) of the mould cause problems such as erosion of the mould wall, rough surface and excessive shrinkage defect. In casting methods when metal is forced into a mould under pressure, the optimum pouring time depends on the fluidity of metal, wall thickness, shape and weight of the casting. The pouring time for aluminium castings is estimated using the following empirical formula (Rajput, 2008),

$$t_p = s(\sqrt[3]{T_{Wg}}) \qquad (4.2)$$

Where, $t_{p=}$ pouring time, s- fluidity factor depending on material composition (aluminum alloy) and pouring temperature, T-mean thickness of casting wall and W_g-gross weight of castings (kg).

After calculating the pouring time, it is required to establish the main control area which controls the metal flow into the mould cavity so that the mould is completely filled within the calculated pouring times. This control area is called choke area. The choke area can be calculated using following Bernoulli's equation as (Ravi and Joshi, 2007),

$$A_c = \frac{W}{\mu \rho_m \, t \, \sqrt{2gh}} \tag{4.3}$$

where A_c- choke area, mm^3, W- casting mass, kg; p_t- pouring time , ρ_m- mass density of the molten metal, kg/mm^3 H-effective height of metal head in the cope side**,** μ- efficiency factor, g - acceleration due to gravity.

4.3 Mold Erosion

In this, case of top and parting line gate, the jet of molten metal succeeds maximized in velocity as it leaves the in-gate and strikes the mould-cavity bottom surface. If the velocity of impingement exceeds a critical value, it results in mould erosion. This can be avoided by using bottom gating system, but it increases the filling time for a given casting as compared to top and parting line gating system, if resolve forces excreted by metal this force (tangential and normal) induce the compressive stress in mould material. So we can define the constraint on mould erosion as follows: (***i)*** Shear stress-induced by melt jet should be less than the shear strength of the mould material. (ii) Compressive stress induced by the melt jet should be less than the compressive strength of the mould material (Beeley, 2001),

Force F = rate of change of momentum $= \frac{\text{mass flow rate in kg/sec} * \text{change in velocity}}{\text{time}}$

$$\sigma_Y = \rho_m * V_g * \sqrt{2g(h_t - 0.1)} \; compressive \tag{4.4}$$

To avoid mold erosion, compressive stress ≤ compressive strength of mold ($\sigma_Y \leq S_Y$)

S_Y =mold compressive strength = 117.19 kpa, S_H=mold shear strength = 68.94 kpa

$$V_g \leq 40.59 \frac{m}{sec}$$

Tangential force exerted by the melt –jet

To avoid mold erosion, shear stress ≤ shear strength of mold (Ruddle, 2008),

$$\rho_m V^2{}_g \leq S_H, \quad V_g \leq 5.382 \ m/\sec \tag{4.5}$$

4.4 Gating System Element

The gating system components in sand casting foundries commonly consists of elements such as gating, sprue, runner, sprue base, pouring cup, filter, riser(s) and choke. Among these the three principal elements are sprue, the runner and the in-gates (Ravi and Joshi, 2007),

A) **Types of gating system**

(i) **unpressurized system** has the advantage of reducing metal velocity in the gating system as it approaches and enters the casting which results in laminar flow. (ii) **Pressurized gating systems** have advantage of reduced size and weight for a given casting, thus increasing mold yield (Ravi and Joshi, 2007),

B) **Design of gating system components**

The dimensions of the gating system can be designed using laws of fluid dynamics namely Continuity law and Bernoulli's theorem. The gating system can be designed with the assumption that same quantity of metal is passing per unit time through each of the elements. The volume flow rate of metal is considered uniform throughout a system and determined from the continuity law using the following Equation (Choudhari et al., 2014b; Ravi and Joshi, 2007),

$$Q = \ A_1V_1A_2V_{2=}A_3V_{3=\ A_n}V_n \tag{4.6}$$

Where, Q-volume of metal passing per unit time, A-Cross-sectional area of the passage, and V-linear velocity of flow, and A_n *and* V_n – are area of passage and velocity of flow at n-location of the passages.

C) **Design of ingate areas**

Flow rate of molten metal aluminum alloy which entered to the mold cavity of the parts may be controlled by properly determined the number of in gates and designed their dimensions. Authors discussed that proper designed of these areas controlled the pouring time. The total ingates used in the casting of this parts were calculated from the following formula (Rajput, 2008),

$$\sum A_i = \frac{Wg}{\mu\rho_m t_p\sqrt{2gH}} \ cm^2 \tag{4.7}$$

Where, Ai-total in-gate area, W_g -Gross weight of casting (Kg), ρ_m - density of metal H-effective height of metal head in the cope side, μ- efficiency factor, g - acceleration due to gravity, t_p - pouring time in seconds.

D) Gating system ratios

In gating system, the shape and dimensions of the passages are the most important characteristics, which determine the rate and type of flow and the position at which the metal enters the mould cavity. The dimensional characteristics of any gating system areas are expressed in term of gating ratio by the following relations (Masoumi et al., 2005),

$$\text{Sprue (exit) area: Runner area: total ingate areas} \tag{4.8}$$

E) Design of sprue sectional area

While a casting is made the average flow rate of the casting for individual castings can be determined by dividing the casting weight with the measured filling time and also the mold filling time can be estimated from the ratio of volume of the mold cavity to the average volumetric flow rate using the following formula respectively,

$$Q_{ave} = \frac{W_g}{t_f} \tag{4.9}$$

Where, Q_{ave}– average flow rate of casting, Wg -Gross weight of casting, and t_f- measured pouring time. The sprue entrance and exit areas, the sprue and the pouring cup heights can be also related using the following Equation, (McGuinness and Roberts, 2001),

$$A_{stop} = A_{Sexit}\left(\sqrt{1 + \frac{h_s}{h_p}}\right) \tag{4.10}$$

Where, A_{stop}- sprue entrance area, A_{Sexit} -sprue exit area,h_s - height of sprue and h_p -height of pouring cup.

F) Riser Design

Riser is a supply of molten metal which is used for shrinkage injury especially in metal casting, types, shapes and size, the need and use of chills. Sound casting can be produced without internal shrinkage defect reduce and external shrinkage defects like sink when riser solidify completely only after the casting has solidified (Masoumi et al., 2005; Shafiee et al., 2009).

G) Riser size

For a given size, the riser can be designed with a high volume to surface area ratio. For metal casting aluminum the total freezing (solidification) time for a riser is proportional to square the ratio of Volume to Surface area expressed by Chvorinov's rule and determined using the following Equation (Yu, 2001),

$$\text{Solidification time}, t_s = \boldsymbol{c}[\frac{\text{Volume of riser}}{\text{surfase area of riser}}]^2 \quad (4.11)$$

Where, **C** is a constant that reflects mould material, metal properties like latent heat, and temperature.

I) Riser volume

The total volume of the riser required would depend on, the shrinkage characteristic of the metal, and the shape of the casting. Hence, the solidification shrinkage of metal (aluminum) is quite high. Casting yield is an important quantity while considering riser volume. For low casting yield, the weight of castings produced compared to weight of melted metal can be less, the energy spent in melting is wasted considerably, even though runner and risers are re-melted. Every effort should be made to reduce the riser volume, thereby increasing the yield and saving energy. The total yield of the casting can be calculated using the following Equation (Di Sabatino, 2005; Rajput, 2008),

$$\text{Casting Yield} = \frac{\text{Net weight}}{\text{Gross weight}} = \frac{mass\ of\ casting\ required}{\text{total mass of metal poured}} \quad (4.12)$$

J) **Relative freezing time of riser and casting**

When the casting solidifies infinitely rapidly, the feeder/riser volume should be equal to the solidification shrinkage of the casting, and when the feeder and casting solidify at the same rate, the feeder should be infinitely large which is expressed by Caine's method. Relative freezing time or freezing ratio (R_F), volume ratio (R_v) and freezing volume relations are determined using the following formula respectively (Beeley, 2001),

$$R_F = \frac{(\frac{V}{A})\text{casting}}{(\frac{V}{A})\text{riser}} \quad (4.13)$$

$$R_v = \frac{V_{\text{riser}}}{V_{\text{casting}}} \quad (4.14)$$

$$R_F = \frac{a}{R_v - b} + C \quad (4.15)$$

Where, R_F -Relative freezing time **a**-freezing characteristic constant for the metal, **b** -contraction ratio from liquid to solid and **C**-relative freezing rate of riser and casting.

K) Feeder function

Solidification of the casting occurs by losing heat from the surface and the amount of the heat is given by the volume of the casting. Hence, the cooling characteristics of a casting can be represented by the surface-area-to-volume ratio. Since, the feeder/riser characteristics can also be specified by the ratio of its surface area to volume. *Chvorinov* has shown that the solidification time of a casting is proportional to the square of the volume-to-surface area of the casting. The constant of proportionality called the *Mould Constant* depends on the pouring temperature, casting and the mould thermal characteristics (Choudhari et al., 2014b),

$$t_s = \text{K } (\frac{V}{SA})^2 = KM^2 \tag{4.16}$$

When t_s- solidification time, V- volume of casting; SA-surface area; K-mould constant; M-modulus of casting.

4.4 Reynolds Number /Metal Flow A long Channels

Molten metal flows through the gating system to the mould cavity, due to complexity of mould cavity it is not possible to get laminar flow in the mould cavity. Low Reynolds number reduces the casting yield because it increases the dimensions of sprue, runner and in gates. The properties of liquid metal may change, particularly the viscosity of metal due to drop in temperature during the flow. The viscosity is characterized by Reynold's number, that is, the ratio of two kinds of forces inflow of liquid which are viscous force promoting the laminar flow and inertia forces promoting turbulent flow. The Reynold's number can be calculated using the following formula (Yu, 2001),

$$R_e = \frac{\rho VL}{\mu_m} = \frac{Vd}{\gamma_m} \tag{4.17}$$

Where, Re-Reynold's number, ρ - the fluid density, μ_m- the dynamic viscosity V-velocity of metal flow d-diameter of the channel and υ-kinetic viscosity. According to this method the lower critical velocity for flow in the channel corresponds to Re= 20000 for all fluids and the upper critical velocity generally corresponds to the Re = 30,000-40,000. From this method the critical velocity of liquid metal flow (V) along the channel is determined using the following Equation,

$$V_C = \mu\sqrt{2gH} \quad (4.18)$$

Where, V_c-critical velocity of the fluid flow, H- Metallostatic head, and μ- flow coefficient and g-acceleration due to gravity.

4.6 Effect of Pouring Temperature

The liquid metal is poured in to the mold cavity at a temperature too higher than the freezing temperature, the temperature above which pure metals are completely liquid and below it completely solid also called equilibrium melting temperature, to allows sufficient time for the liquid metal to follow into all corners of the mold cavity before it begins to freeze (the difference between the pouring temperature and freezing temperature is known as super heat). Cooling curves are useful to find out the low pouring temperature, which will cause partially filled cavities (Gajbhiye et al., 2014).

4.6.1 *Temperature loss to the gating system*

To penetration defects happened, metal should be poured at an optimum temperature and pouring rate. However, due to heat losses in the gating system, molten metal does not enter the mould cavity at the pouring temperature. Metal should be poured at an optimum pouring rate and temperature (Di Sabatino, 2005). The temperature loss (in ℃) of liquid metal in the gating system due to the mold surface irregularities can be estimated using the formula below,

$$\Delta T = \frac{Asc(T_p - T_{mi})(\sqrt{t_p})}{W_g ci} \sqrt{K_m \rho_m C_m} \quad (4.19)$$

Where, A_{sc}-Surface area of channel used (cm^2) T_P- pouring temperature (^{0}C),T_{mi} -initial temperature of the mould(^{0}C), t_p-pouring time(in sec),W_g-weight of the casting and the gating system(kg), Ci -specific heat of liquid metal, J/Kg ^{0}C, Km-thermal conductivity of the mould, J/h_r/cm ^{0}C, ρ_{md},-density of the mould, Kg/cm^3, C_m - specific heat of the mould material, J/Kg 0C and e-units conversion factor.

4.6.2 Estimation of metal fluidity

Fluidity of molten metal depends upon its pouring temperature, inoculants, and alloying elements and also on the amount of superheat absorbed within it in order to enable to fill the required mold cavity. By increasing the pouring temperature, the fluidity of the molten metal pool can be

increased. Lack of fluidity of metal flow caused to misruns defects and shrinkage defect occurred in the casting part. The fluidity of an alloy of molten metal that is poured in to channel in a mould with some superheats ΔT and a mould which conducts heat rapidly is estimated using the following formula (Di Sabatino, 2005; Tiryakioglu et al., 1993),

$$L_f = \frac{(Ams * \rho * v)(H_f\, c\Delta T)}{h * (T - T_r)} * 1 + \frac{\frac{h * \sqrt{\alpha m * \Delta y}}{k_m \sqrt{v}}}{2} \qquad (4.20)$$

Where, L_f- final fluidity length, (mm), Ams- mould surface area (mm^2), Δy -Choking range(mm), C- specific heat capacity metal (KJ/kg K), $(T-T_r)$-liquid metal temperature minus room temperature(^{o}c), h- heat transfer coefficient at mold-metal interface(W/m^2K), ΔT-superheat (^{o}c) Km- thermal conductivity of mold material (W/m K), ρ -density of metal, v -velocity of metal flow H_f- heat of fusion of metal(kJ/kg), αm -thermal diffusivity of mould [m^2/s].

4.6.3 Estimation of heat transfer during solidification

Solidification and cooling of castings process depends on heat transfer from the part of metal to the mould. Two possible modes of heat transfer occur during solidification of castings namely, conduction (due to molecular interaction particularly in the cast part i.e., both liquid and solid states and is the primary mode through the mould (i.e., solid state only) and convection (due to movement of liquid metal both during mold filling and after the mold is filled as well as cooling of the mould exterior to the atmosphere) (Beeley, 2001).

The heat transfer rate per unit area (heat flux) by conduction at any distance in the mould is proportional to the temperature gradient and estimated using Fourier's law from the following formula (Rajput, 2008),

$$q_x = -k_m \frac{\partial T}{\partial x'} \qquad q_y = -k_m \frac{\partial T}{\partial y'} \qquad q_z = -k_m \frac{\partial T}{\partial z'} \qquad (4.21)$$

Where, qx, qy, and qz- Heat fluxes in the x, y and z- directions of the mold respectively, Km-thermal conductivity of the mould material and the minus sign (-) indicates that heat is transferred in the decreasing temperature direction(from high to low) and $\frac{\partial T}{\partial x}$, $\frac{\partial T}{\partial Y'}$and $\frac{\partial T}{\partial Z'}$- temperature gradients in the x, y and z- directions of the mold respectively. Similarly, the heat conduction in Cartesian

coordinates including the heat generation term, the density, the specific heat and time taken can be also determined using the following formula (Yu, 2001),

$$Q' = -\rho_{\Delta} H_f \frac{\partial f_s}{\partial t} \quad (4.22)$$

Where,- density, Q- heat generation term, C-the specific heat, t- time, H_f - heat of fusion of metal. The hot liquid metal takes time to lose its heat and solidify. The rate at which it can lose heat is controlled by a number of resistances. The major fundamental resistances to heat flow from the interior of the casting are the solidified metal casting, the mould interface and the mould (Campbell and T.S. Piwonka 1966 et al).

4.6.4 Casting resistance to heat transfer

For the unidirectional flow of heat from a metal poured exactly at its melting point temperature, T_m, against a mould wall initially at a temperature T_o, and time t, the transient heat flow in the casting is estimated using the formula (Campbell, T.S. Piwonka and M.C. Flemings: 1966),

$$\frac{\partial T}{\partial t} \alpha_s \frac{\partial^2 T}{\partial x^2} \quad \text{and } H\alpha_s \left(\frac{\partial s}{\partial t}\right) = k_s \left(\frac{\partial T}{\partial x}\right) \quad (4.23)$$

Where, αs-thermal diffusivity of the solid, Ks -thermal conductivity of the solid, H- latent heat of solidification of the solution. The temperature distribution in the mold during the solidification as a function of time and location can estimated based on Fourier relationship using the following formula,

$$\frac{\partial^2 T}{\partial x^2} = \frac{1}{\alpha_m} * \frac{\partial T}{\partial t} \quad (4.24)$$

Where, α_m= thermal diffusivity of the mould = $\frac{k_m}{C_m \rho_m}$

The temperature at any location within the mold as a function of time following the pouring of the metal can be estimated using the Equation bellow (Beeley, 2001),

$$T(x , t) = Tc + (T_o - Tc)\ \mathrm{erf}\left(\frac{X}{\sqrt{\alpha\ (t)}}\right) \quad (4.25)$$

Where T_O- initial temperature of mould, Tc- metal melting temperature, $\alpha = \frac{k_m}{\rho_m C_m}$ = $4.5 * 10^{-7} m^2/s$- thermal diffusivity of mold material estimated using Appendix.7.6, t- time duration after pouring (solidification time) erf -is the Gaussian error function. From these

parameters temperature gradient in the mould can be also calculated from the following formula (Shafiee et al., 2009),

$$\frac{\partial T}{\partial x} = \frac{T_c - T_0}{\sqrt{\pi\alpha_{th}}t} exp\left(-\frac{x^2}{4\alpha_{ht}t}\right), \frac{\partial T}{\partial Y} = \frac{T_c - T_0}{\sqrt{\pi\alpha_{th}}t} exp\left(-\frac{x^2}{4\pi\alpha_{th}t}\right), \frac{\partial T}{\partial Z} = \frac{T_C - T_O}{\sqrt{\pi\alpha_{th}}t} \exp(-\frac{x^2}{4\pi\alpha_{th}t}) \quad (4.26)$$

The heat flux away from the interface in to the mould is determined using the following eqn.

$$\boldsymbol{q_{t(\,m,x,y,z)}} = \mathrm{Km}\ \frac{dT}{dx}\ \mathrm{x}=0\ +\ \mathrm{Km}\ \frac{dt}{dy}\ y = 0\ +\ \mathrm{Km}\ \frac{dt}{dz}\ z\ =\ 0 \quad (4.27)$$

The heat flux across the mould-metal interface is estimated using the following equation (Beeley, 2001), Where, K_m- thermal conductivity of mold material (green sand) taken from.

$$\mathrm{q}_{,(\mathrm{m,x=0})} = \sqrt{\frac{\mathrm{k_m\rho_m C_m}}{\pi \mathrm{t}}} * (\mathrm{T_m - T_o}) \quad \text{or} \quad q_m(x, y, z = 0) = \sqrt{\frac{C_m\rho_m K_m}{t\pi}} * (T_c - T_0) + \sqrt{\frac{C_m\rho_m K_m}{t\pi}} * (T_c - T_0) + \sqrt{\frac{C_m\rho_m K_m}{t\pi}} * (T_c - T_0) \quad (4.28)$$

Where, ρm and Cm are density and specific heat of the mould material respectively.

When the metal is allowed to cast at the melting temperature, then the heat inlet the mould can only be come from the latent heat of solidification of the metal. The heat transfer coefficient 'h' across the metal/mould interface is simply defined as the rate of transfer of energy. For the unidirectional flow of heat, the rate of heat released during solidification across the mould-metal interface can be determined using the formula(Campbell and T.S. Piwonka2009),

$$q' = \rho_s H_f V_s\, A_{mi} \frac{\partial s}{\partial t} \quad (4.29)$$

Where, q- rate of heat released, ρs - density of a solid and H_f- latent heat of solidification, S-thickness of solidified metal casting, A_{mi}- area of the mould-metal interface, Vs-volume of solidified metal equivalent to area of the mould-metal interface times thickness of solidified metal

The heat released from the interface has to transfer to the mould. For unidirectional conditions and metal poured originally at the temperatureT_o, but whose surface is suddenly heated to melting temperature (T_m) at t=0, the transient of heat flow in the mold is estimated using the formula (Beddoes and Bibby, 1999),

$$\frac{\partial T}{\partial t} = \alpha_m \frac{\partial T^2}{\partial x^2} \tag{4.30}$$

Where, α_m-thermal diffusivity of mold material and $\frac{\partial T}{\partial t}$- transient of heat flow. The solidification time of the casting can be estimated considering the heat flux away from the mould-metal interface must be equal to the heat flux to the mould-metal interface using the following equation (Beeley, 2001),

$$S = \frac{2}{\sqrt{\pi}} * \frac{T_m - T_o}{\alpha_m \Delta H_f} * \sqrt{k_m \rho_m C_m t} \tag{4.31}$$

$$(\frac{V}{A})^2 = \left(\frac{2}{\sqrt{\pi}} \frac{T_m - T_o}{\rho_m \Delta H_f} * \sqrt{k_m \rho_m C_m}\ \right) \tag{4.32}$$

Where, S=V/A, V -volume solidified at time t, and A- the area of the metal/mould interface (i.e., the cooling area of the casting), then when t= t_f(the total freeing time of a casting of Volume). According to this method the solidification time of the casting material can be find out and calculated using the following formula (Beddoes and Bibby, 1999; Beeley, 2001),

$$t_{c=} \quad [\frac{\pi}{4}(\frac{\rho_C \Delta H_f}{T_m - T_o})^2 \left(\frac{1}{k_m \rho_m C_m}\right)](\frac{V}{A})^2 \tag{4.33}$$

Where, t_c-time casting, ρ_m, C_m and K_m-are density material, specific heat and thermal conductivity of the mould material respectively, H_f-latent heat of solidification, ρc-density of casting, V-volume solidified, A- interface area, T_m- melting point temperature and To- initial temperature of mold wall.

The heat flux due to convection at the solid surface can be estimated based on the Newton's law of cooling using the following formula (Yu, 2001),

$$q, = h(T_s - T_\infty) \tag{4.34}$$

Where, q-heat flux normal to the surface h- convection heat transfer coefficient, ($Ts-T\infty$) - difference in surface and free stream fluid temperatures.

4.6.5 Estimation of heating the metal

The total amounts heat energy required to melt the metal to a molten temperature sufficient for casting is the sum of (a) the heat of fusion to convert it from solid to liquid (b) the heat to raise the temperature to the melting point, and (c) the heat to raise the molten metal to the desired temperature for pouring and can be estimated using the following formula (Ruddle, 1956),

$$H_t = \rho_{mt} v_{mt}\{C_s(T_m - T_a) + H_f C_1(T_p - T_M)\} \quad (4.35)$$

Where, H_t- total heat required to increase the temperature of the metal to the pouring temp (J), ρ_{mt}- density ($^{g}/_{cm^3}$), V_{mt}- Volume of metal used for heating (cm^3), Cs- Specific heat for the solid ($J/g℃$), T_m - Melting temperature of the metal (℃), Ta- Ambient temperature (or starting) (℃) , H_f - Heat of fusion (J/g), Cl- specific heat of the liquid metal ($J/g℃$) , T_p- Temperature of the pouring liquid (℃).

5 CHAPTER

5. MATHAMATICAL APPROACH AND ANALYSIS

Design of the gating system, metal flow conditions, metal melting, pour parameters and solidification conditions, and modes of heat transfer from casting to mold are discussed in Chapter 5. Detailed analysis mathematical approaches related to study as well as analyzed the mechanism of reducing defect sand casting process and control parameters influence on aluminum alloy casting product used techniques.

5.1 Design Specification of Model and Pattern Preparation

The design specifications of model in ordered to materials were given as net weight of 0.586kg and final dimensions of 136x115mm corresponding to total dimension, diameter and thickness.

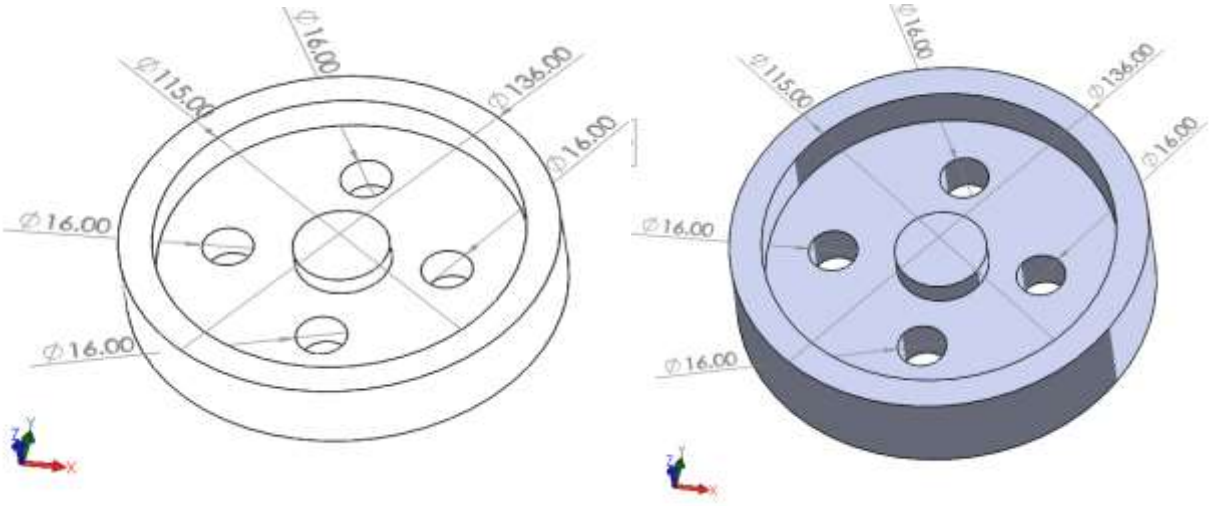

Figure 5.1 Flywheel-view with final dimension

The casting geometry pattern with the given specifications (initial) was built using soldwork software. Hence, its net weight was checked and its density, total volume and total surface area were obtained respectively as 2700kg/ m, 3 4836 $mm^3$and 1452.7mm^2 using material analyzing tool of the solidwork software *(Lee et al., 2001)*.

$$\text{Total vol. pattern} = \left(\frac{\pi}{4}2D * D_i\right) - (2\pi H * hl) - \left(\frac{\pi}{4} * 3D_i\right) + \left(\frac{\pi}{4} * 2h_s H\right) - \left(\frac{\pi}{4}h_s D_i\right) = 34836mm$$

The actual 3D of the geometry flywheel model is shown in Figure 5.1. The net weight, total volume, surface area and density of the pattern used in produce part component casting were also obtained using analyzing tool of solidwork as shown in table 5.1

Table 5.1 Pattern Specification dimensions

Constraints(main)	Weight and Size pattern specifications	Designed pattern specifications
Mass casting required	0.586 kg	2.49kg
Total Mass pour	2.50 kg	2.8kg
Mass pour in mold	1.8 kg	2.3kg
Density	2700 kg/m^3	2700 kg/m^3

The pattern size in Table 5.1 above obtained from the solid work software predicts about the overall size of casting produce part (flywheel) mould cavity pouring by 2.49Kg of molten metal. This is considered as the minimum weight of metal that pouring in the mould cavity.

5.2 Estimation of Casting Gross Weight

The gross weight of casting can be defined as the weight of metal in mold cavity and weight of all gating system elements, i.e., net weight of the geometry part pattern casting plus the yielding material (excess weight of parts removed from casting by machining and grinding). For this work, the casting yield of aluminum material was taken as 40% (Appendix 7.1. So, casting gross weight was determined using Equation (4.12) as following (A. Reis, Z et al,2012, 2017; John et al., 2013),

$$\text{gross weight of casting} = \frac{\text{Net weight of geometry part pattern casting}}{\text{maximum yield of alunimum casting}} = \frac{0.586}{40\%} = 1.5kg$$

This weight was considered as little good to get the desired geometry part pattern weight of 0.586kg and also to fill the gating system cavities which take part in the casting process.

A) **Casting Yield**

The casting yield is the proportion of the actual casting mass to the mass of metal poured into the mold expressed as a percentage.

$$\text{Theoretical casting yield} = \frac{mass\ of\ casting\ required}{\text{mass of metal poured into the mold}} * 100 = \frac{0.586*2}{2.008} * 100 = 58.4\%$$

$$\text{Actual Yield casting from pouring} = \frac{\text{Net } mass\ of\ casting\ required}{\text{total mass of metal poured}} * 100, \frac{0.586*2}{2.150} = 54.5\%$$

It is also clear that actual casting yield is less than that of the theoretical casting yield since the actual amount of metal poured is always more than that of theoretical value due to various factors like mould cavity errors, oxidation loss through the sand mould, volumetric contraction of the molten metal absorption of metal in the sand. Feeding of metal during solidification also accounts to this factor. The following these orders parameters details discuss in chapter four, in this chapter to analysis data result for used. These parameters constraints are described in detail to analysis data results as the following section.

5.3 Analysis of Clay Content in Molding Sand Used

The clay content of the sand which used for mold making in produce casting part process was determined using the Equation (4.1) after washed and before washed measured of weight in content of water. The result of each measured test conducted is given as percentage in Table 5.2.

Table 5.2 Water content test clay.

Trial	Weight before washed(kg)	Weight after washed (kg)	Clay content (%)
1	12	11.1	0.90
2	12	10.47	1.53
3	12	10.98	1.02

Therefore, clay content of the molding sand used in produce part (flywheel) casting was calculated as the average clay content of high water and low water result of the three times taken in table 5.2. This was simply estimated from sum of all the clay content percentages divided by the number of takes and found as 1.15%. This is acceptable sand and its mud effect was small.

5.4 Estimation of Pouring Time

The pouring time of molten metal of aluminum alloy geometry part produce casting (flywheel) poured to filling mold cavities was estimated and compared to the actual mold filling time which was taken during pouring. To estimate this time of filling the fluidity factors of composition and pouring temperature was taken as from Appendix .7.2. Therefore, this time of pouring was calculated using the empirical formula given in Equation (4.2) as,

$$t_p = s\ (\sqrt[3]{TW_g})\ (seconds)\ \ = 9.8sec.$$

This is the minimum time of pouring taken for the metal weight of 0.586 Kg to completely fill the gating system and mold cavities.

After calculating the pouring time, it is required to establish the main control area which metal flow into the mould cavity so that the mould is completely filled within the calculated pouring time is called choke area (Heine et al., 1976; Ruddle, 1956). The choke area can be calculated using following Bernoulli's equation as [4.3],

For Aluminum alloy maximum pouring rate=0.3kg/s, Assume C=0.9*2 because double runner tapered sprue, parting gate is used so effective sprue height =70mm

$$A_c = \frac{W}{\rho_m \, t \, C\sqrt{2gH}} = \frac{0.3}{0.9*0.00000265\sqrt{90*9.81}} = 82.97mm^2.$$

5.5 Mold Erosion

In case of top and parting line gate, the jet of molten metal succeeds maximized in velocity as it leaves the ingate and strikes the mold-cavity bottom surface. If velocity of impingement exceeds a critical value, it results in mold erosion. This can be avoided by using bottom gating system, but it increases the filling time for a given casting as compared to top and parting line gating system, if resolve forces excreted by metal this force (normal and tangential) induce the compressive stress in mold material using equation [4.4] and [4.5] (Ruddle, 1956),

To avoid mold erosion, compressive stress $\leq$ compressive strength of mold($\sigma_Y \leq S_Y$), from aluminum, S_Y =mold compressive strength = 117.198 kpa, S_H=mold shear strength = 68.94 kpa

$2700 * V_g\sqrt{2 * 9.81(0.175 - 0.1)} \leq 117198, \quad v_g \leq 40.59\, {}^{m}/_{sec}$

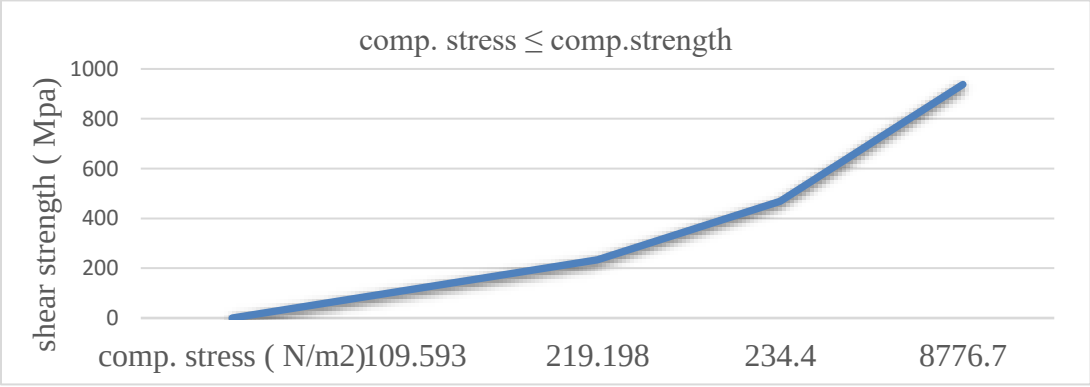

Figure 5.2 Compressive stress melt jet process to avoid mold erosion

This figure indicated at all the point the compressive stress induced by the melt jet should be less

than the compressive strength of the material. At all the point graph where compare the compressive stress less than the compressive strength the mold material. This means the mold erosion completely reduce approach to zero. Tangential force exerted by the melt –jet. To avoid mold erosion, shear stress ≤ shear strength of mold equation. [4.5],

$$\sigma_H \leq S_H,\ \rho_m * V^2{}_g \leq S_H,\ 2700 * V_g^2 \leq 68.94 * 10^3 \quad = \quad V_g \leq 5.382\ m/\sec$$

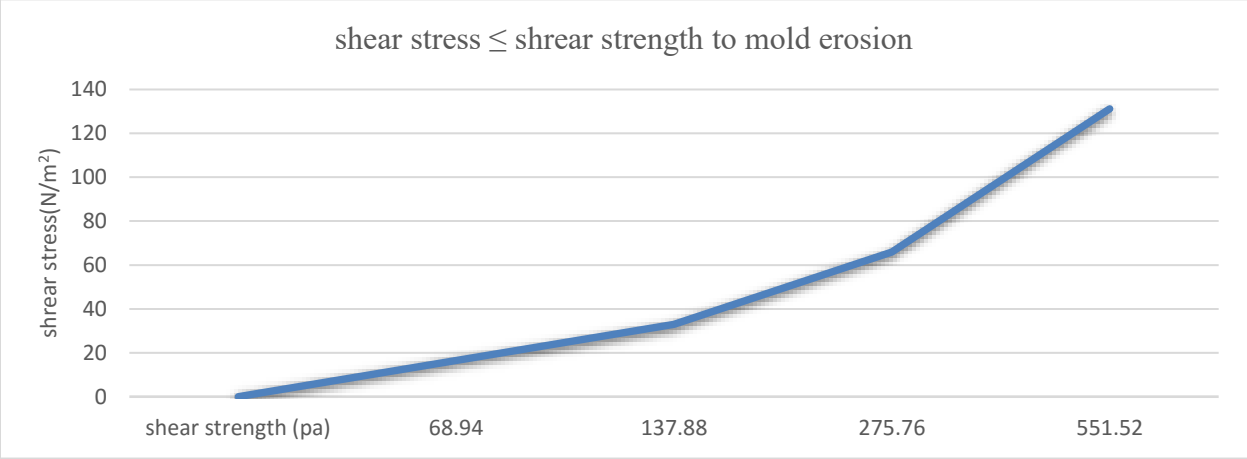

Figure 5.3 Shear stress melt jet process to avoid mold erosion

From the equation of 4.4 and 4.5, it clear that this constraint givens maximum limit of velocity of molten at the ingate. To avoid mold erosion where shear stress less than shear strength of the mold material. Hence the equation 4.5 used the value of shear stress analysis less than the value of shear strength mold material. From this calculation fill the mold erosion completely reduced.

5.6 Basic Gating System Elements

Shrinkage defect is a very normal nature of molten metal during solidification. The function of a gating with element is to feed the casting during solidification so that no shrinkage defect is formed. For that reason, it is also named feeder. In this analysis the optimum gating system (riser size) is determined using Modulus method. Two center risers are used for this casting which provides directional solidification and the gating system modulus are calculated using following formulas.

Modulus of casting, $Mc \quad = \frac{DH}{2(D+2H)} \quad = 3.6,$ Modulus of gating, Mg =6Mc = 22

This necessary of Modulus method two center risers are used for this casting which provides directional solidification to determine.

5.6.1 Design of total in gate areas

Ingate area is the smallest in the feeding channels which controls the flow rate of metal into the mold cavity and in turn controls the pouring time. The total in-gate areas of the system in castings are determined using equation (Ingle and Sorte, 2017; Rajput, 2008),

$$\sum A_i = \frac{W_g}{\mu \rho_m t_p \sqrt{2gh}} = \qquad \Sigma Ai = Ai = 30 cm^2$$

Where, Ai-total in gate areas, W_g -gross weight of casting (Kg), ρ_m- liquids density of metal, take from in table (5.12) , μ- efficiency factor commonly used as 0.2**,** g - acceleration due to gravity**,** t_p - pouring time in seconds. Hence, substituting all the values and was found that

This size ($30cm^2$) is the using area and discuss as sum of all in gates areas constructed to the entrance of the part produce mold cavity. Since one in gate was used for metal entrance to mold cavity, this total area could be taken equal to area of single ingate. From this result, dimensions of ingate were estimated taking in to consideration the geometry that constructed on drag part of mold using the following equation,

$$\text{Ingate area, Ai} = a_i \text{ x hi} \qquad (5.1)$$

Where, a_i-width of ingate and hi –height of ingate

Thus, ingate dimensions were obtained as 10.5cm of width and 5.5cm of height (depth) using the width to depth relation of in gate sizes taken from Appendix.7.3. The actual pattern near to these estimated in gate dimensions were 7cm width, and 4cm thickness was used in construction of the in-gate cavity. Hence, the total volume of metal at ingate section was estimated from the actual dimensions of the pattern used based on the following equation,

$$\text{Volume of metal in the ingate (Vi)} = (A_{ic}) \text{ x(h)} \qquad (5.2)$$

Where, A_{ic}- current in-gate area, t-thickness of the in-gate section and so found as $0.00319 m^3$.

From the volume calculated above, weight of molten of aluminum alloy in the ingate section was estimated taken density of the material (242 Al alloy) as 2700Kg/m^3 using the following formula,

$$\text{Wi} = \text{(volume of ingate) x (density of in} - \text{gate material).} \qquad (5.3)$$
$$= 0.086\text{Kg}$$

This amount of molten metal was accumulated in the ingate portion of the gating system during filling of the produce part cavity and later considered as casting yield.

5.6.2 Runner design

The other areas of gating system elements namely runner and sprue were calculated using gating ratio design rule for aluminum castings using the following ratio formula (Masoumi et al., 2005),

$$\text{Area of ingate: Area of runner: Area of sprue} \quad (5.4)$$

Based on this method area of runner was determined from the gating ratio of ingrate area to runner area using Equation (5.4) as,

Cross-sectional area (or size) of runner (A_{run}) = (ingate areas, Ai) x1.2

= 0.058cm^2 x1.2 = 0.00696cm^2

Hence, dimensions of runner were determined using standard law of proportion taken from Appendix 7.3. for width (∂_r), depth or height (h_{cut}) and length (L_r) using the following formula,

$$\text{Cross} - \text{sectional area of runner} = 0.624m^2 = \partial_r h_{cut} \quad (5.5)$$

∂_r (width)= 12.9cm and h(depth) =4.5cm

Width was estimated using 1.25 times its width and obtained as 16 cm (taken from Appendix.7.3. For this part produce(flywheel) cast, the runner cavity was constructed using pattern sizes of width as 10cm, depth as 4.5cm and length as 14cm geometry of runner used the particular flywheel casting as shown in Figure from appendix.7.10. Based on the selected dimensions the actual size of runner constructed in cope side of mold was calculated using Equation (4.5) and found as following,

$$A_{run} = a_r * h_{cut} = 45\ cm^2$$

Therefore, the actual volume of the molten metal accumulated in the runner was estimated and found as 0.0003132 m^3.Then, the actual weight of metal in the runner was estimated using Equation (5.3) and found as 0.34 Kg.

The above result predicted that weight of the metal feed in to riser base was less as compared to designed runner and this may be produced lack of metal pressure on the in-gate section to entrance

of the cavity. But this weight was considered as small yield in the runner cavity and reduced further works and energy consumption.

5.6.3 Sprue

The passage which connects the pouring basin to the runner or in-gate is called sprue. It is generally designed taper shaped in downward to avoid aspiration of air in sand casting because straight cylindrical shape creates a low-pressure area around the metal of the sprue (Ruddle, 1956). A sprue is molten metal receiver section, after passing over the dam of pouring basin. The exit area of the sprue was determined from the specified rule of the gating area of in-gate to sprue ratio given in Equation (5.4) as following,

$$\text{Sprue area } (AS_{exit}) = \text{(in-gate area) x } 1.6 \qquad = 92.8cm^2$$

From this area the exit diameter of the sprue was determined using the following equation,

$$\text{Ae sp} = \frac{\pi d^2}{4} \tag{5.6}$$

$$= d_{exit} = 9.5cm$$

The entrance diameter of the sprue was determined from 1.15 times the exit diameter (Beddoes and Bibby, 1999), and hence equal to 11.85. Hence, the top cross-sectional area of sprue ($A_{s,top}$) was calculated similarly to Equation (4.6) and found as $10.9cm^2$.

The minimum height of a sprue was considered and taken as equivalent to the height of mold in the cope side, i.e., 280mm. The actual sprue diameters which near to the designed values used were 110mm as top diameter and exit diameter of 80mm with fillet radius 1.5mm. Therefore, the actual entrance and exit areas of sprue were calculated and found as $95cm^2$ and $50cm^2$ respectively. Geometry of sprue used in casting, 3D view of proposed sprue with sprue base well draw show in figure from appendix.7.10.

3D view of proposed sprue with sprue base well, Since the sprue has frustum like shape, the volume of the metal in it was calculated using the frustum formula of the following (Ravi and Joshi, 2007)

$$\text{Volume of sprue, } V_S = \frac{1}{12}\pi h\{d^2top + d^2ext + d_{exit}d_{top}\} \tag{5.7}$$

$$V_s = 0.001107m^3$$

From the total volume found above, weight of molten metal in the sprue was estimated (density of the sprue material taken as 2700Kg/m3) using the formula of Equation (5.7).

Wi = (volume of in-gate) x (density of in-gate material) == .0.4 kg

As per the designed dimensions of sprue pattern amount of metal hold in the sprue cavity could be predicted and believed that higher than the actual metal weight of 2.98kg. This casting weight may be produced less pressure on the sprue base and yield at the sprue cavity was considered less which consumed less both time and energy while fettling.

5.6.4 Sprue base design

Aluminum pattern with 3cm top diameter, 2.5cm end diameter ,2cm height and 15mm thickness was used in construction of sprue base cavity to received molten metal from the sprue exit area and entrance to runner. Geometry of sprue base used in part produce casting (flywheel) show in figure from appendix.7.10. Hence, volume of the sprue base was determined similarly to Equation (5.7) using the following formula;

$$\text{Volume of sprue base} = \frac{1}{12}\,\pi \text{h}\left\{d^2top + d^2exit + d_{top}d_{exit}\right\} \quad = 0.0085m^3$$

This was comparatively good and hence produced pressure to the metal in the runner. This amount of casting yield in the sprue base cavity was acceptable with respect to the given weight of part produce casting.

5.6.5 Pouring cup design

A pouring cup with 2.5cm and 1.5cm entrance and exits diameters and 0.8cm height constructed on a square of 1.4cm was used for entrance molten metal into the cavity. The exit of the basin is larger than the entrance of the sprue to avoid air aspiration at the basin/sprue connecting location. Geometry of pouring Cup used in fly wheel producing casting used see in figure appendix.7.10. Similarly, to discussions of eqn. (5.7), the volume of the metal and its weight in the pouring cup was estimated using the measured values stated above as following,

$$\text{Volume of pouring cup} = \frac{1}{12}\pi h\left\{d^2top + d^2exit + d_{top}d_{exit}\right\} = 0.04cm^3$$

From the total volume above, weight of metal in the pouring cup was estimated and found as 1.08Kg. This was also yield of the casting at the pouring cup of the gating system and it created pressure on the sprue cavity but lead to sand erosion because of its location. As a result, this made narrowed and even closed the sprue exit area and caused to metal solidification in the gating system.

5.6.6 Selection of gate &riser design

Feeder acts as a liquid metal reservoir provides liquid feed metal until the end of the solidification. Riser also serves as a heat reservoir, creating a temperature gradient that induces directional solidification. Two criteria determine whether or not a riser is adequate. Common types of feeders are: top feeder and side feeder. The major considerations in the casting design are the quality of the final product and the yield, which heavily depend upon gating system and feeders.

While designed a riser used in casting produce component, it was considered to be large enough to satisfy requirement so that it solidifies after the casting according to Chvorinov's rule and it must contain a sufficient volume of metal to supply the shrinkage contraction which occurs on cooling from the casting temperature to the completion of solidification. This condition of solidification in produce part by casting process was estimated using the following formula (John et al., 2013),

$$t_s(\text{riser}) > t_s(\text{casting}). \tag{5.8}$$

Where, t_s–solidification time of riser or casting which is related to properties of mold and metal which take part in the process and estimated using the formula of Equation (4.13). Hence substituted the solidification time equation in to Equation (5.8) above, the relation between section modulus of both the riser and produce component by casting was derived and found out using the following formula (Shafiee et al., 2009),

$$C_s(r)\{\frac{V}{A}\}2\text{r} > \text{CS(c)}\{\frac{V}{A}\}\text{c} \tag{5.9}$$

Where, C_s(r) and c_s(c) are the mold constants for the riser and casting respectively, and $(V/A)_r$ and (V/A) c are the volume to area ratios of the riser and casting respectively. In the discussion, constants C_S(r) and cs(c) were considered the same because both the riser and part produce were

molded in to same material, i.e., green sand. From Equation (5.9) the ratio of V/A can be defined as the modulus (M) which used as a critical parameter in riser design of sand-casting process. So that, $(V/A)_r$ is termed as modulus of riser (M_r), and (V/A)c as modulus of casting (M_c). Thus, the riser used in part produce casting process was successfully designed by considered the C_S(r) equal to the C_S(c) using the following formula,

$$(Mr)^2 > (Mc)^2 \tag{5.10}$$

Where, $M_r > M_c$ - the criterion that must be met to insure that the riser solidified after the casting Sound casting produces when the solidification of the riser is taken as 1.5 times the solidification of the casting and also for side mounted height of the riser varies from 1 to 1.5 times diameter of the riser can take as satisfactory condition of feeding (Masoumi et al., 2005)

Therefore, according to this method and Equation (5.10), diameter of the riser was calculated using the following formula,

$$\mathrm{tr} = 1.5\mathrm{tC} \tag{5.11}$$

Substituted t_C with Cs(c){Mc}^{2} and t_r with Cs(r){M_r}^{2} in to Equation (5.9) and using Appendix 7.9, for side mounted riser in to Equation (5.11) the top and exit diameters of the riser were found as following,

$$\left.\begin{aligned} \{V/A\}^2\mathrm{r} &= 1.5\{V/A\}^2_{\mathrm{C}} \\ (V/A)_r &= 1.22(V/A)_c \end{aligned}\right\} \tag{5.12}$$

The shape of the riser is cylindrical like frustum, hence the volume to surface area ratio was found using the following formula (Masoumi et al., 2005),

$$\frac{V}{A} = \frac{\frac{\pi hr}{12}(de^2 + dt^2 + d_e d_t)}{A_l A_t A_e} \tag{5.13}$$

Where, A, A_l, At and Ae- total surface area, latent area, top cross-sectional area and exit cross sectional area of the riser respectively also L-latent length of riser which was given in equation below,

Substituted equation (5.11) in to equation (5.10) and L= $\sqrt{(\frac{d_e - dt)^2}{4} + h^2}$ = 1.50142dt

d_t =1.15de and h_r.=1.5dt, in to the following equation then found all dimensions of the riser.

$$\left(\frac{\frac{\pi hr}{12}(de^2+dt^2+d_e d_t}{\frac{L}{2}(\pi d_e+d_t)+\left(\frac{\pi dt^2}{4}+\frac{\pi d^2}{4}\right)}\right)r = 1.22\left(\frac{0.10cm^3}{2.66}\right)c \qquad (5.14)$$

Hence, d_t = 0.244m or 244mm and possible maximum height of the riser, h = 1.5*d = 366mm was found.

The exit diameter of the riser was determined by considered the top riser diameter is equal to 1.15 times the exit diameter to avoid air aspiration (away) that can be induced in the wall of the riser cavity during metal pouring (Lee et al., 2001), and found as 105mm. Hence, a pattern (near to the estimated values) with sizes of 244mm, 22omm and 366mm as top diameter(d_t), exit diameter (de) and height respectively was selected riser and used in construction of flywheel cavity as shown in Figure from appendix.7.10,

5.6.7 Riser volume

Total volume of metal reserved in the riser was estimated on basis of the actual dimensions using Equation (5.7) of the following formula (Masoumi et al., 2005),

$$\text{Volume of riser} = \frac{1}{12}\pi h\{d^2\text{top} + d^2\text{exit} + \text{dtopdexit}\} = 0.00386\ m^3$$

The weight of riser from the total volume and the density of the riser material (aluminum) was estimated also using Equation (5.3) as following,

Weight of the riser (W_r) = (V r) x (density of the riser material) = 0.0461Kg

According to this method the weight of metal in the riser cavity was high because excess cavity was constructed. This could be in fact compensated the metal shrinkage but casting yield was large and hence consumed time and energy.

5.6.8 Riser neck

Riser has a neck attached to it at the lower end. The neck facilitates easy to directed metal flow from riser to the riser base and then through in-gate to the mold cavity of the produce part. In addition, it also facilitates easy separation of the riser from the riser base. Hence, the neck was considered as an important part of the riser. Therefore, for side mounted riser, diameter of the riser neck was determined from top riser diameter and its neck height using the following formula (Masoumi et al., 2005; Shafiee et al., 2009),

$$dn = 0.5\,Ln + 0.1dr \quad (5.15)$$

Where, dn –end riser neck diameter, Ln-riser neck distance from the casting, dr-riser top diameter. For this design the actual top diameter of the riser pattern was considered and the neck distance was considered same as the length of the in-gate which is 50cm.

Therefore, dn = 1.25 x50cm + 0.18 x40.5cm =70cm

Hence, the actual riser neck which used in part produce casting process was with a pattern dimension of 70 cm end diameter and 29cm of height.

5.7 Estimation of Pouring Speed and Dimensionless Reynold's Number

The gap between the ladle lip and the pouring cup (entrance of the sprue) was measured and found as head variation from 25cm (when the molten started to leave the ladle tip i.e., fall freely from a starting velocity of zero) to 15cm (at the optimum ladle level).

The maximum velocity of the molten metal at the pouring cup base was estimated after falling a distance of 25cm and 15cm plus the height of pouring cup respectively as, using Equation (4.18)

Therefore, velocity of the metal at the pouring cup bottom and or sprue entrance from the two heads respectively, by ignored the coefficient of friction equation.

$$V_{0.25} = \sqrt{2 * 9.81\frac{cm}{sec} * (0.25 + 0.7cm)} \quad = 4.173\text{cm/sec.}$$

$$V_{0.15} = \sqrt{2 * 9.81cm/se * (0.15 + 0.7)} = 1.44\text{cm/sec}$$

From the velocity results, the first velocity was believed to occur for short duration whereas the second velocity was performed up to pouring completion. The first velocity may be created erosion of sprue lip. Thus, for this work the velocity of 1.44m/sec was taken for other analysis of metal flows in the channel used in part produce casting.

The maximum critical velocity of the metal arrived at sprue bottom or exit was estimated by considered the surface friction coefficient (μ) of the sprue-wall using Equation (4.18) and used hs-sprue height in cm which is 150mm (for Aluminum dynamic viscosity ,μ_m =0.012 N-s/m$^{2\cdot}$ from taken properties of aluminum table 5.12.

Therefore, $V_{p,exit} = \mu\sqrt{2g\mu_m} =$ 2.5 cm/sec

This is considered as the critical velocity of metal in the sprue exit which was influenced the metal speed in the critical gating systems channels and treated as moderate speed for alunumim casting flow on the sprue base. The dimensionless Reynold's number (Re) was also determined using Equation (4.17) to estimate the fluid flow condition at the sprue entrance and exit section

$$R_e = \frac{\rho V L}{\mu_m} = \frac{Vd}{\mu_m} = \textit{40670 and 35730 (in sprue entrance and exit respectively).}$$

At the sprue entrance and exit(estimated), L- important length dimension for the flow (for pipe flow, L is taken as the pipe diameter which is sprue diameter). **μ** - the dynamic viscosity taken from Appendix 7.4, and υ - the kinematic viscosity where υ =μ/ρ. Molten metal flows through the gating system to the mold cavity. Due to complexity of mold cavity it is not possible to get laminar flow in the mold cavity. It is either turbulent or semi turbulent flow. Low Reynolds number reduces the casting yield because it increases the dimensions of sprue, runner and ingates. Conversely high Reynolds number leads to turbulent flow. So in order to avoid highly turbulent flow, Reynolds number should be less than 20000, which results in semi-turbulent flow.

5.8 Estimation Pouring Temperature

The temperature of pouring is very vital for the surface finish of the castings. The tapping temperature of aluminium alloy should be 630–750^{o}C. High pouring temperature causes poor surface. When we pour aluminium alloy then its fluidity is completely dependent upon pouring temperature. Generally, a better fluidity in higher temperature is connected with the decreasing viscosity and surface tension of molten metal with the increasing of pouring temperature, which leads to the increasing filling speed. At the same time, the heat capacity of molten alloy rises with increasing temperature of the pouring, which increases by filling time. The pouring temperature also affects the microstructure formation at a greater extent and which in turn affects the final structure and toughness of casting product.

5.8.1 Estimation of average flow rate of mold cavity filling

The average flow rates the molten metal of the part produce was estimated simply dividing the gross weight of casting divided by the actual time of filling, using Equation (4.9) of the provided formula (Masoumi et al., 2005; Ravi and Joshi, 2007),

$$Q_{ave} = \frac{Wa}{t} = \frac{1.5}{8} = 0.2kg/sec$$

This is the average of metal weight flow to the mold channel cavities and predicted that 0.2Kg per every second may be feed in the cavities of the gating system. The mold filling time of the part produce mold cavity was also estimated using Equation (4.9) of the following formula (Ahmad, 2015),

$$\text{MFT} = \frac{mold\ cavity\ volume}{\text{Volumetric flow rate}} = \frac{V}{Q} \quad = \quad 25 \text{ sec.}$$

Where, V-volume of the mold cavity of the part produce which is $0.10cm^3$ and Q-volumetric flow rate of metal along the mold channels which estimated from the velocity and sprue bottom cross-sectional area ($0.5cm^2$/sec),

This is the minimum time required to filling the one produce part mold cavity only (by ignored the gating system elements' cavity). Here, the way of feeding metal to the complex cavity geometry was not considered and hence the actual our produce part mold filling time may be longer.

5.8.2 Estimation of casting to riser freezing temperature ratio

To ensure the solidification shrinkage or macro porosity in the part produce to be avoided solidification time of the riser to solidification time of produces part casting was compared in terms of relative freezing time or freezing ratio of casting to riser. Therefore, relative freezing time or freezing ratio (RF) of riser to casting was estimated using Equation (4.13) based on modulus method as following,

$$R_f = \frac{(\frac{\text{Volume}}{\text{surface Area}})\,riser}{(\frac{\text{Volume}}{\text{surface Area}})casting} = \frac{(\frac{0.000386}{0.3545})\ riser}{(\frac{0.10}{2.66})} = 1.24$$

According to this method the volume to area (V/A) ratio of the riser is 0.0386, as compared to the casting V/A ratio of 0.0362 (i.e., V/A of riser is 1.24 times V/A of casting longer). As a result, the riser was solidified after the casting and should feed properly.

The ratio of volume of the riser to volume of the casting, was estimated using Equation of [5.13] and found as 0.1650. From this result and based on Caine's method, the relative freezing ratios of the riser to casting was also estimated using Equation (4.15) taken constants of **a**-freezing

characteristic for the metal, **b**-contraction ratio from liquid to solid and **C**-relative freezing rate of riser and casting given in Appendix.7.7,

$$\boldsymbol{R_f = \frac{a}{R_v - b} + c = 2.042}$$

According to this result the riser freezing period predicted that much larger than the casting freezing period and hence produced sound part produce castings.

5.8.3 Estimation of riser solidification time

The total freezing (solidification) time of a riser part produce casting was estimated using Equation (4.33) by considered riser and casting constants same(Ahmad, 2015), Therefore, Total solidification time

$$t_r = \left[\frac{\pi}{4}\ \left(\frac{\rho_c \nabla H_f}{T_M - T_o}\right)^2 \left(\frac{1}{k_m \rho_m c_m}\right)\right]\ (V/A)^2 = 2{,}635.8 \text{ seconds} = 44 \text{ minutes}$$

Where, t_r-solidification time of riser, ρ_m, C_m and K_m-are density, specific heat and thermal conductivity of the mould material respectively (Appendix.7.6, and H_f- latent heat of solidification, ρc-density of liquid metal casting (Appendix.7.4), V-volume of riser solidified, A- interface area of the riser, T_m -melting point temperature (^{o}c) and To - initial temperature of mold wall (^{o}c) taken from Table 7. In this, the properties are assumed to be constant all over the casting process.

According to this result, the riser solidified after casting solidification completed and predicted that the design carried out was acceptable in produced sound cast, free shrinkage defects part produce casting.

5.8.4 Estimation of flow rate metal along mold to channels

While estimated the volumetric flow rate of metal in the passages which take part in produce casting, the initial velocity of metal at the ladle tip was assumed as zero. The velocity of metal at the entrance of sprue was estimated after falling through the heights and found as 4.173 m/sec and 1.44 m/sec. respectively. But the metal can be entered with a velocity of less than the estimated one of due to the fact that the difference of the pouring cup bottom and sprue entrance dimensions (sprue top diameter is less). By assuming the volumetric flow rate of metal remains constant and then metal velocity at top of sprue was estimated by applying the continuity law of Equation (4.6) as following (Tiryakioglu et al., 1993),

$Q_1 = A_1V_1 = A_2V_2$, Hence, Q= 0.023m^3/sec and V_1=0.25m/s

Where, Q-Volume rate of flow in the mold channels, A_1-entrance sprue cross-sectional area, and V_1- velocity of flow at sprue entrance, A_2-exit sprue cross-sectional area, and V_2- velocity of flow at sprue exit(estimated).

This is, the maximum flow rate result 0.023m^3/sec) of molten metal flow through the entrance of the sprue without considered the surface tension. Thus, actual flow rate can be believed lower than from what is estimated above. The metal velocity at the runner inlet and outlet was estimated based on the continuity law after sprue base cavity filled was also estimated from the Equation (4.6) analysis the following,

$$Q_2=A_2V_2=A_3V_3 = A_4V_4, \text{ where } Q_2= 0.023,\ A_2= 0.56,\ V_2=0.46,\quad A_3= 0.45,\quad V_3 = 0.43$$

Where, A_2 – actual sprue exits sectional area V_2 - velocity of metal at sprue exit, A_3 and A_4 - actual runner inlet and exit sectional areas (same) and $V_3$and V_4 –velocities of metal at the runner inlet and outlet sections.

Similarly, velocity of the metal at in-gate inlet and outlet was estimated (loss in riser base due to irregular shape not considered) based on the velocity of metal in runner section which considered as fourth reference point using the following equation,

$$A_5V_5 = A_6V,\ \ A_5 = 0.57\ ,\ V_5 = 0.42,\ \ A_6 = \ 0.52, v_6 = 0.52$$

Where, A_5 and A_6=A_i– actual in-gate inlet and exit areas V_5 and V_6 - velocity of metal at ingate inlet and outlet section.

Table 5.3 volumetric flow rate in the respective channels of the produced cast gating system.

Parameter	Locations					
	1	2	3	4	5	6
Area (cm^2)	0.092	0.56	0.45	0 .4	0.57	0.52
Velocity(m/sec)	0.25	0.46	0.43	0.54	0.42	0.40
Flow rate (m3/se)	0.023	0.023	0.023	0.023	0.023	0.023
Re	40670	35730	32700	34200	37001	30960

The numbers1, 2, 3, 4, 5 and 6 given above represent locations of gating system elements respectively to sprue entrance, sprue exit, runner inlet, runner outlet, ingate inlet and ingate outlet. The liquid metal with a maximum velocity of 0.54m/sec and flow rate of 0.023 m^3/sec may be

entered to the used form of calculation mold cavity. Hence, the actual metal speed may be less due to the effect of surface tension and other factors of the mold.

5.8.5 Estimation of temperature loss to the gating system

To penetration defects happened, metal should be poured at an optimum temperature and pouring rate. However, due to heat losses in the gating system, molten metal does not enter the mould cavity at the pouring temperature. Metal should be poured at an optimum pouring rate and temperature (Di Sabatino, 2005).

Table given below discusses about the critical casting process temperature parameters taken through direct observations during metal melting, filling, pouring and part removal activities.

Table 5.4 Data related to melting and casting of part produce used.

S.n	Parameter	Parameters used for Experimental	Unit	remark
1	Pouring temperature	630, 680, 750	℃	
2	Starting metal temperature	615	℃	
3	Atmospheric temperature	27	℃	
4	Mold filling time (Estimation)	15	sec	
4	Part take off time (TST + Solid solidification)	2.50	hrs.	(part removal from cavity)

While the molten of aluminum alloy was poured from the furnace, the pouring temperature was taken as 680^0C. Further, due to heat losses in the gating system, believed that molten of aluminum alloy could not enter the mold cavity at this temperature (680^0C) and hence less fluidity caused misrun defect or penetration defect on the casting product. Therefore, the amount of temperature of the molten aluminum alloy loss in the gating system was estimated using Equation (4.19) (Lee et al., 2001),

$$\Delta T = \frac{(As(T_P - T_{mi})\sqrt{T_p})}{W_t C_i}\sqrt{k_m \rho_m c_m}$$

$$\Delta T = \frac{0.280908 cm^2((680-27)^O C\sqrt{8sec}}{(1000kg)(0.9J/Kg.c^o)} * 3.4x10^3\left(\frac{J}{m^2 k}s^{\frac{1}{2}}\right) = -20℃$$

The minus sing indicated loss of temperature in the gating system channels and hence hot metal was arrived to in-gate outlet cavity with a temperature of approximately 630^{O}C. Where, As-surface area of the mold channel used/sum of the surface channels of in-gate system (cm^2), P_T-pouring temperature(^{0}C),T_{mi}-initial temperature of the mold (^{0}C), t_p- pouring time(in sec),W_t- weight of the casting and the gating system(kg), Ci - specific heat of liquids metal(taken from Appendix.7.4), J/Kg ^{0}C, Km -thermal conductivity of the mould material , J/se/m ^{0}C, ρ_m,-density of the mould material, Kg/cm^3, C_m - specific heat of the mould material, J/Kg ^{0}C which given by$\sqrt{K_m \rho_m C_m}$ - Heat diffusivity (J/m^{2}Ks1/2) (taken from Appendix.7.7). In this case, the total surface area of the mold channel, that made in contact with fluid, was estimated believed that more heat may be loss within the channel surfaces and found as 0.029cm^2 (sum of all surfaces in contact with fluid as shown in table5.5,

Table 5.5 Surface area of mold channels in the contract with fluid.

N/o	Channel	Total surface area	Area in contact	unit
1	Sprue	AL +At +Ae = 1,042	AL= 98.46	mm^2
2	Sprue base	AL +At +Ae = 283	AL +Ae= 203.65	mm^2
3	Runner	2Ac +AL = 496	AL = 406	mm^2
4	Riser base	2Ac +AL = 1131	2Ac+AL =1130.97	mm^2
5	Ingate	2Ac +AL = 274	AL =170	mm
	Total		0.029	cm^2

The results above given in Table 5.5 discuss about the total surface area of the mold channels which take part in flywheel casting and areas of these channels that only made contact with fluid flow during mold cavity filling from sprue entrance to ingate section. Where, AL – lateral area, At –top area, Ae- exit area and Ac-cross sectional area of the passages (mold channels) used in the produce part casting.

5.8.6 Estimation of metal aluminum alloy fluidity

The fluidity of the metal (aluminum alloy), which is a measure of its capability to flow into and to fill the mold cavity before freezing, was estimated without considering losses in the channel. Since vertical gating system was used, metal fall through down of sprue that made to fill sprue base

cavity directly and so believed that its effect in the fluidity reduction is less. Hence, the fluidity of metal was assumed as that started from the runner towards the mold cavity. This was estimated using Equation (4.20) of the following formula (Ahmad, 2015; Ruddle, 1956),

Where, L_f- final fluidity length, (cm), A_{sr}, A_{sing} and A_{TP}- are surface areas of mold channels of runner, riser base, ingate and part produce respectively (mm^2), Cr, C_{ing} and C_{TP}- are circumferences of mold channel of runner, ingate and on part practice respectively (mm), Δy -Choking range(mm) taken from table 5.12, C-specific heat capacity of metal KJ/kgK from Appendix.7.4, $(T-T_r)$ -liquid metal temperature of aluminum minus room temperature (K) (used as melting temperature minus mold temperature), h - heat transfer coefficient at mold-metal interface(W/m^2K) taken from Appendix.7.4, ΔT- superheat of aluminum (K) taken as pouring temperature minus melting temperature, K- thermal conductivity of mold material (W/mK) from Appendix.7.6, ρ -density of liquid metal (kg/m^3), H_f - heat of fusion of metal (kJ/kg) taken from Appendix.7.4, α-thermal diffusivity of mould material m^2/s (estimated), and V_3, V_5 and V_7 - Velocities of metal flow(mm/s) in the mold channels of runner, ingate and cavity (V_7= LTP/ MFT),

$$l_f = \frac{(\rho H_f + c\Delta T)}{h(T - T_r)} \left\{ \frac{A_{sr}V_3}{C_r} + \frac{A_{isng}V_5}{c_{ing}} \left(1 + \frac{\frac{h * \sqrt{\alpha * \Delta y}}{k\sqrt{V}}}{2} \right) + \frac{A_{PT}V_7}{C_{PT}} \right\} = 6.39\text{cm}$$

This is the maximum length of the metal flow in mold channels (gating system elements) used in casting produced by ignored the surface effects that could retarded to the motion.

5.8.7 Estimation of heat transferred from liquid metal to mold

While solidified the casting believed that heat was transferred from its liquid phase (part) to the solid phase (mold). The amount of heat transferred was estimated using conduction and convection modes of heat transfer. Conduction can be occurred at the liquid and solid state (i.e. liquid of alloy aluminum -mold) and also through the mold (solid state only). Here, temperature distributions at the metal-mold and mold phases were carried out by considered the assumptions of steady state conditions.

After pouring completed, the pouring cup and the top riser surface was insulated by insulating material (asbestos) to reduce heat lost to air and to keep air away from molten metal (Prajapati and Sutaria, 2013; Ravi and Joshi, 2007). Tables 5.6 and 5.7 below discuss about gab between metal

cavity and mold outer edge of the mold which used in all of the positive x, y and z-directions and the respective surface areas of the mold used in the positive x, y and z- faces by taking the cast end as reference point that can be arranged for analysis purpose.

Table 5.6 Data related with cast end and mold surface used in heat transfer analysis

Description	Initial coordinate	Final coordinate	Δ	Unit	Reference point
Thickness of mold, cast end to	x_0 =0	X= 0.24	0.24	cm	Cast end
mold end in the $+v_e$direction	y_0 =0	Y= 0.029	0.029	cm	Cast end
	z_0 =0	Z= 0.036	0.036	cm	Cast end
Thickness of mold, cast end to	x_0 =0	X=0.029	0.029	cm	Cast end
mold end in the -v_e direction	y_0 =0	Y= 0.24	0.24	cm	Cast end
	z_0 =0	Z= 0.036	0.036	cm	Cast end
Mold initial temperature, To	27	T_s	T_s-T∞	℃	Room temp.
Free stream temperature, T∞	20	20	------	℃	Room temp.
Temperature at cast end, Tc	680℃ at t=o sec	T_s at t-sec	Tc- T_s	℃	Cast end
Free stream temperature, T∞	20	20	-	^{o}c	Room temp.

Table 5.7 Data related with surface areas of mold used in the produce flywheel casting

Mold face area	Area description	product	Size	Unit	Remark
$A_{x,m}$	Area of mold in X-face	$W_m x\ H_m$	0.65	cm^2	Two Areas
$A_{y,m}$	Area of mold in Y-face	$w_m x L_M$	2.9	cm^2	Two Areas
$A_{Z,m}$	Area of mold in Z-face	$H_m x L_m$	1.9	cm^2	Two Areas

Considering 3D heat flux per unit area or state, the heat flow rate and time transferred from liquid casting to mold surfaces, along the mold length x-direction using side chill, along the mold height y-direction and along the mold width z-direction was estimated using Equation (4.22) as following,

$$Q_t = Q_X+Q_Y+Q_Z = -KmA_X\frac{dT}{dx} + -Km\ A_Y\frac{dT}{dy} + \ -Km\ A_Z\frac{dT}{dz}$$

Q_t = (-6.141 watt) + (-21.2 watt) + (-12.66 watt) = - 40.001 KJ/sec

Where, Q_t-total heat flow rate, Q_X, Q_Y, Q_Z - Heat flow rates in the x, y and z- directions of the mold, A_X, A_y, A_z- mold face areas in the x, y and z- directions of the mold, K_m-thermal conductivity of the mold material (Appendix.7.6) and the minus sign (-) indicates that heat transferred in the decreasing temperature direction (increase to decrease) and $\frac{\partial T}{\partial x'} + \frac{\partial T}{\partial y'}$ and $\frac{\partial T}{\partial z'}$,- temperature gradients in the x, y and z- directions of the mold (table 5.8). This result show that almost -40 KJ/sec heat was out (- sign) from the casting through all of the positive sides of the mold without considered the heat extracted by chill effect. This is taken as the average heat transferred to the molding material. For the same condition, the amount of heat flux transferred from metal (liquid) to mold (solid), taking convection heat transfer coefficient at the metal- mold- interface, can be estimated using convection mode of heat transfer of Equation (4.34) of the following formula,

$$q = h\,(Tc - To), \text{ Therefore, } \quad \mathbf{q} = 50520 W/m^2$$

Where, q-amount of heat flux, h- heat-transfer coefficient at the metal-mold interface in (w/m^2C) taken from appendix.7.4, Tc – metal cast end temperature immediately after cavity filling in (^OC), To- initial temperature of mold in (^OC) and substitute to the provided equation above.

This is the maximum amount of heat flux from cast that can be transferred from the liquid (metal) phase to solid (mold) phase during the solidification of the 242-alunumim analysis produce part casting (flywheel).

The temperature at any location (X- Y -Z-axis) within the mold as function of time following pouring of the metal and using the mold initial temperature (T_o) and the cast end temperature (T_c) was estimated from the Equation (4.25), analyzed in this the following table value. Table 5.8 below discusses about temperature distribution along the mold in + x-direction (length) from cast end.

Table 5.8 Temperature variation results in mold (+X, Y& Z-direction)

Mould initial temp. ^{o}c (T_o)	End cast temp.(c) (T_c)	Time (sec)	Distance from casting (X, Y and Z in m) /Direction			$Erf\frac{x}{\sqrt{\alpha(t)}}$	T (x, t)
			X	Y	Z		
27	750	90	0	0	0	0	750
27	750	120	0.019	0.013	0.015	0.932507	654.82
27	750	150	0.14	0.016	0.013	1	653.00

27	750	120	0.12	0.023	0.020	1	653.00
27	750	150	0.017	0.014	0.024	0.856592	656.87
27	750	90	0.016	0.018	0.012	0.924576	655.04
27	750	150	0.15	0.022	0.017	0.924576	655.03
27	750	90	0.022	0.017	0.023	1	653.00
27	750	150	0.011	0.015	0.015	0.656252	662.28
27	750	120	0.24	0.029	0.036	1	653.00

In this table 5.8 temperature distribution result with respect to the mold thickness in the positive x-direction and length y and z from cast end. In the done only x-direction, similarly, the temperature distribution in the positive y and z-directions can be obtained. The temperature gradient in the mold at any distance from the casting end to +x, +y and +z –directions can be estimated respectively using Equation (4.26) (Montgomery, 2017).

Table 5.9 given below discusses about the temperature gradient along the length of the mold of the three positive directions. In this case, the minimum temperature gradient magnitudes of the molten metal along mold wall in the positive three directions and shown in gradient reduction as the distance of the increased from the casting end.

Table 5.9 Temperature gradient results in the mold distance

T_0℃	T_c ºC	Time in sec.	(+x)	(+Y)	(+Z)	$\frac{\partial T}{\partial x}$	$\frac{\partial T}{\partial y}$	$\frac{\partial T}{\partial z}$
27	750	90	0	0	0	202861.3	02861.2676	202861.2676
27	750	123	0.019	0.013	0.015	42582.18	2582.17729	42582.17729
27	750	150	0.14	0.016	0.013	26677.73	5423.23087	17021.59086
27	750	123	0.12	0.023	0.020	6236.907	517.7807802	3644.262947
27	750	150	0.017	0.014	0.024	777.4951	212.4060005	212.4060005
27	750	90	0.016	0.018	0.012	166.8188	10.13290265	166.818812
27	750	150	0.15	0.022	0.017	36.03005	0.079397084	36.0300539
27	750	123	0.022	0.017	0.023	7.828812	0.003020811	0.457514898
27	750	90	0.24	0.029	0.036	1.70992	1.661105	0.000701614

The total heat flux away from the interface of the part cast in to the mold at a distance was estimated from the estimated temperature gradients using Equation (4.27). Table 5.10 below discussed about the estimated heat flux away from the cast interface in to the mold and then to environment in the positive directions (+X, +Y and +Z).

Table 5.10 Heat flux values at metal-mold interface and the mold inside wall.

$\frac{\partial T}{\partial x}$	$\frac{\partial T}{\partial y}$	$\frac{\partial T}{\partial z}$	q_m(X)	q_m(Y)	q_m(Z)
202861.3	20861.2676	202861.2676	65827*	66432.63	65046.088
42582.18	2582.17729	42582.17729	57626	62257.02	57043.90
26677.73	5423.23087	17021.59086	50426	56714.00	49672.89
6236.907	517.7807802	3644.262947	43225	50974.00	43843.00
777.4951	212.4060005	212.4060005	36025	46004.69	37203.47
166.8188	10.13290265	166.818812	28824	40867.19	27690.06
36.03005	0.079397084	36.0300539	21624	29002.00	16063.6
7.828812	0.003020811	0.457514898	14423	12001.01	96.4046
1.70992	1.6611.05	0.000701614	7222.6	217.20	46.70656
0.65721	8.66268.12	7.34891-07	22.093*	76.038	24.07612

The results in Table 5.10 above direct the maximum amount of heat flux applied from casting interface to mold interface in which at x=0, is 65827 (J/m^2s) and at the outer mold surface as minimum $qt_{(m,x,y,z)}$=0.24,0.029,0.036) is 22.093 (J/m^2s). This is only in the selected points and positive direction of the mold from the reference initial point of the casting end.

The heat flux across the mold-metal interface (away or mold initial) was also estimated using the thermal conductivity (K_m), density (ρ_m) and specific heat (C_m) of the mold material and the cast end temperature using equation (4.28) analysis this result,

Where the result is $\left(\sqrt{\frac{70J/m/s*1000kgm^2/s*2570kg/J}{\pi t}} * (T_c - T_0)\right) * 3 = 2773.98 J/m^2 s$

Where, $q_m(x,y,z)$- total heat flux in the metal –mold interface (away), q_m(x=0) - heat flux in the metal –mold interface (away), q_m(y=0) - heat flux in the metal –mold interface (away) and (z=0)- heat flux in the metal –mold interface (away) in the x, y and z-directions respectively. This is the

amount of heat flux at the metal-mold interface/away mold initial point) which indicated that reduction by 3776 (i.e., 6550 -2774) J/m^{2}s from the heat flux at the cast end of table 5.10 due to the fact metal solidification occurred in the interface. The solidification time of the part produce (flywheel) was estimated based on Chvorinov's rule using Equations of (4.11) and (4.32) of the following formula (A. Reis, Z et al,2012, 2017; Choudhari et al., 2014b),

$$t_c = [\frac{\pi}{4}\{\frac{\rho_c \nabla H_f}{T_m - T_c}\}^2 (\frac{1}{\rho_m C_m K_m})(\frac{V}{A})^2] \text{ = 15 min.}$$

Where, t_c-solidification time of casting, ρm, Cm and Km-are density, specific heat and thermal conductivity of the mold material respectively (Appendix7.6), and H_f- latent heat of solidification of metal),ρc-density of liquid metal casting (Appendix.7.4), V-volume of cast solidified, A-interface area of the casting, Tm -melting point temperature (℃) and To - initial temperature of mold wall (℃) taken from table 5.4. Therefore, Total solidification time (TST), tc = 900 seconds From the result of casting solidification period, it indicated that the produce part (flywheel) casting solidified before riser solidification period and hence the design produced sound casting.

5.8.8 Estimation of heat transferred from mold to environment

The amount of heat flux transferred from mold wall to environment by convection mode of heat transfer (steady state condition) was estimated using Equation (4.34) as following,

$$q = h(T_s - T_\infty), \quad \text{then the result is , q = 2.347 J/}m^2\text{s.}$$

Where, q- heat flux normal to the surface of mold which was taken from table 5.10, h- convection heat transfer coefficient (which is not a thermodynamic property of the material, but depend on geometry of surface, flow characteristics and thermodynamic properties of the fluid, etc. (W/m^2 and $\Delta T = (Ts - T\infty)$ - difference in surface and coolant (free stream fluid) temperatures (^{O}C). This result was the minimum amount of heat flux transferred from mold surface to environment indicated that gases bubbles out through the mold wall to environment.

5*.8.9 Estimation of energy to heating of Al242, aluminum alloy*

The amounts/total heat energy required to melt the metal to a molten temperature sufficient for casting is the analysis estimation. Hence, this energy was calculated using Equation (4.35) of the following formula(Choudhari et al., 2014b),

$E_t = \rho V \{Cs(Tm - T_{st}) + H_f + Cl(T_P - Tm)\}$ Therefore, $\mathbf{E_t} = 0.00351X\ 10^3 J = 3.51KJ/kg$

Where, E_t- total heat required to increase the temperature of the metal to the pouring temp (J), ρ-density of metal (g/cm^3), V-volume of metal used for heating (estimated as volume of the gating system elements and the mold cavities) equal to 48363 mm^3,from calculation, C_s - Specific heat of solid metal (J/g℃) taken from Appendix.7.8, Cl - Specific heat of liquid metal taken from Appendix.7.4, Tm -melting temperature of the metal (℃), Tst- starting temperature of metal (℃), taken from Table 5.5, H_f - Heat of fusion (J/g) taken from Appendix.7.4, T_p- temperature of the pouring metal (℃), This was the maximum heat energy used for melting the gross weight of 1.58 Kg in the induction furnace up to pouring stage of the metal. It indicated that for complete melting up to pouring stage of the given metal weight took longer time. Hence, the molten metal entered to the gating system cavities was assumed with this heat value by ignored heat losses during pouring operation.

5.10 Material Properties

In this table discuss Themophysical properties of alunumim alloy used analysis of the simulation

Table 5.11 Themophysical properties of alunumim alloy (*Al-242) used in the simulation.*

Material properties	value
Solid temperature	515°c
Liquid temperature	686°c
Ambient temp.	2839kg/m^3
Specification heat	1531J/kg-k
Solid density	2729.8 kg m^3
Liquid density	2502kg/m
Thermo conductivity	141W(m^2/k)
LHF	352.5 J/kg
Dynamic viscosity	4.5*10^{-7}kg/m/s
Tensile strength	214mpa

The above table discus material properties of using in simulation, the interfacial heat transfer coefficient (IHTC) between the mold and atmosphere used was 11.2 W/ m^2K (Nadiah J. Ahmad,

2015). The properties of sand mold used in the simulations are shown in table5.13 (Nadiah J. Ahmad, 2015, et al).

Table 5.12 Sand mold properties used.

Property	value
Conductivity	0.8W/m-k
Specific heat	1172.4J/Kg-K
Density	1520Kg/m^3

5.11 Minitab software

Minitab is a statistical analysis software package designed for carrying out statistical, numerical, and graphical activities. Minitab offers several graphical tools to explore and detect quality problems and improve process and hence it is an interactive program (i.e., supply Minitab with input data, or tell it where the input data is, and then Minitab responds instantaneously to any commands with that data) (Moore and MCCabe's, 2010).

5*.11.1 Design of experiments (DOE)*

Tables of 5.16 to 5.19 given below discuss about the designed levels of selected variables which take part produce in flywheel casting, the L9 standard orthogonal array (OA)of three levels factors determined using array select, the actual position of the selected factors determined using Minitab software/Taguchi's DOE and the measured responses' (trials), length/depth (in vainer caliper and µm) variations of the flywheel were taken as response variable and measured using caliper and micrometer, results of the experiment respectively.

Design of experiments is systematic techniques to determine the relationship between factors affecting a process and the output of that process. It is used to find cause-and-effect relationships and needed to manage process inputs in order to optimize the output. Experimental design can be used at the point of greatest leverage to reduce design costs by speeding up the design process, reducing late engineering design changes, and reducing product material and labor complexity. Designed of Experiments are powerful tools to achieve manufacturing cost savings by minimizing process variation and reducing rework, scrap, shrinkage defect and the need for inspection (Moore and MCCabe's, 2010; Roy, 2001).

5.11.2 Taguchi method

The three important input parameters have been considered for this process, pouring temperature, pouring ingate/ riser size and pouring time selected. The present study as associated with sand casting process which involves various parameters at different levels and significantly affects the casting quality. In generally the objective of this method is minimize the process parameters shrinkage defect of in sand-casting product (Moore and MCCabe's, 2010; Roy, 2001).

5.11.3 Factorial design experiments

Factorial design is used for determining experimental design used for scenarios with a small number of parameters and levels (1-3) and where each variable contributes significantly, it can work well to determine the specific interactions between variables. Factorial design gets increasingly complex with an increase in the number of variables. The main advantage of the factorial design is enables to examine the interaction effect of the independent variables on the dependent parameter effect of one independent variable has on a dependent variable is not the same for all levels of the other and can lead to more powerful test by reducing the error (within cell) variance (Montgomery, 2017).

5.11.4 Selection of Orthogonal Array (OA) and process parameter

Selection of an orthogonal array depends upon the number of control factors and interaction of interest. It also depends upon number of levels for the control factors of interest. Therefore, for designing experiment and to visualize the effect of process parameters such as pouring temperature, pouring riser size and pouring time on the quality characteristics of produce part made by the investigating casting process, three levels are selected (Montgomery, 2017; Roy, 2001) orthogonal array is selected with nine (L9) experimental runs and three columns. In following table with replace number corresponding values for levels.

Table 5.13 Experimental layout of L9 orthogonal array.

	Trial No.									
Input parameters	1	2	3	4	5	6	7	8	9	Corresponding value for levels
Pouring temperature(^{o}c)	1	1	1	2	2	2	3	3	3	1=630, 2=680, 3=750
Pouring riser size(cm)	1	2	3	1	2	3	1	2	3	1=50,2=60, 3=70
Filling time(sec)	1	2	3	2	3	1	3	1	2	1= 90, 2=120, 3=150

The software used for this purpose is the MINITAB statistical tool and the arrangement of the factors in arrays is represented in the table below. Here the parameter with at three different levels, therefore orthogonal array (L9) is selected for the experimental work. As per L9 orthogonal array nine experiments were performed randomly as shown in table The following table is discussing method of parameters select and factorized method.

Table 5.14 Orthogonal array of three variables and three levels using Minitab software

↓	C1	C2	C3
	Pour temperature(deg.C)	Pour riser size(Cm)	Pour time(sec.)
1	630	50	90
2	630	60	120
3	630	70	150
4	680	50	120
5	680	60	150
6	680	70	90
7	750	50	150
8	750	60	90
9	750	70	120

In table 5.16 trial conduct in nine experiments replicate each factor level present (conduct all the nine experiments and observe the surface defect counts per unit area). The percentage of measured defects surface for each trial was evaluated and the report generated was obtained from MINITAB-18 statistical software. The experimentally results shown in Table 5.16 predicted that the selected input parameters have an effects of on the length variations of castings produce during casting process. At sand casting process is performed according to L9 OA of Taguchi approach. Table 5.16 represents the experimental mean values of casting defects which are relate/visually inspected. Rejection rate cause of parameter is determined from the ratio rejected metal cast due to casting defects to the amount of metal poured. The performance characteristic factors of the process namely, the average elimination (mean) and standard deviation of each experiment were determined to predict the effects from the replicate results using the following equations respectively (Montgomery, 2017; Pyzdek and Keller, 2003)

$$veg.(mean(\overline{X})) = \frac{\text{sum of individual trials of each experiment}}{n} \qquad (5.16)$$

$$std.\ deviation\ of\ each\ experiment = \sqrt{\frac{\sum_{i=1}^{n}(\mathrm{Xi}-\bar{\mathrm{X}})^2}{n-1}}\ \ or\ \sqrt{\frac{(T1-\bar{\mathrm{X}})^2 + (\mathrm{T2}-\bar{\mathrm{X}})^2}{n-1}} \qquad (5.17)$$

Where, T_1- trial one, T_2- trial two or n- number of trials of each experiment, X_i-individual trials of each experiment and $\bar{X}$-mean of the trials of each experiment. In table 5.17 below discuses about the mean and standard deviation of each experiment calculated using Equations of (5.16) and (5.17) respectively. Mean and standard deviations of the experimental trials and conducted in nine experiments with two replicate of each factor level.

Table 5.15 Mean trials conducted in nine experiments two replicate of each factor level

	Pouring Temperapture (^{o}c)	Pouring Riser size(cm)	Pouring time(sec.)	Trial(1)	Trial(2)	Trial(3)	Arg. mini. area casting defect
1	630	50	90	0.0334	0.0330	0.0332	3.32
2	630	60	120	0.0402	0.0200	0.0301	3.01
3	630	70	150	0.0436	0.0368	0.0300	3.68
4	680	50	120	0.0600	0.0400	0.0500	5.00
5	680	60	150	0.0420	0.0380	0.0400	4.00
6	680	70	90	0.0460	0.0360	0.0403	4.01
7	750	50	150	0.0436	0.0432	0.0434	4.34
8	750	60	90	0.0600	0.0400	0.0500	5.00
9	750	70	120	0.0470	0.068	0.0466	4.68

Table 5.16 above indicated that the average defect surface area of product by using (mean) and standard deviation results of each trial (measured values) of the response variable of each experiment conducted on the castings produce part.

5.11.5 Analysis of Signal-to –Noise (SN) ratio

The effect of each variable on the length variations of casting produce part were determined using Signal –to-Noise ratio method. There are three different ways of calculating the *S*/*N* ratios. These are the nominal-is-best, the smaller the better and the larger-the-better approaches. In the present study, the smaller-the-better option of the *S*/*N* quality characteristic was utilized to obtain the best combination for the free casting surface defect with respect to the desired low cast defect. Hence,

SN ratio for each experiment was determined using the following formula (John et al., 2013; Montgomery, 2017),

$$n{=}{-}10Log10 \text{ [Mean of sum of squares of measured data]}$$
$$Small\ the\ better, SN\ ratio(\eta) = -10\log[(\sum y^{2i})/n \quad (5.18)$$

Where, n= the number of the outputs of the test, y= is the response of the output characteristic for the test. The experiments were conducted thrice for the same set of parameters using a single-repetition randomization technique (Roy, 2001). The average for elimination value and SN ratio of each factor of experimental level was calculated using the following formula (John et al., 2013; Montgomery, 2017),

$$SN_{A1} = \frac{SN_1 + SN_2 + SN_3}{3} \quad (5.19$$

5.11.6 Analysis of Variance (ANOVA)

Analysis of Variance (ANOVA) is a computational method to quantitatively estimate the relative contribution, which each control factor makes to the overall measured response and expressing it as a percentage. In ANOVA, effect plots were used to visualize the impact of each factor combination and identify which factors are most influential**. i**t was consisting of simultaneous hypothesis tests to determine if any of the effects are significant. ANOVA was used to estimate the relative effects or magnitudes of the input variables which high affect (defects) in this input parameter on casting product part (flywheel) casting process and expressed it as a percentage contribution. The total sum of squared deviations (SST) was calculated from the total mean SN ratio using the following formula(Montgomery, 2017; Roy, 2001),

Total sum of squares = Sum of all the squared effects for each factor, $= \sum_{i=1}^{9} SN_i^2$ (5.20)

Over all mean of responses (SN),M $= \frac{1}{9}\sum_{i=1}^{9} SN_i$ (5.21)

F ratio and p-value were also calculated using the following formulae

$$\text{F ratio } = \frac{MS}{MSE}, = \text{P} - \text{value } = (\text{F} - \text{ratio}, \text{DOF}, \text{DOF error}) \quad (5.22)$$

6 CHAPTER

6. RESULT AND DISCUSSION

In this, chapter presents the main results and discussions of the study. This study was carried value of for numerical modelling in process sand cast and free shrinkage defect and to minimize shrinkage defect in product free casting (sound casting) discuss understanding. The study used experimental and simulation results obtained based on the availability of parameter data were discussed concerning to the facts that occurred and compared to the literature. The analysis focuses on studying the behaviour of the causes of shrinkage defects parameters on casting product affects the early stage of the solidification process when the metal melt still powerful behaved as liquid inside the castings material.

6.1 Discussion of Numerical Results

. Casting gross-weight

The gross weight (net weight) of metal used casting (1.5Kg) that acquired (obtained) using the increased/ maximized yield may be used to fill for the given casting product part mould cavity and the gating system cavities which take product part (flywheel) in casting. As per the related to standard design considerations this weight indicated that a little less due to the small-sized pattern and moulding use. casting gross weight as well as casting yield determined used Equation (4.12)

The casting yield is the proportion of the actual casting mass to the mass of metal poured into the mould expressed as a percentage. The theoretical casting yield value (58.4%) and actual yield casting (54.5%). It is also clear that actual casting yield is less than that of the theoretical casting yield since the actual amount of metal poured is always more than that of theoretical value due to various factors like mould cavity errors, oxidation loss through the sand mould, volumetric contraction of the molten metal absorption of metal in the sand. Feeding of metal during solidification also accounts to this factor.

6.2 Gating system elements

The overall sizes of gating system elements used in pattern casting were designed and obtained based on the principle of pressurized gating area ratio rule applicable for Aluminum castings. The gating areas ratio used in this work was “1:1:2:4” respectively to total ingate areas, sprue exit area, sprue entrance areas and runner area and this may be give small sizes results of the critical gating

system (channel) dimensions as compared to the standard gating areas ratio of 2:3:4 that applied for metal castings as given in the literatures. In this case, the ingate system area presented by "1" was estimated from the net weight of the metal, can be used as small size and resulted to give in small sizes of the other gating system elements used in casting produce part. Therefore, small sizes of these gating system elements lead to turbulence flow condition within the channels/not necessary in castings) and cause for metal solidification before cavity poured and resulted to volumetric solidification shrinkage occurred in the part producing.

A) **Freezing periods of riser and casting in part produce**

As per the analysis used the result of freezing time/freezing ratio (RF) of the riser to casting that using Equation (4.13) based on their modulus ratio method is 1.24. This indicates that volume to area ratio of the riser is 0.0386 and that of casting is 0.0362 and hence volume to area ratio of the riser is 1.24 times greater to the volume to area ratio of the casting. Accordingly, to the riser used freeze after completing of part produce freezing by 1.24 times later. Based on the **modulus ratio** method the riser analysis can be satisfactory for the given weight of specification of cast produce the part to feed properly.

B) Comparison of riser and casting part production solidification

As per the rule used, these results indicate that the total time was taken of the molten liquid of the aluminium alloys to solidify from the pouring stage to its freezing completed stage. In this work, the time taken of solid to freezing completed to out from the mould cavity was not taken into consideration. From this value, the riser solidification period is 2635.8 second/ 44 minutes late to that of the casting part produce solidification completed time. As a result, the riser used can be feed and compensate metal for the given weight and effective in producing sound castings part with minimizing shrinkage defect, misrun and porosity formation.

6.3 Pouring Time Result

The pouring time of result through the experimental and numerical methods indicates the same and can help as the total time required to fill the given weight of metal into the gating system elements' and mould cavities is 9.8 seconds, using equation (4.2). This filling time result predicts that as compared to the solidification time or freezing time of metal produce part casting (flywheel) is much less than the time at which solidification started. The actual pouring time for the given

furnace and gating system cavities can be greater than to what is given above help the provided equation and or experiment considering on the skill of the ladle operator and used part product (flywheel) casting.

On the other hand, longer pouring time (greater than to 9.8seconds) caused in temperature decreased of molten in the system cavity (with time) which lead to its fluidity reduction. Therefore, metal pouring temperature falls to overcome the liquidus temperature line, molten metal can be started solidification and results in cold shut, shrinkage porosity defect and misrun defect in the final casting, which is unacceptable. So, the optimum pouring time of the given produce part (flywheel) casting considered, as 9.8 seconds and metal solidification could not start before cavity filling completed and produced sound flywheel casting.

6.4 Flow rate metal along mold to channels result

The Reynold's number (Re) results in channels predict that the fluid flow condition was laminar flow (Re < 340 called laminar and Re $\leq$ 40670 turbulent flow at the entrance). Since the results were estimated by ignored the channel surface tension effects on flow retardation, the actual flow results can be greater than from what are found using Equation (4.17). The flow also reduced (damped) as both viscosity and density of metal increased along the channels, turbulent flow in long channel very this impossible because the high turbulent flow it is creating mold erosion. This figure 6.1 indicates the result turbulent flow and laminar flow into channel.

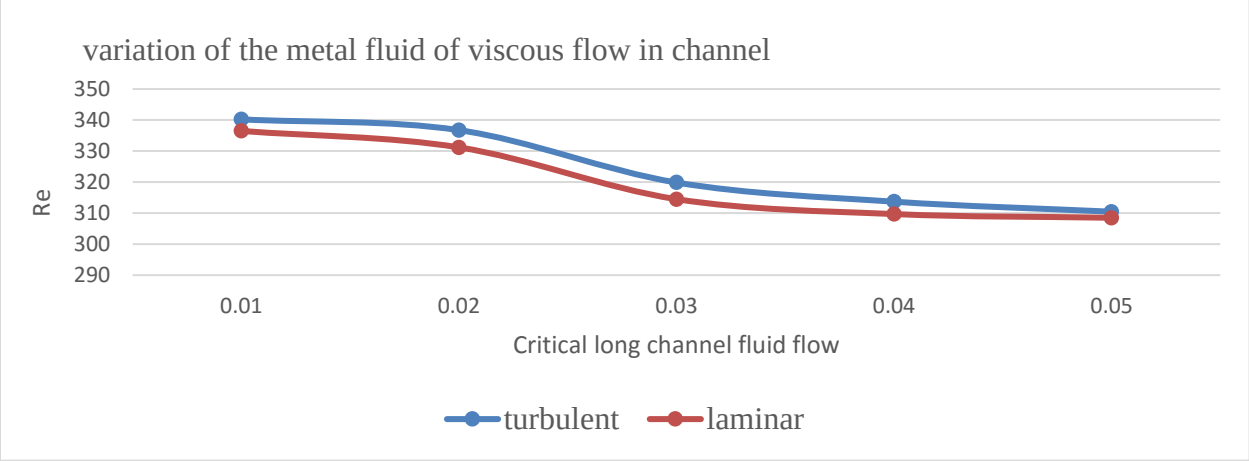

Figure 6.1 metal fluid flow in the laminar and turbulent

The properties of liquid metal may change, particularly the viscosity of metal due to drop in temperature during the flow. The viscosity is characterized by Reynold's number, that is the ratio

of two kinds of forces inflow of liquid, which are viscous force promoting the laminar flow and inertia forces promoting turbulent flow. The metal fluid flow of compering the qualitatively, the force inflow of liquid metal which are viscous forces laminar flow better than inertial forces promoting turbulent flow.

6.5 Heat transfer to metal and from liquid to mould Result

Based on the condition method, the total rate of heat transferred from the part produce cast (flywheel) cavity end molten-liquid state to mold surface of respective directions (±X, ± Y and ± Z) during solidification was estimated using conduction heat transfer method Equation (4.25). From this equation the result, 40KJ/sec heat out, the metal released high amount of heat per second and subjected to fast solidification time and fast cooling which is not desired in solidification of alunumim metal castings.

While the metal loses its sensible heat and the rate of heat transfer from the solidifying metal to the mould is high. During the formation of the gap between the solid skin and the mould wall, *h* decreases and it is continuing to decrease as the thickness of the solid increases. The temperature at any location (x, y, z-axis) within the mold as function of time and pouring of the metal and using the mold initial temperature (T_o) and the cast end temperature (T_c) was result in table 5.8, estimated using Equation (4.25) discusses the result temperature distribution along the mold thickness in length + x-direction from cast end. This is temperature distribution result with respect to the mold thickness in the positive x-direction only during the provided solidification period and y and z similarly process to the x- direction.

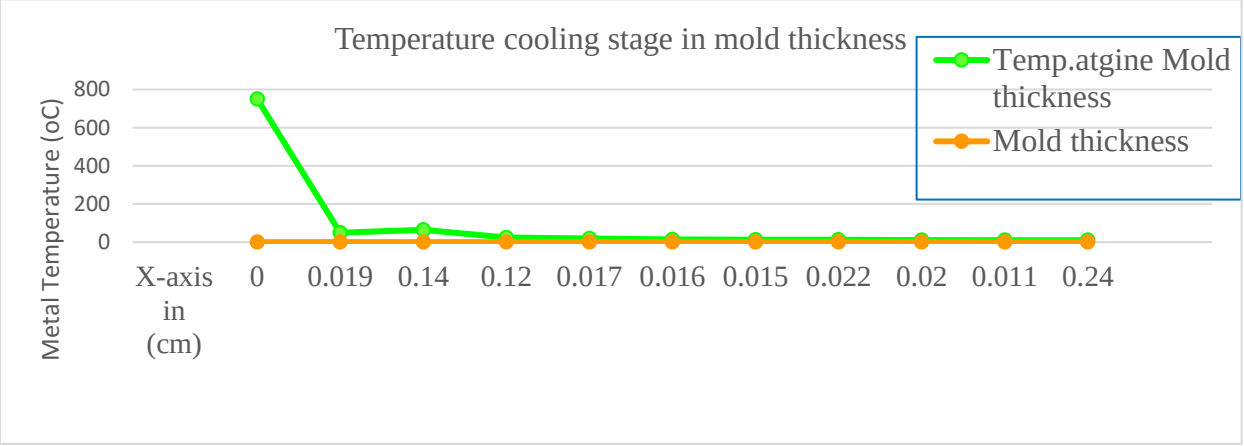

(a) Temperature cooling in +X- direction

Similarly, the temperature distribution in the positive y and z-directions can be obtained.

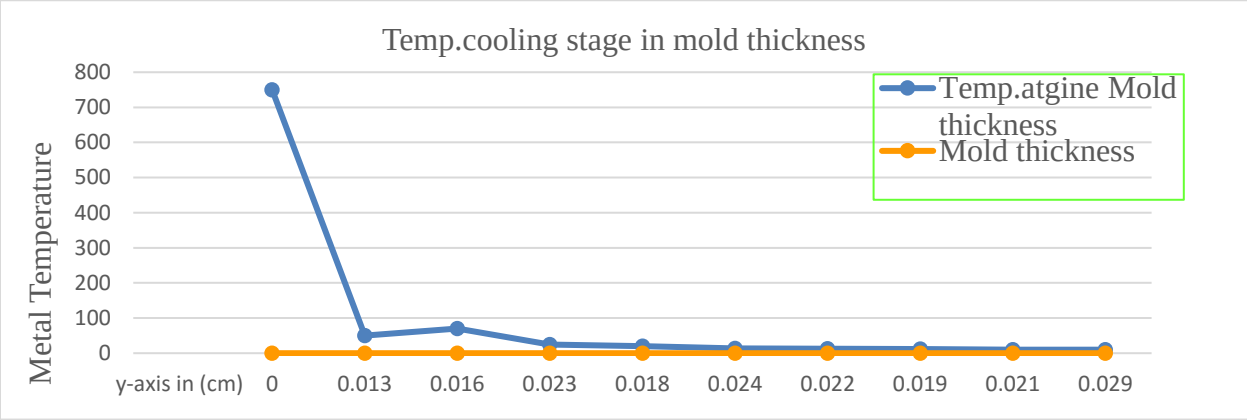

(b) Temperature cooling in +Y- direction

Temperature change results in mold thickness in +z-direction

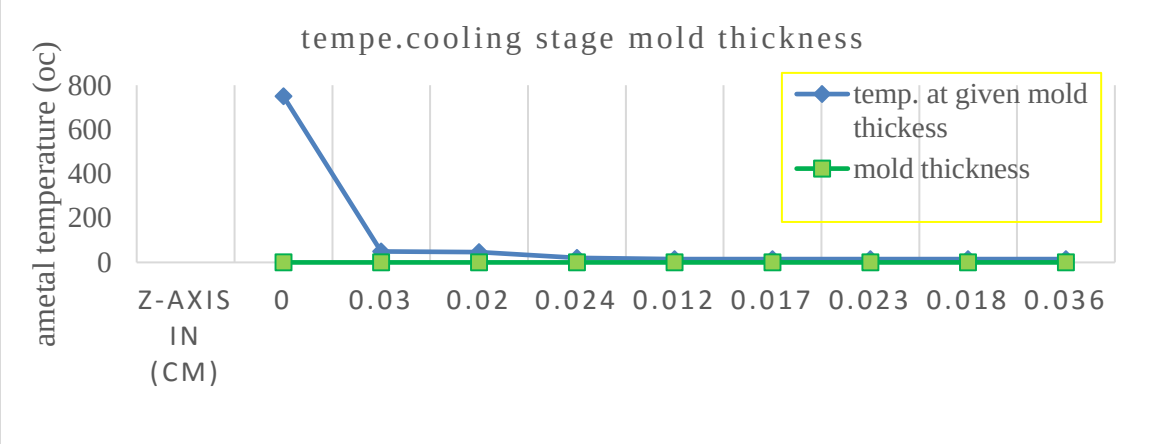

(c) Temperature cooling in +Z- direction

Graphs (a), (b) and (c) of Figure above show the temperature distribution of the metal in the mould during the cooling/freezing stage. Here, the metal temperature can be highly dropped its hotness along with the mould thickness of about 24mm in X-axi positive sides. Therefore, the total freezing period taken by the metal up to this thickness was around 44 minutes which is almost equivalent to the results obtained by the simulation process.

Table 5.8 results indicate that temperature variation of molten metal from cavity end to mould outer surface within the estimated solidification time. According to this method, the variation

shows from 680°c (at initial point) to 27 (a distance of X = 24mm) during the provided period of 2640 seconds and almost same in all of the positive directions of the mould.

Similarly, the amount of heat flux transferred in the metal to mould interface by considered the convection mode of heat transfer was obtained as around of 250000W/m^2. As per the result indicated, the maximum amount of heat flux was away from cast per a unit area and this can be caused to fast heat transferred out from the liquid cast metal phase to solid (mould) phase during the solidification aluminium casting. So, this caused fast freezing period resulted in volumetric shrinkage defects in the castings produce part (flywheel).

In the table 5.10 the result value of total heat flux by using Equation (4.27) in any direction (x, y, z). discussed about the estimated heat flux away from the casting interface into the mould and in the positive directions (+X, +Y and +Z). Heat flux values at the metal-mould interface and the mould inside wall. In this the selected points and positive direction of the mold from the reference initial point of the casting end. The graphs discussed at the (X, Y, Z) direction amount of heat flux transferred to during cooling stage.

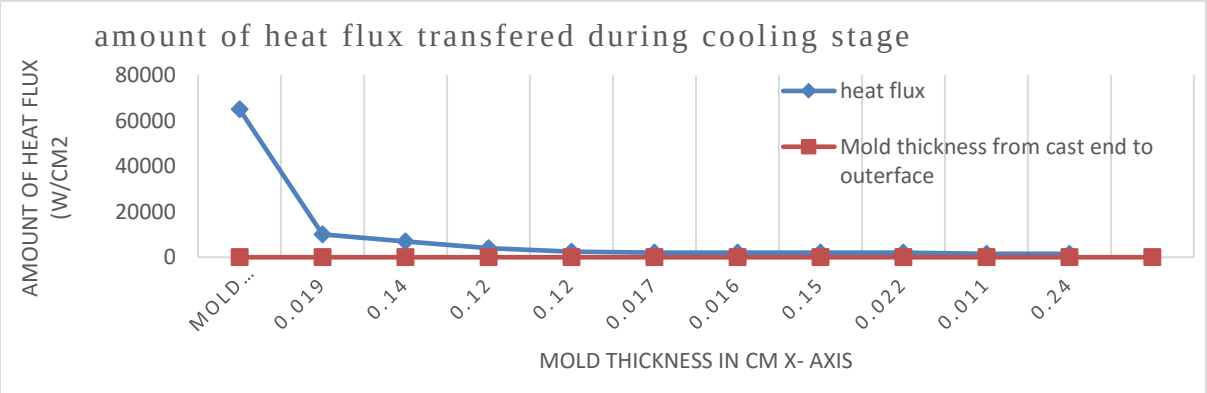

(a) Heat flux transferred to mold in +x-direction

Similarly, the amount of heat flux transferred in the positive y and z-directions can be obtained

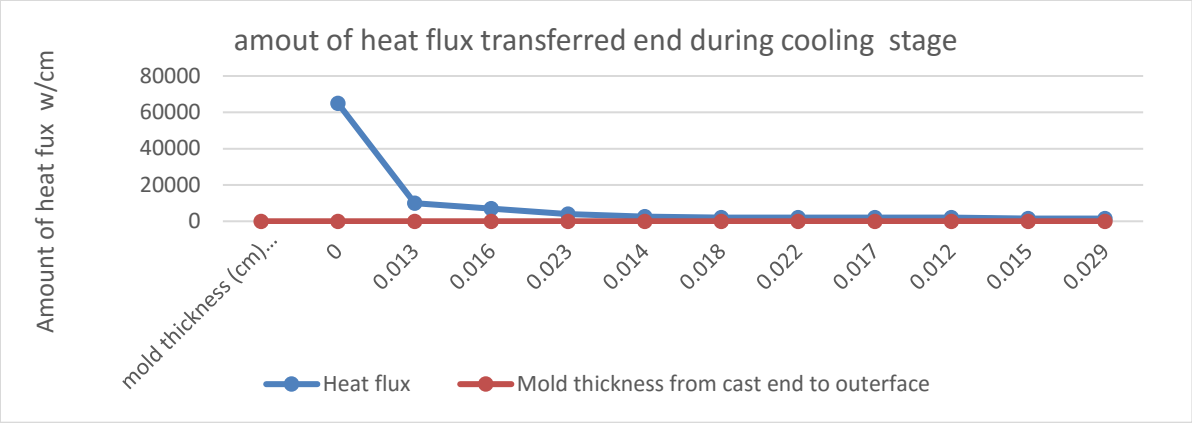

(b) Heat flux transferred to mold in +y-direction

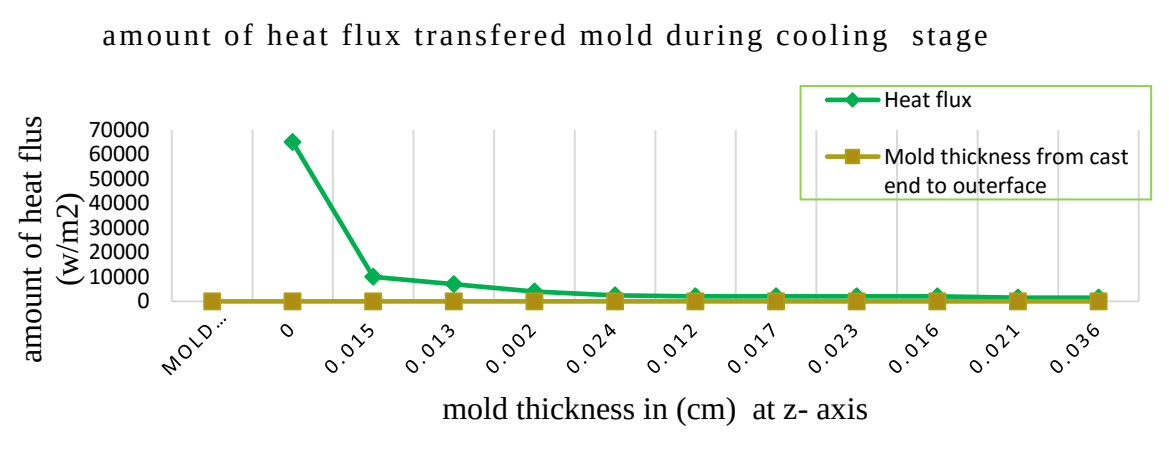

(c) Heat flux transferred to mold in +z-direction

Charts (a), (b) and (c) above graphs show that the amount of heat flux transferred through mould and environment during the freezing stage. Here, increase heat flux can be transferred from the metal cavity and absorbed by the mould through all the positive sides only. Charts of the above graph also show the amount of heat fluxes occurred beyond the mould thickness which predicted that heat flux can be transferred to the environment to the mould wall thickness with small magnitude. Table 5.8, results show that the amount of heat flux during the solidification period in the positive sides of the coordinate systems. This can be performed due conduction occurred in the given directions of the metal to mould interfaces during the solidification stage.

The amount of heat flux at the metal-mould interface in to the other mould wall directions can be estimated using Equation (4.27) and the total heat flux from the metal to mould interface at respective reference points can be taken as the sum of heat flux emitted from X, Y and Z directions

(-ve and +ve sides), i.e., qt (x=0), is equivalent to 670 KJ/m^2/s, and the minimum of qt (m, x, y, z = 0.24,0.029, 0.036) 9.37J/m^2 /s at the end surfaces of the mold. This was due to the heat was absorbed by the mould and transferred to the environment. In the table 5.9 result the value of temperature gradient by using Equation (4.26) in any direction (x, y, z). The temperature gradient in the mould at any distance from the casting end to +x, +y and +z –directions can be estimated discuss by the following graphs. The below graphs discusses the temperature gradient along the length of the mould of the three positive directions. In this case, the minimum temperature gradient magnitudes of the molten metal along the mould wall in the positive three directions and as shown in gradient reduction as the distance of the increased from the casting end. The value of temperature gradients distribution in table5.9 are plotted distance respective direction.

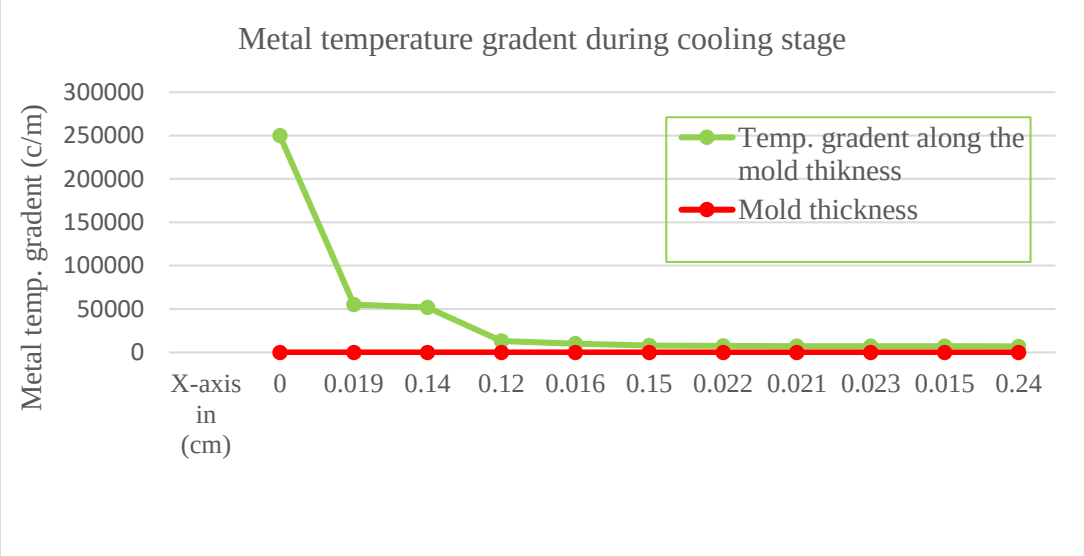

(a) Temperature gradient along the +X-direction

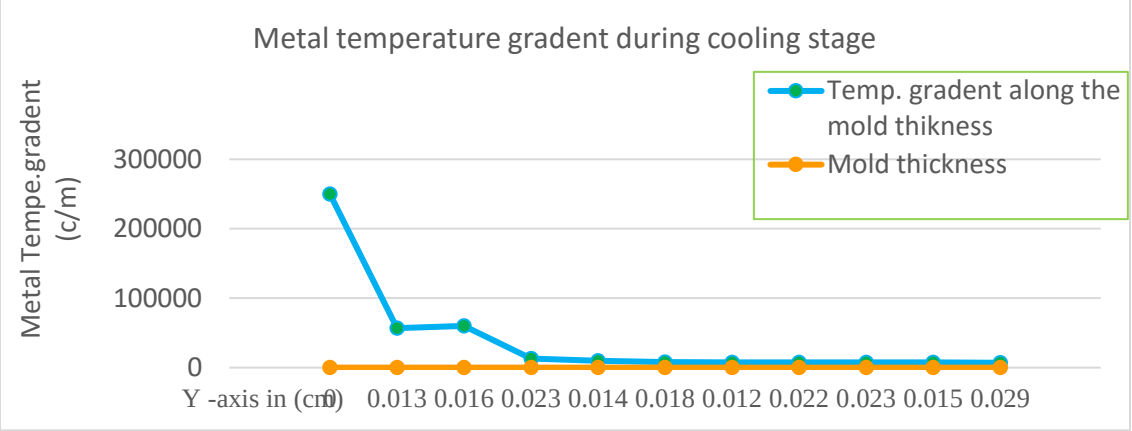

(b) Temperature gradient along the +Y-direction

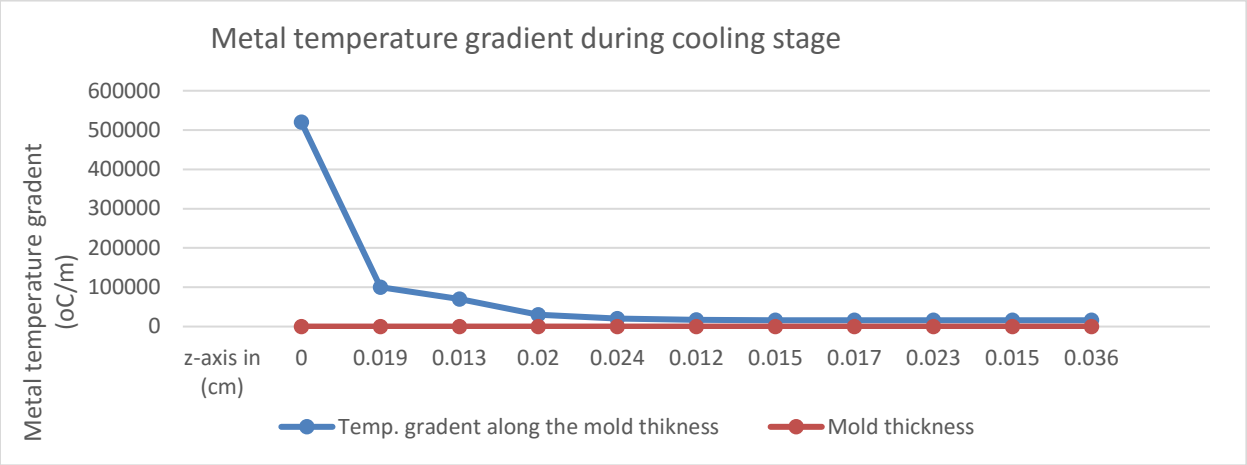

(c) Temperature gradient along the +Z-direction

(a), (b) and (c) of the graph above discuss the temperature gradients of the metal in the mould thickness during the cooling stage. Here, the amount of temperature gradient can be dynamically reduced up to 65mm of the mold thickness along all of the positive sides of mold used and this condition can be predicted that solidification of the metal may be fast around the mould cavity but almost smaller and uniformly distribute after 50 mm of the mold thickness to the outer faces.

A) Average heat transfer coefficient

The average heat transfer coefficient is simply defined as h= $\frac{q''}{\Delta T_{avg}}$, which is determined based upon the heat flux density applied to the body of the substrate and the temperature difference between the average surface wall temperature and the bulk liquid temperature ($\Delta T_{aveg} = T_w - T_l$). The average heat transfer coefficient variation for these three cases can be determined and the natures of output results are comparable with conventional results. The local heat transfer is not as accurate or detailed as the case for the Z- y- and x-direction. However, the resolution is sufficient to aid in the design of micro heat sinks for industrial applications and also to provide information and insight in to the fluid flow characteristics in the flow direction. Here we plot the average heat transfer coefficient variation along the channel length for different heat flux of magnitude 50W/cm^2, 90W/cm^2 and 150W/cm^2 in Figure (5.4).

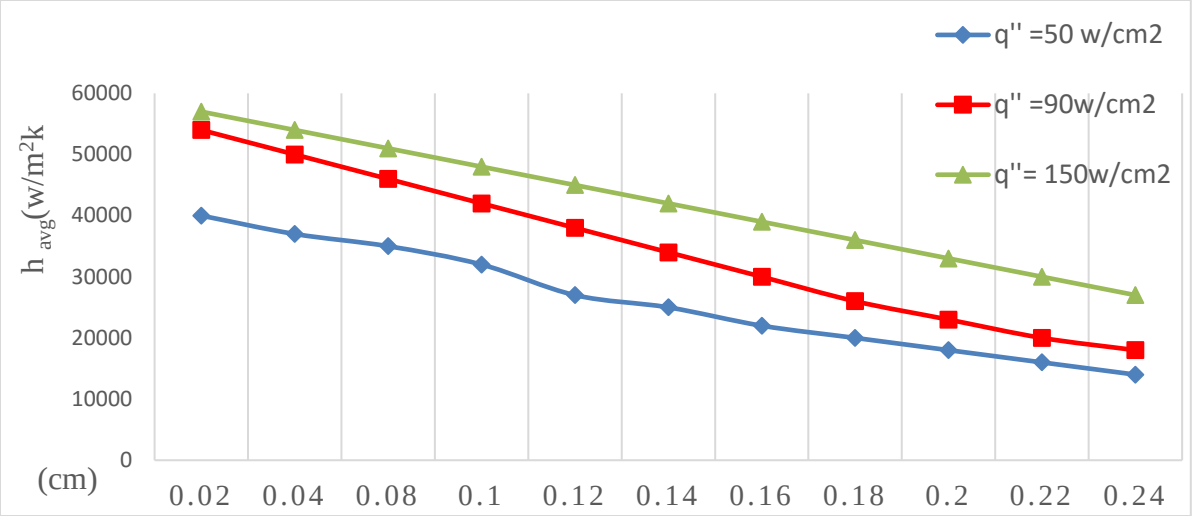

Figure 6.0.2Axial variation of average heat transfer coefficient for different heat fluxes

While the metal loses its sensible heat and the rate of heat transfer from the solidifying metal to the mould is high. During the formation of the gap between the solid skin and the mould wall, *h* decreases and it is continuing to decrease as the thickness of the solid increases.

6.6 Experimental Result

In this, the experiment riser/feeder, pour temperature and poring time/solidification period are used observed, quality stage of casting and Analyze the shrinkage defect reduce. There are several defects on casting product that identified, the defect is shrinkage defect. The metal is melted in the furnace used pour temperature; Metal temperature is measured from time to time. As observed from experimental the pouring temperature is important for the quality of castings product. The molten metal is poured into the pouring ladle at a higher temperature than the pouring temperature better. From this experimental, the parameter caused shrinkage defect/shrinkage porosity higher temperature, lack of riser/feeder size and solidification time (pouring time) and as well direction of solidification. This solution is optimal (maximum riser/feeder size) used pouring temperature and pouring solidification time as well change the position of feeder are used reducing defect (free casting product). And this happened when the thin section in a casting solidify sooner than thicker regions, so the molten metal flows into the thicker regions that have not yet solidified. The porous regions may develop at their centers because of contraction as the surfaces of the thicker region begin to solidify first. Shrinkage defect is detrimental to the ductility and strength of casting and its surface finish, potentially making the casting permeable. Shrinkage defect reduced these

parameters are control must be important: (i) poor design gating system/riser size (ii) too much-pouring temperature (ii) Non-uniform cooling rate. For the cavities defect occurred in the form of shrinkage defect. Due to surface area of the casting was remained molten the shrinkage reduced occurred. A minimize occurs as the material solidifies forming a shrinkage defect when there is no sufficient amount of molten metal to feed the shrinkage. The following figure show the surface of shrinkage defects.

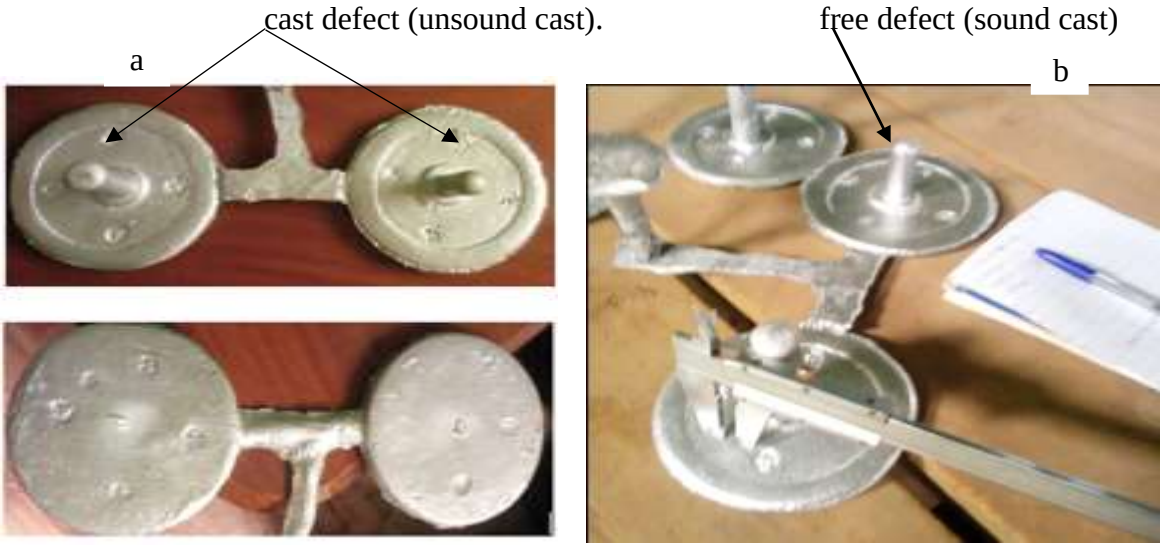

F*igure 6.3 casting show Shrinkage defect and without defect*

There are several ways to prevent the defect in the casting. For the above figure defect which is shrinkage defect, it can be prevented by melt the metal with a suitable temperature, uniform the cooling rate. It promotes directional solidification back to the molten riser/feeder. As this casting freezing/cool, there is still a molten path open that will feed the liquid and solidification shrinkage, which give a part with minimal shrinkage defects. Another method of reducing the shrinkage defects is adding a riser near using method optimum. Risers require additional metal for the casting process, removal and additional finishing.

And the temperature, too high pouring temperature one of reason cause of shrinkage defect. This increases pouring temperature with increase shrinkage defect, because the temperature melting metal very increasing the fluidity liquid melting metal increase (the pouring temperature optimized with decrease shrinkage defect and the pouring temperature used range 630-750^{o}c), according to

aluminium metal. At the optimized pouring temperature 680^{o}c the shrinkage defect-free surface (sound) casting.

The method of reducing the shrinkage defects is to adding a riser neck and the optimized pouring riser sized. The pouring riser used range 50-70cm. At the optimized size of riser (70) the shrinkage defect-free surface (sound) casting, because when a riser near and height adding shrinkage defect reducing from surface casting according to experimental observed. But at the riser size (50cm) the shrinkage defect shows on surface casting figure 6.3 (a). At the pouring temperature (optimized 680^{o}c) with adding a riser near size (70) is used the cast product is not shown shrinkage defect surface (agreement sound casting) as to refer figure 6.3(b).

At the pouring temperature (630^{o}c) and with riser size (60cm) used the shrinkage defect is shown on the surface area of casting produced, but small refer as figure (6.4). and at the pouring temperature increase (750^{o}c) with riser size (50cm) shrinkage defects show on surface casting (unsound) as refer figure (6.4).

Therefore, in this experimental study the pouring temperature, adding pouring riser size and pouring time very Signiant to shrinkage defect minimizing. However, the high pouring temperature and small size riser probability of cause shrinkage defects on the casting product and because high Pouring temperature influences fluidity, porosity, strength and structure of the casting.

Figure 6. 4 Directly on surface area show defect

Generally, the fluidity of molten metal depends upon its pouring temperature, inoculants, and alloying elements and also on the amount of superheat absorbed within it to enable to fill the required mould cavity. Pouring temperature is an important parameter in foundry for

manufacturing quality castings. Casting trials were carried out without optimum feeder, with optimum feeder and feeder with exothermic sleeve. It can be seen that casting without optimum feeder directly shows shrinkage defect at the center as shown in Figure.6.4, when the feeder of small (50mm) diameter was placed no surface defects were present but when the component was machined shrinkage porosity was found as shown in Figure.6.4. it is which was a sound casting with Al242 alloy, showed scattered small shrinkage porosities defect present throughout the riser/feeder and the region in the casting below the riser/feeder. note that this alloy also had a surface sink shrinkage at the top of the riser which is a common form of shrinkage defect. High pouring temperatures causes shrinkage defect and hence most be maintaining correct pouring temperature reduces such as shrinkage porosity defect and cold shut defect

The lower pouring temperature of molten metal causes premature solidification of the metal without reaching the entire volume. Fixing the proper pouring time helps increase flow rate and it reduce the shrinkage defect and cold shut defect. optimum pouring temperature, ingate design/riser size and solidification period leads to minimized shrinkage defect as shown in the Figure 6.5.

Figure 6.5 cast free shrinkage defect

Generally, this defect occurs due to lack of poor design gate, insufficient feeder feeding metal and solidification time is the maximum reason, as well Causes non-uniform solidification, Pouring temperature, incorrect venting, Extreme release of gas-poor gate again the maximum reason**.** Remedies**:** Location of riser should be proper, Proper position and using chills for better solidification, providing good venting and shrinkage defect minimized greater used optimal parameter.

6.7 Quantitative Distribution of shrinkage Porosity

Area percentage of the defect was measured in five longitudinal sections, each of 20mm length, in all test product. Thus, the values given here are the area of shrinkage porosity defects related to the area of the inspected 20mm length section, (20x 50, 20x55, 20x60 and 20x70 for the 50, 55, 60 and 70 mm diameter product, respectively). Area percentages of defects as functions of position along the longitudinal sections of the test product are shown in Figure 6.6.

Generally, the area of porosity defect tended to decrease with the increasing model of diameter. The highest porosity content was found in the small area (10 mm) diameter model whereas the maximum measured area of porosity was 10.8 % at a position of between 20 to 60 mm from the feeder. The maximum area of porosity in the 60 mm diameter model was 4% at a distance of 100 mm from the feeder. The minimum area of the (smallest area) 70mm of porosity with a maximum value of 1.8% at a position between 100 and 140 mm from the feeder where the thin section of the model (at about 120 mm from the feeder) had a cross section of approximately 50 mm diameter. The end effect can be described by heat was extracted from three surfaces instead of two. The cooling effect of the end surface, (the penetration of the end effect extended into the model surface), was in the region of 20 mm from the free end of the 15 mm diameter of the model, increased to about 40 mm in the 25 and 35 mm diameter of cast product part.

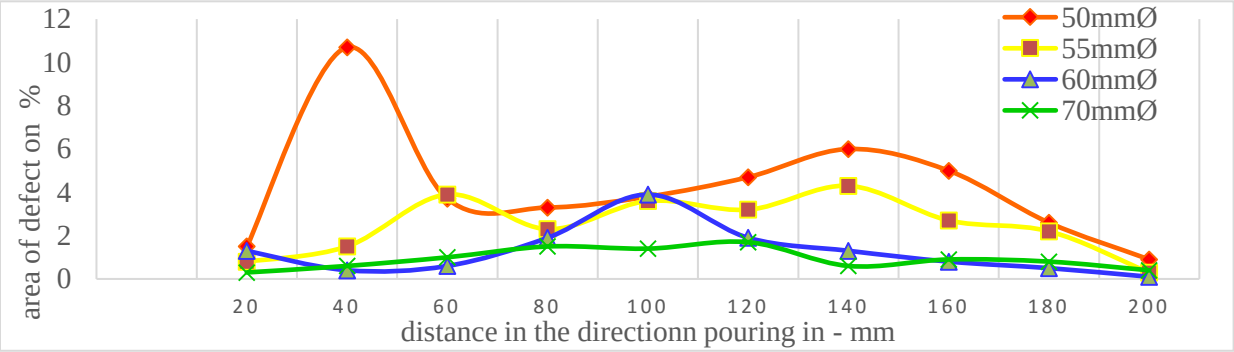

Figure 6.6 Comparison of area of defect in the longitudinal sections of the test products

6.8 Taguchi Method Analysis Results

In this process sand casting is performed according to selected L9 orthogonal array (OA) of Taguchi approach. Table 5.15 represents the experimental mean values of shrinkage casting defects which are visually inspected. Minimization rate is determined from the ratio of minimized metal due to casting defects of the amount of metal poured. As observed from the analysis in table

5.16 in column seven (average minimization) that the minimum value reduced for casting shrinkage defects is estimated 3.01 % which achieved at pouring temperature of 630^{o}c, with riser size diameter of 60 cm and pouring time 120 second. As demonstrated in the bar graph show in figure 6.7 each trial amount of average minimized in casting shrinkage defects determined.

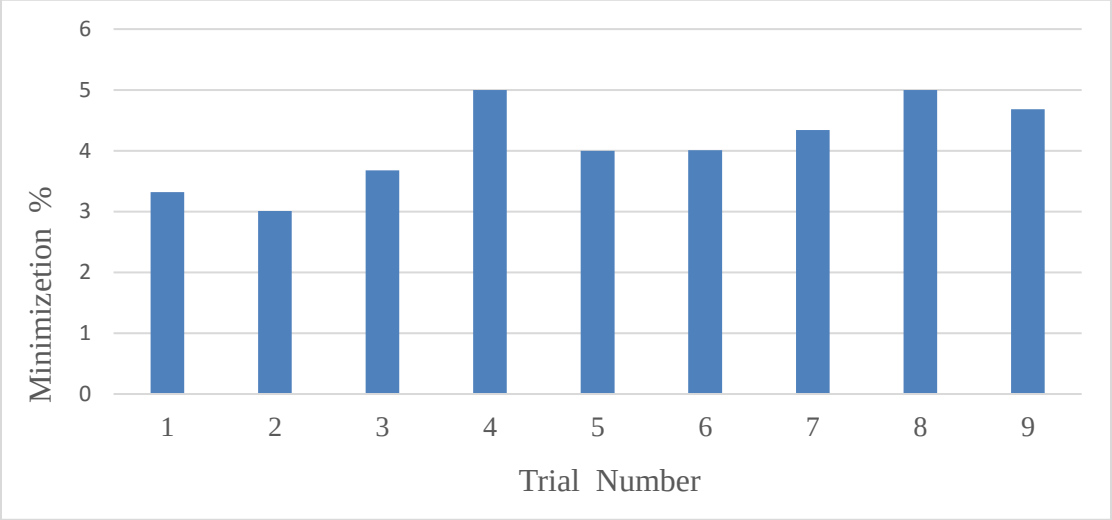

Figure 6.7 Percent of elimination for casting defects at each levels

6.8.1 Regression analysis result

The regression analysis is a numerical means for the examination of interaction between various parameters. In this study, the optimal elimination rate for casting defect is obtained by means of regression analysis using MINITAB 18. The feature of the regression equation is formed by providing input and output parameters in the Taguchi L9 orthogonal array (OA).

This helps to determine the cause result of one variable upon another. The equation is formed based on the value of three factors and two interactions. In this study, the regression equations of elimination rate for casting defects are obtained by the input parameters such as pouring temperature (^{o}c), pouring riser size (cm) and pouring time (min.). The regression equation for elimination rate optimum is shown below.

$$\text{Average cast defect } (\Delta X)\% = 4.116 - 0.779\,x_1 + 0.221x_2 + 0.558x_3 + 0.104\,y_1 - 0.112\,y_2 + 0.008\,y_3 - 0.006\,z_1 + 0.114\,z_2 - 0.109\,z_3 \quad \text{----------eqn.}$$

Where, x_1= pouring temperature @ the level 1, x_2 = pouring temperature @ the level 2, x_3 = pouring temperature @ the level 3, y_1= Pouring riser @ the level 1, y_2 = pouring riser @the level 2, y_3 =

pouring riser @ the level 3 and z_1= pouring time @ the level 1, z_2 = pouring time@ the level 2, z_3 = pouring time @ the level 3.

The above represents the experimental values predicted (from regression equation) and residuals of casting defects for in nine trials.

Table 6.1 Residuals of average elimination rate for casting defects in various trials.

T/N	Experimental values of elimination rate for casting defects in pouring metal (%)	Optimum values of elimination rate for casting defects in pouring (%)	Residuals
1	3.500	3.32	0.77
2	3.075	3.01	0.983
3	3.97	3.68	0.286
4	5.3	5.00	0.07
5	4.06	4.00	0.056
6	4.3	4.01	0.286
7	4.44	4.34	0.11
8	5.2	5.00	0.196
9	4.72	4.68	0.04

The table above represents the experimental values of elimination rate and using optimum values of elimination rate for casting defects in metal casting pouring residuals of casting defects. The regression results are a numerical means for the examination of the interaction between various experimental value and optimum value comparing. The optimal elimination rate for shrinkage defect is obtained by means of regression analysis using MINITAB 18 and depend on the regression equation is formed by providing input and output parameters in the Taguchi L9 orthogonal array. This regression equation is formed based on the value of select factors.

This below graphs is indicating Experimental values of elimination rate for shrinkage defects in pouring metal proposed casting and Optimum values of elimination rate for shrinkage defects in pouring casting proposed.

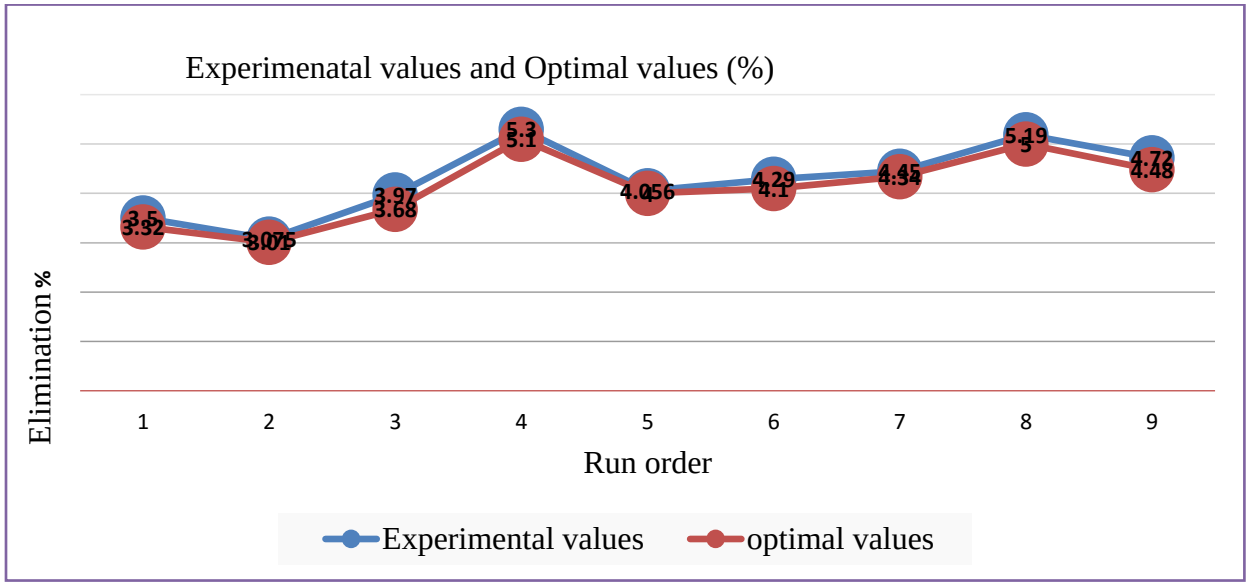

Figure 6.8 Indicate experimental value and optimum value of result

The above graphs represent compare optimal value and Experimental values of average elimination rate for casting defects in nine trials casting. The corresponding value of input factors are considered for calculating the minimum casting defects of work piece by using regression equation. The reducing rate for casting defect is 3.01% obtained from above regression equation, corresponding values for each factor pouring temperature (^{o}c), pouring riser size(cm) and pouring time (sec) are 630^{o}c,60cm and 120min. respectively. The values are substituted in the provided equation. Experimental values and optimum values (from regression equation) of rejection rate for casting defects for means are also clearly described as shown figure 6.7.

From the above graphs, orange color shows optimum value and blue color illustrates experimental value. The minimum value for experimental is 3.01% and its maximum value is 5% and also for optimum value case 3.65% and 5.97% is minimum value and maximum value respectively. Generally, by comparing these two graphs, experimental value is global minimum value and optimum value is global maximum. The value of above graph calculate case of optimum value used regression equation and experimental value from the experimental input (pouring temperature, pouring riser size and pouring time) software.

6.8.2Analysis of Signal-to-Noise (SN) ratio result

The casting defects that occur in each trial conditions were found and recorded. The average of the casting defects was determined for each trial condition as shown in table 6.2. The casting defects

are the "small- the better" type of quality characteristics. Lower the better S/N ratios were computed for each of the nine trials and the values are given in table 5.16 Casting defects was selected as a quality characteristic to be measured. The smaller the better number of casting defect implies better process performance using equation 5.18 determine SN ratio. Maximizing η' leads to minimization of quality loss due to defects. Where *S/N* ratio is used for measuring sensitivity to noise factors, *n* is the number of experiments OA, and *yi* the *ith* value measured. Table 6.2 below discuses about the mean and standard deviation of each experiment calculated using Equations of (5.17) and (5.18) respectively

Table 6.2 *SN ratio results of each experiment conducted for factors and levels*

Worksheet 1 ***

→	C1	C2	C3	C4	C5
	Pouring Temp. (oC	Pour Riser Size (cm	Pouring Time(sec.	Minimized per Area Cast defect%	SN Ratio
1	630	50	90	3.32	-10.4228
2	630	60	120	3.01	-9.5713
3	630	70	150	3.68	-11.3170
4	680	50	120	5.00	-13.9794
5	680	60	150	4.00	-12.0412
6	680	70	90	4.01	-12.0629
7	750	50	150	4.34	-12.7498
8	750	60	90	5.00	-13.9794
9	750	70	120	4.68	-13.4049

Table 6.2 discussed SN ratio value distribution of each experiment conducted and varied from minimum of -9.5713 (#2th) to maximum of -13.9794(#4th). The average SN value of each factor and level was calculated from the SN ratio of each experiment discussed in above table using the eqn 5.19. The range of each factor was determined in which the larger the change (**Δ)** value for a factor, the larger the affect the parameter has on the cast product variation. Then, rank of each factor was determined using Minitab software as shown in table 6.2.

Table 6.3 Means of reject rate for produce part defects at various levels of input parameters

Level	Means of elimination rate for shrinkage casting defects		
	A(Pouring temperature)	B(Pouring riser size)	C(Pouring time)
1	3.337*	4.322*	4.110
2	4,337	4.003*	4.230*
3	4.673*	4.123	4.007*

Delta /max-min./	1.337	0.319	0.223
Rank	1	2	3

Table 6.4 S/N ratios of reject rate for cast product at various levels of input parameters

Level	S/N ratios of elimination rate for shrinkage casting defects		
	Pouring temperature	Pouring riser size	Pouring time
1	-10.44*	-12.38*	-12.16
2	-12.69	-11.86*	-12.32*
3	-13.38*	-12.26	-12.04*
Delta (max-min)	2.94	0.52	0.28
Rank	1	2	3

Table 6.3 and 6.4 above indicated range, optimum levels (*) and rank of the selected variables which take part in flywheel casting processes based on the response values. Hence, as per the results of the experiments conducted the optimum settings of pouring temperature, riser size and pouring time were at A1, B2 and C3 respectively.

6.8.3 Main effect plot results

The main effect plot is an outcome of the optimization that gives the uniform difference between the different levels of a factor. When there is a consistent trend among the different levels of a factor then the situation is same as these outputs. The effect of each selected variable was identified using Minitab from the overall mean value and SN ratio. The effects of levels are shown in Figures 6.9 and 6.10 below respectively to pouring temperature, riser size and pouring time. The below figure Main effects plot for pouring temperature, pouring riser size and pouring time at the means values on casting produce part length.

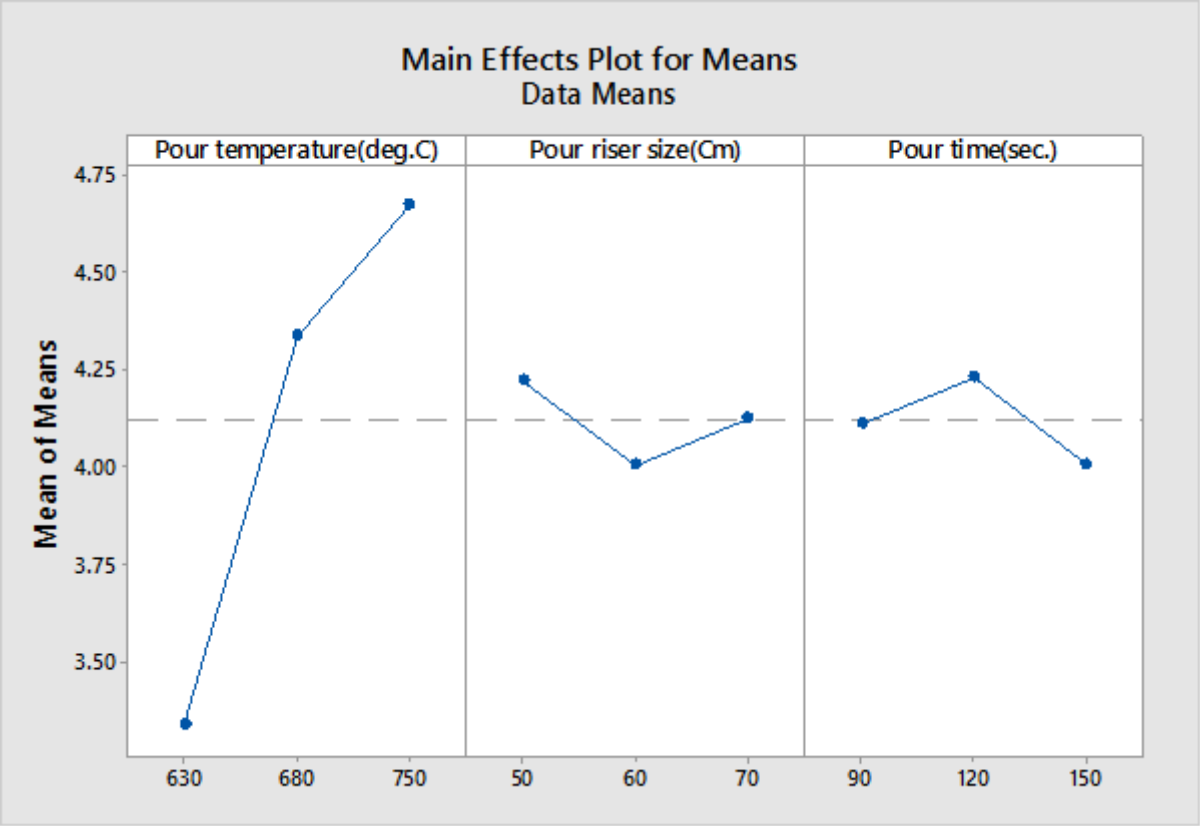

Figure 6.9 Main Effects Plot for Means for different factors and for each level

The main effect plot results in figures 6.9 discussed that effect of the selected factors' levels from the overall Main effect plots for mean values and Main effects plot for SN ratios of the experiment conducted in the flywheel castings producing. As per the design used the overall mean and SN ratios of the placed at a line of 4.125 and -12.1753 respectively, in the horizontal direction. Hence, pouring temperature deviated from 4.694 above the mean line to 1.968 below the mean, pouring time deviated from 4.169 above mean line to 4.120 below mean line and riser size deviated from 4.198 above the mean line to 4.122 below the mean line.

As per the experiment conducted, results shown as length variations occurred from below to above of the clients' specification limits of the flywheel produced and these can be minimized the quality and considered as castings shrinkage porosity defects. Therefore, based on the experiment level used for the given metal weight of part producing (flywheel) the optimum level of the selected parameters namely pouring temperature, riser size and pouring time A1, B2 and C3 corresponding to values 750 ^{o}C, 70cm and 120min. as shown in table 6.2 (level) and Figures 6.9 and 6.10 (values).

Hence, the part casting (flywheel) produced using these settings are with a minimized shrinkage defects and taken as sound casting.

In the figure 6.11 below, a quality, analysis that wants to improve the performance of its products has created a line plot that finds a strong interaction between pouring temperature, pouring riser size and pouring time (solidification time) at which it is applied. The main effects plot by plotting the means for each value of a categorical parameter variable and a line connects the points for each parameter.

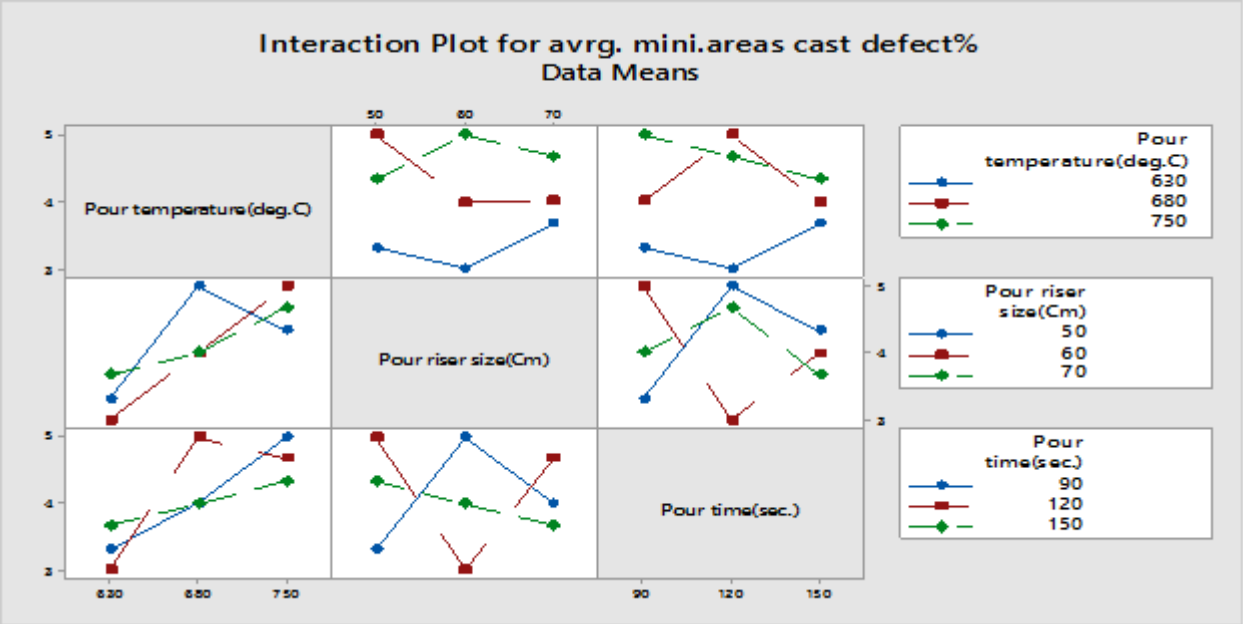

Figure 6.10 Interaction plots of main effects

The blue and red line discuss mean response increase factor change of defect low to high length and green line discuss when factor of parameters at its high level, means response decrease (change) high to low length. It is found that in the presence of noise, the interaction between the different factors increases and becomes stronger and more significant and it appears clearly between pouring temperature and solidification time. blue line when factor low level the mean responses increase. Red and green line change in means response factor of low to high interaction effect high(increase).

6.8.4 ANOVA analysis results

Analysis of variance (ANOVA) is a statistical decision making tool used to test the adequacy of model for the response in experiments.

The input factor that has much affected on output factor is identified. The analysis of variance for response quadratic model is summarized in table 6.5 about the DOF of the total sum of squares (number of observations), the DOF of each factor (the number of levels minus one) and the DOF of the error (DOF of the total sum of squares minus sum of the DOF of the three factors) in the process experiment performed. It indicates also the SST, MS MSE, F- ratio, P and Percentage contribution results of each factor selected in the experiment of the part product selected casting. In this table 6.5 ANOVA analysis the average rejection rate for casting defects with percentage contribution of each parameter.

Table 6.5 ANOV process variables

Variation source	Degree of freedom	Sum of squares (SS)	Mean of squares (MS)	F-ratio	p-ratio	Percent contribution (%)
model	6	23.450	2.82	54.66	0.0004	-
Pour temp.	2	3.95002	1.45001	3.03	0.248	35.57
Pour riser size	2	2.78018	0.03534	0.07	0.931	24.93
Pour time	2	o.7849	0.03798	0.08	0.927	7.14
Pour temp.* Pour riser size	2	1.07802	0.47858	0.95	1.31	9.7
Pour temp. *Pour time	2	1.5704	0.2709	2.008	3.074	14.06
Error	1	0.957904	-	-	-	8.6
Total	17	11.1214				100

ANOVA results in Table 6.5 indicated that contribution of each factor on the response variable, DOF of each factor, error and the total (overall) system. According to the experimental method used from the selected factors pouring temperature contribution was larger and has the larger ability to influence (SN) signal- to-noise ratio. From the percentage contribution results of each factor on the response (measured) values, factors can be ranked from largest to smallest and predicted their respective effect.

According to this method, pouring temperature can have made the larger contribution (effect) of length variation of the produce part that counted by 35.57% corresponding to the total sum of squares and it has the larger ability to influence signal- to-noise response (SN). Then pouring riser

size was the next largest contribution by 24.93% to the total sum of squares and pouring time contributed for length variation by 7.14% contribution.

The Model F-value of 54.66 implies that the model is significant. There is only 0.04% chance that a "Model F-Value" this large could be affected due to noise in the experiments.

The model F-value 54.66 indicates that the model adequately represents the process. The p-values less than 0.05 indicate that the model terms are significant and the values greater than 0.10 indicate the model terms are not significant. The parameters pouring temperature and pouring time has the *p*-values less than 0.05 which indicates the pouring temperature and pouring time are the major contributing factors of defects in castings.

The significance of control factors in **A**NOVA is determine by comparing the F-values each control factors. The last column of the table 6.5 shows the percentage value of each parameters Contribution which indicates the degree of influence on the process performance.

Therefore, the optimum setting (condition) of the above factors can be set at A1 B2 C3. Hence, the optimum value of SN ratio under this optimum condition could 57.7 (using Regression equation) and so that the produced part casting (flywheel) using these settings are good quality and sound castings. The following bar graphs show the process parameters in value of Percentage contribution the effect of casting defects

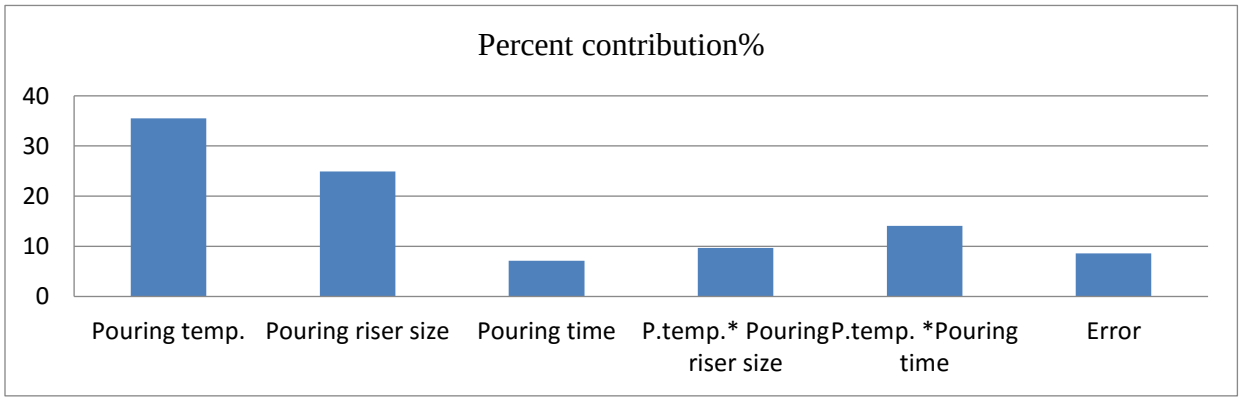

Figure 6.11 Percentage of contribution process parameter eliminate for casting defects

6.8.5 Optimum Level of Process Parameters

The optimum combination of process parameters for minimum volumetric shrinkage is shown below. From detailed study the three factors which can control almost all the defects was found. These factors were called control variables as it controls the output results. The three control variables selected for obtaining were optimum output.

Table 6.6 Optimum values of the selection process parameters

Parameters selection	Process parameters	Optimum value
Pour temperature(^{o}c)	Pouring temperature	750
Pour riser size (cm)	Pouring riser size	50
Pour time (sec.)	Pouring time	120

6.8.6 Confirmation experiment

The confirmation experiment was conducted with two replications based on the optimized settings and it was observed that casting defects are eliminated/minimized. Also it was observed that pouring temperature and pouring time significantly affect the casting quality. Pouring time/solidification period recommended is between (15-20 min). Slow pouring reduces the flow rate of molten metal and hence the metal is incompletely filled in thin sections and remote areas. Fast pouring increases the flow rate of molten metal and causes problems like sand erosion, blow holes, etc. From the conducted experiments, out of nine model of part produced castings tested there is only one casting unsound and the percentage of effect (rejection) on part produced is 11.1% and it may be concluded that casting defect are reduced from (sound casting) 88.9% to 11.1%. The 11.1% before analysis (optimum) parameter of causes casting defect and 88.9% after the analysis (minimized) of parameters the casting defect.

Pouring temperature of molten metal is recommended to be between 630°C to 750°C. If the pouring temperature of metal is below the recommended range, it will reduce the fluidity causing cold shut defect. If the temperature is below the recommended range, it causes cold shut defect as the fluidity is reduced Pouring time recommended is between 90 min. and 150 min. Recommended pouring riser size of used in produce flywheel is between 50 to 70 cm and poor design. If the pouring riser size of used is less than the recommended size, it likely to cause result is shrinkage defect and cold shut defect. Slow pouring reduces the flow rate of molten metal and hence the metal is incompletely filled in thin sections and remote areas.

6.8.7 Optimum control parameters of free casting produce

As per the experiment design of method help the optimum setting of the riser size was 70 cm^2 found at the third (3) level. As a result, the optimum sizes of the other gating system elements can be determined from the optimum riser size using the provided gating ratio for aluminum casting Equation (5.4) and given in table 6.7, Optimum sizes of gating system used in produce part.

Table 6.7 Optimum values of process parameters

	Element of gating system			
	Sprue	Runner	Riser neck	Ingate
Area/size cm^2	42.8	63	70	58

Optimum gating system dimensions, weight and volume of metal that can be accumulated in each cavity can be determined using Equation (5.5) and given in table 6.7.

Table 6.8 Optimum gating system dimensions of produce part casting

Gating element	Dimension (in cm)					Volume in	Weight(kg)
	Entrance dia	Exit-dia	Length	Depth	Width	m^3	
Sprue	11.9	10	30	x	x	0.1107	2.98
Sprue base	10.5	7	x	6	x	0.00084	2.3
Runner	x	x	16	4.5	12.9	0.0003132	0.845
Riser base	20	20	x	8	x	0.00161	4.35
ingate	x	X	5	4	13	0.00319	0.86
Riser	25.3	22	37.96	x	x	0.000386	1.042

6.9 Defect Analysis Simulation Model Result

6.9.1 Modelling pattern with allowances for casting

Modelling can be done with the help of any available solidwork software and can be inserted in FEM based software using geometry transformation. Model can also be generated using FEM based software. In FEM based software (ANSYS®) and ProCAST. Modelling consists of defining two parts one is sand mould and other is the castings with proportional dimensions.

The following model pattern design for casting as show front, top and side views.

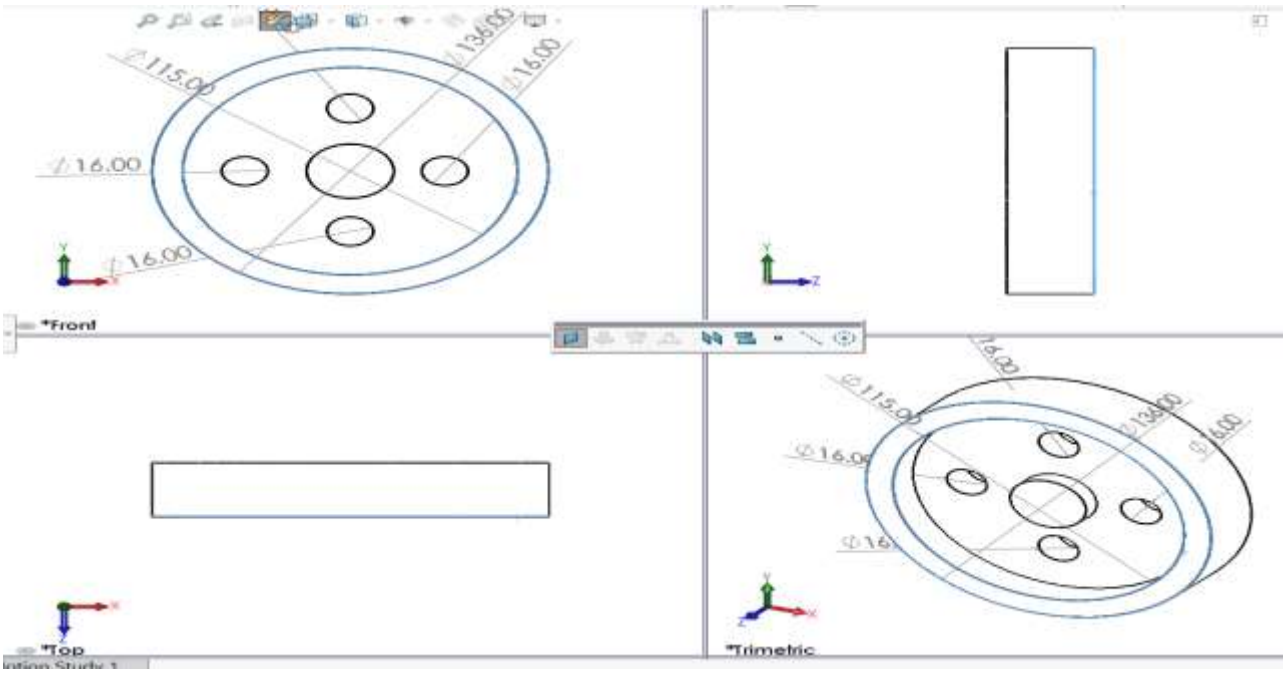

Figure 6.12 wooden pattern with allowances for casting view

This is initial model analysis design solid work software proposed gating and feeding design of part produce. This figures shown as the gating and riser components of the test casting proposed modeling.

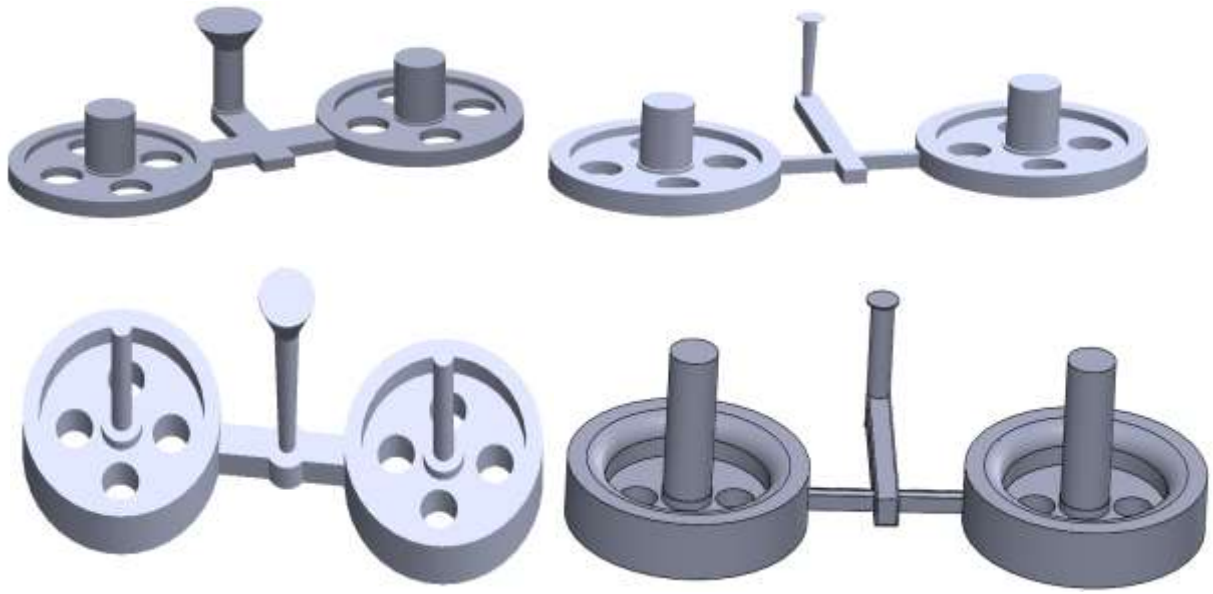

Figure 6.13 wooden pattern with allowances for casting

6.9.2 Meshing with mesh cast

The work steps which you follow when using Mesh CAST depend upon the following: the nature of your model, the intended use of the meshes generated by Mesh CAST and the type and quality of solidwork model you use as the initial input. The model part was meshed using defined small element size that it can be give the more accurate simulation results as compared to experimental done. The parting line is created using the volumetric mesh elements. Parting direction is selected as horizontal.

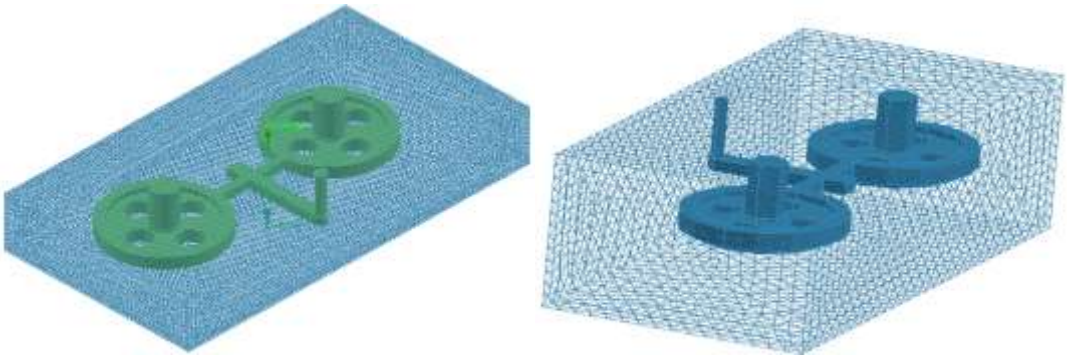

Figure 6.14 Meshing in Mesh CAST

The following box flask where in carrying fluid casting pattern shape and discus inlet mould liquid metal and velocity of filling and the analysis casting shape mould. From this study the maximum temperature at the center of the part so that the maximum chances of shrinkage defect occur at that region. Figure 6.17 indicates the mould for using metal casting shape into analysis that, figure 6.17 (a) proposed for ProCAST software simulation and figure (b) proposed for experimental used to analysis cast shape.

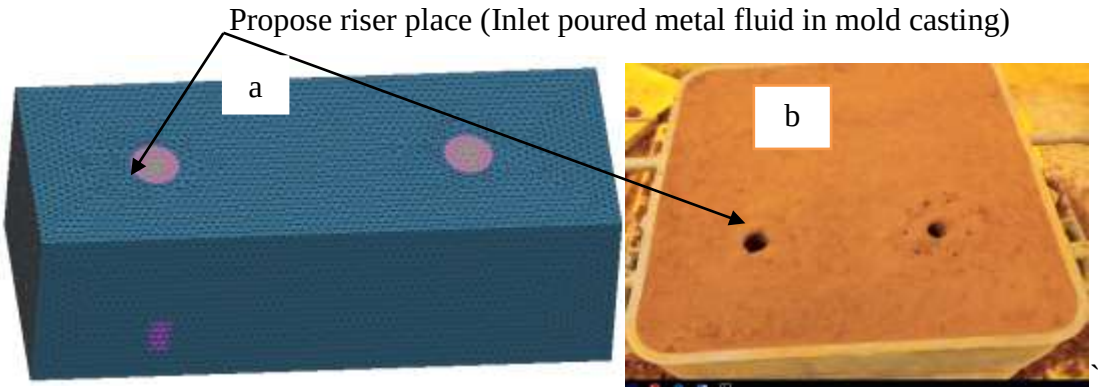

Figure 6.15 Proposed mould experimental and simulation a) mould for software, b) mould for Experiment

The mold cavity order to software simulation with metal cast shape. The mold cavity consists of two parts, cope -the upper part and drag- the lower part show as figure 6.18 and this figure indicates pouring melting metal to inlet that to analysis the casting shape into the mould box. Boundary Condition is applied now and half symmetry Constraint is also selected because it takes lees time for simulation for half of the object then the full itself; apply inlet fluidity to Pouring Cup.

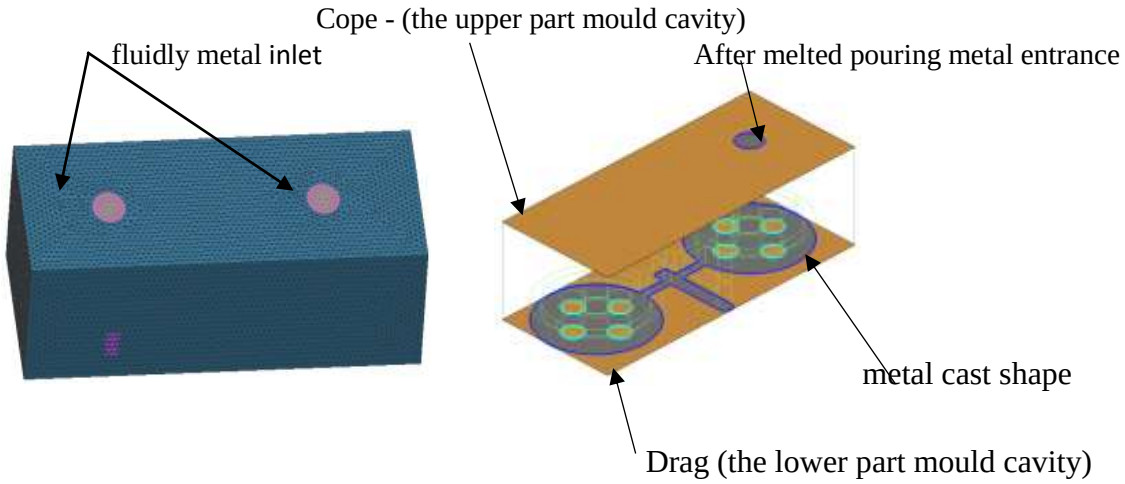

Figure 6.16 Liquid mould of pouring metal analysis and with velocity constraint window

The velocity required to fill in the cast in a minute is applied on the Temperature range of 750 °C. The metal filling in mould cavity, that ensure the smooth flow of Liquid metal and the cold metal is not entering in the mould cavity shown as figure 6.18.

The pouring temperature for aluminium is 630°C to 750°C. The estimated pouring time for complete filling of the mould cavity is 60 seconds. From the iteration 1&2, we can easily predict that the cavity is filling smoothly, uniformly without any turbulence. In any of the iteration, there is no defect associated with fluid flow, in casting component and gating system. Fill time reference is set in the following step and discus area of fluty in the mould. Casting quality largely depends on the filling of the mould, design of gating system and solidification of the liquid metal. In this study, we employed the any Casting software package to determine the order in which the liquid metal fills the mold cavities and solidifies.

(a)

(b)

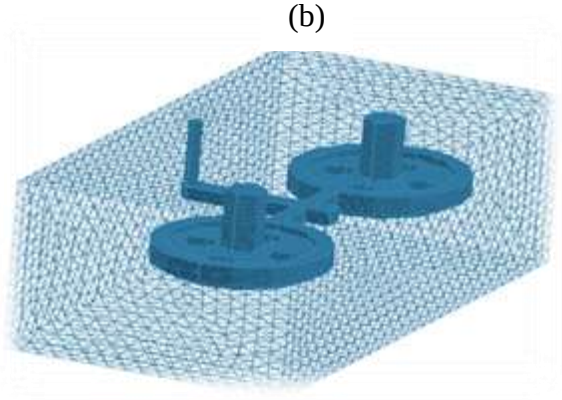

Figure 6.19 (a) shown the initial modelling and proposing a new design gating system for minimizing shrinkage defect. We also sought to characterize air entrapment, shrinkage defect and turbulent flow conditions. Severe defects in the center of the keys indicated the need for improvements in the design model. As shown in Figure. 6.19(a), we adopted a single vertical sprue in the revised scheme, while retaining the process parameters used in the initial model. In this, the function of the gating system and with elements are control shrinkage defect from main part product casting. Figure 6.19 (b) indicates the experiment processes were simulated by a finite element method software ProCAST. The number of tetrahedral meshes was about 460,000. The tetrahedral mesh element simulation has good quality mesh and save time (mesh in short time).

Figure 6.19(c) shows severe shrinkage defect location of in the center of keys part produce using the initial scheme. The speculate that the shrinkage pores are associated with physical hot spots at the ingate of keys, which formed during pouring. The simulation show the material product is affect by shrinkage porosity defect. This is reasons lack of poor solidification, velocity of fluid and poor gating system design. An increase in the likelihood of shrinkage defects in the top key can be

attributed to the fact that the riser neck is too small diameter. Figure 6.19(c)(d) as show as predict location defect.

(c) (d) (e)

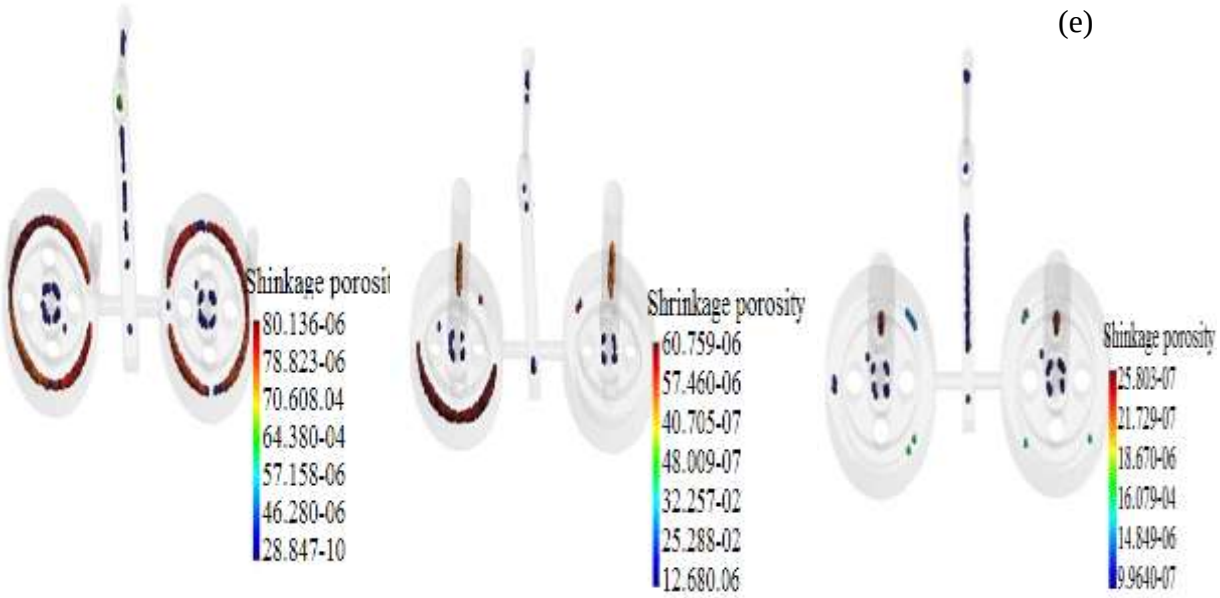

Figure 6.19(d) shows that the solidification sequence resulted in a short pour from the ingates, which resulted in the formation of shrinkage defect. The surface key in the center was the least susceptible to defects because the riser and runner helped to maintain it at a higher temperature while providing sufficient feed. Defect formation is associated with cause of flow velocity; i.e., higher velocity causes shrinkage porosity and turbulent flow in the mold cavities, which in turn creates defects is using gating system. Thus, reducing pour velocity should decrease the probability of defect formation. the velocity fluid high figure 6.19 (c)& (d) as show 80.14 and 60.8cm/sec. During pouring, the liquid metal first filled the cavities below the ingates before flowing to the sides as shown in Figure 6.19 (e). This greatly hindered the filling process and thereby decrease the probable of shrinkage defects. According this simulation presented the fluid velocity and condition of solidifications decrease with detect minimized. The revised scheme clearly reduced the pour velocity, which resulted in the formation of fewer defects. intense defects in the center of the keys indicated the need for improvements parameters in the design models, pour temperature and pour solidification time. The revised scheme helped to maintain the melt modulus, which in forward significantly reduced the likelihood of forming shrinkage defect (Figure 6.19(f) and nearly eliminated the formation of shrinkage cavities. By using optimum simulation of parameter helped minimized defects. The figure 6.19 (f)-(g) as show minimized casting simulation defect/ full sound

casting. nearly eliminated the formation of shrinkage defect used optimum parameters cause defects.

Thus, liquid metal flowing into the runner ran back and forth continuously between the bottom runner and the ingate, resulting in turbulent flow. Increasing the length of the bottom runner or moving up the wax piece on the right side should reduce the probability of shrinkage pores forming at the bottom. From this molten metal volume increase during solidification due to the atoms drawing nearer and coming to fixed lattice positions resulting in decrease shrinkage defect. It is

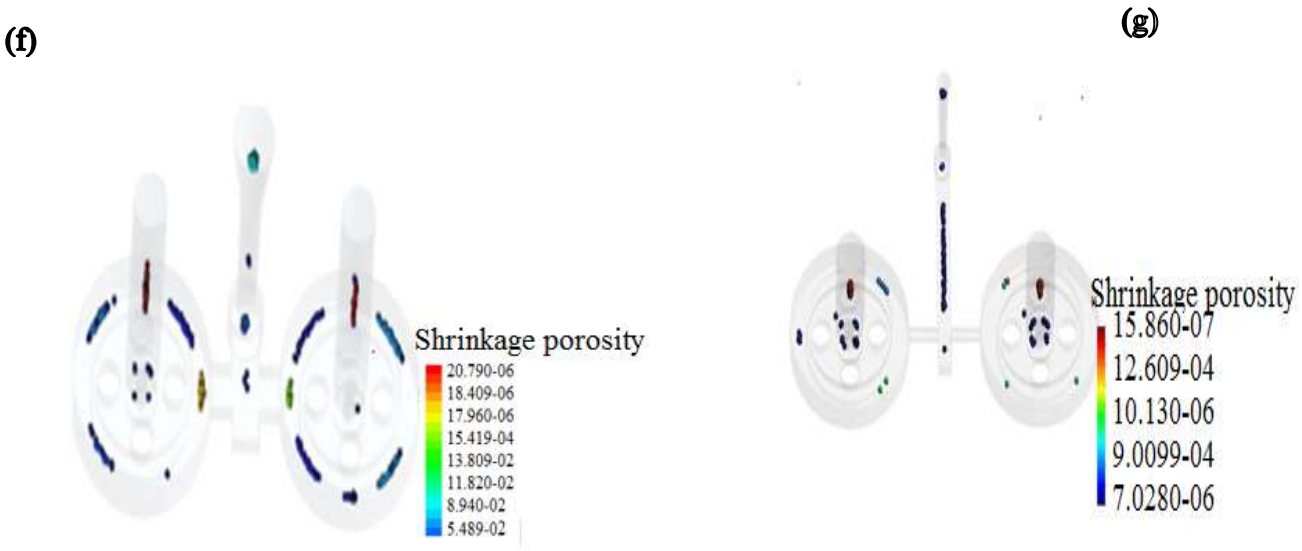

Figure 6.17 (a-g) Shrinkage defect predicted and reducing analysis simulation

observed that produced castings are sound and have no defects (Figure 6.19(d)(f)(g)). Shrinkage defects are predicted to form in the region where the ratio is smaller than a critical value. In principle, it predicts that shrinkage decreases with optimum solidification time and using pouring temperature.

9.3 ANSYS Simulation Analysis Model

The heat transfer during casting was studied first by available literature and then by successfully implementing simulation in ANSYS software. The main aim of the analysis is to get the condition of solidification and temperature distribution with respect to time. Element, PLANE 55 is chosen in ANSYS® which has the capability of transient heat transfer analysis. The element has four nodes with a single degree of freedom, temperature, at each node. It has generated the element of in nodes and out of which 1263 numbers of nodes belong to casting region generated.

Figure 6.20 indicates the meshed model of the flywheel which was done using the meshing operation. The model part was meshed using defined small element size that it can be given the more accurate simulation results as compared to experimental done. So, transient thermal simulation results related to the nature of the meshed surface of the part produce (flywheel) used.

Simulation results shown in Figure 6.21 indicated that temperature variation of the modeled flywheel during solidification in case of transient-thermal modes of heat transfer analysis carried out using ANSYS 17.0 software. The solidification process and temperature field of the original model casting process are shown in figure 6.21 Red indicates the highest temperature of surface defect and impact areas of shrinkage defect. Purple indicates the solidus temperature of 750^{o}c.this temperature and solidification predictable by ANSYS software using.

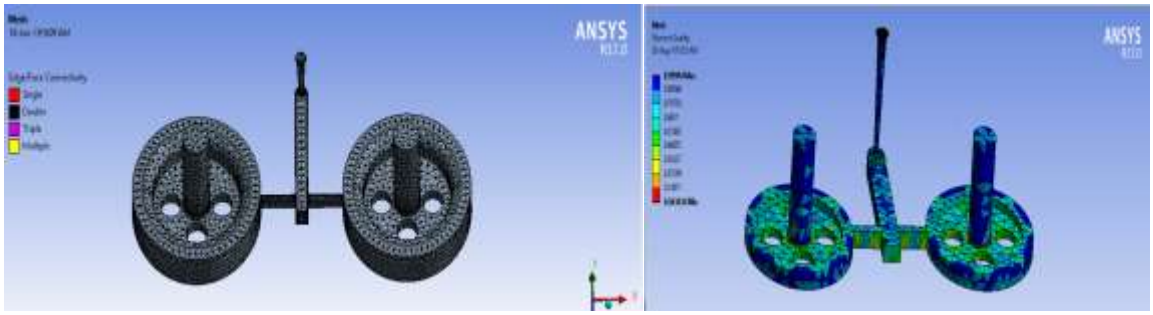

Figure 6.18 Element quality mesh in mesh size

Casting solidification was mesh and simulated to view the progress of cooling from casting surface to interior, and to predict the location of shrinkage defects such as porosity and cracks. This helps in verifying and optimizing the design of feeders'/gating system so that the desired quality and high yield are achieved product casting part.

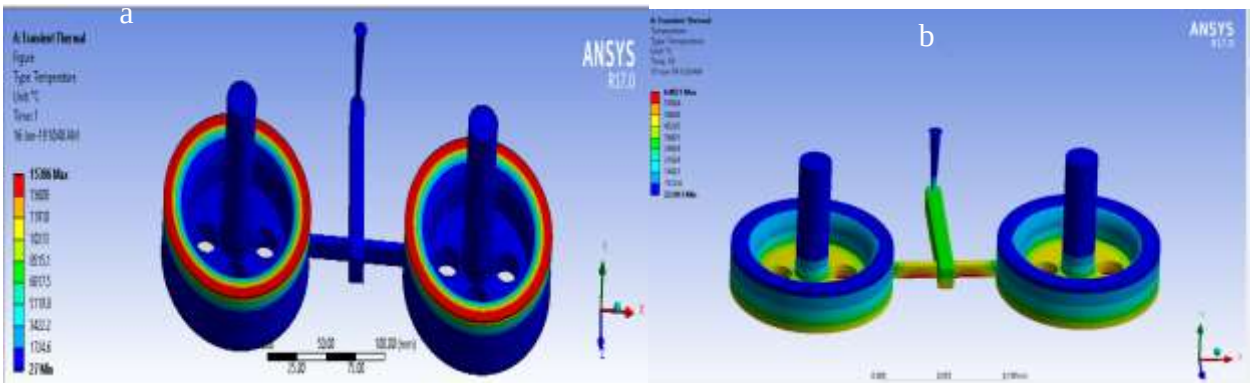

Figure 6.19 Solidification process and temperature analysis

Figure 6.21(a) red on the top indictor discuss shrinkage defect surface due to caused short freezing/cooling period. Shrinkage defect is quantitatively predictable by ANSYS built-in "shrinkage porosity criterion" function. The criterion function automatically calculates the degree of solidification shrinkage and feeding for each of the control parameters. The shrinkage porosity appears at feeders, runners, the bottom of discharge round and the parts. Pouring temperature is between (630-750℃), and pouring time is between (60 to150s). The solidification process and temperature field before optimum as shown in figure 6.20 (a) & (b) before optimum the part produce casting is the chilled in the solidification process.

The figure 5.21(a) shrinkage defect indicator before optimum show on surface casting product. Pouring temperature is 680℃, and filling time is 10s. The solidification process and after the parameters optimum defect not show on surface casting produce as shown in figure 6.21(b). The size of the time step, controlled by various stability criteria associated with fluid flow, may also be small compared to the total solidification time of the casting as show figure 6.22 (a). It is discussing cooling curves at varying aluminium cast and for the solidification of aluminium alloy.

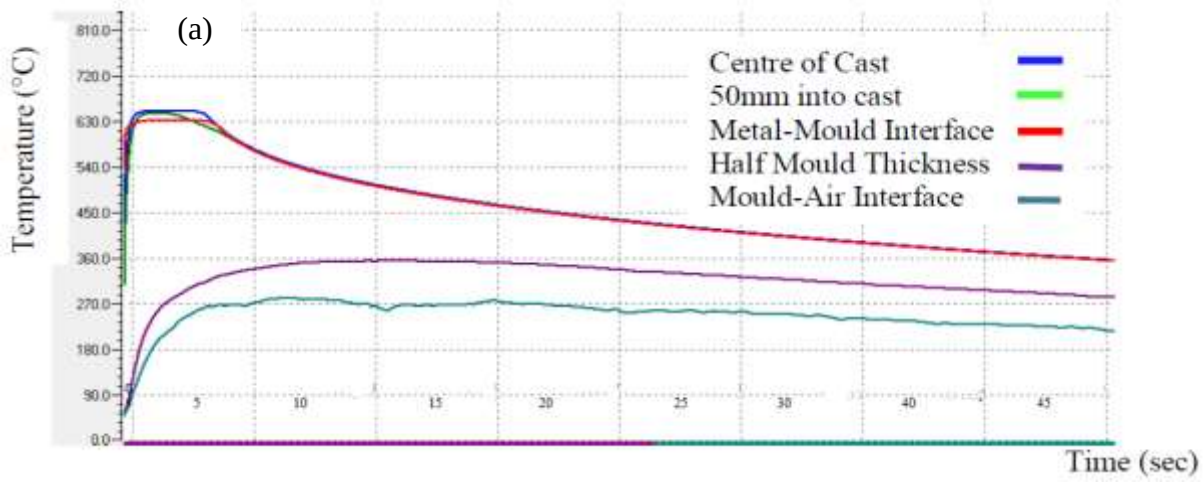

Figure 6.22 (a) give the cooling curves of the aluminium cast and the mould heating curves during the casting process of solidification. Figure 6.22 (a) present the result mould heating curves as well as the cast solidification and cooling curves for 50 mm thick mould.

Figure 6.22 (b) presents the solidification time of the aluminium cast increasing as the mould thickness increases and result mould heating curves as well as the cast solidification and cooling curves for 40 mm thick mould. This indicates that the solidification period is longer in thicker Moulds. Figure 6.22 (a)and (b) shows the trend corresponding to the nodes located in sand region. Initially sand was at ambient temperature. As soon as the cavity was filled, the molten metal was

started liberating the latent heat and was picked up by sand particles. It can be seen by the trend of the graph shown in Figure 6.22 (a, b). Ansys simulation has also been performed using Thermal Solid-PLANE55 as a plane element with a 3-D thermal conduction capability. Results obtained with triangular element are better than Thermal Solid PLANE55 element with reference to experimental result. Figure 6.22 (b) Cooling and heating curves at varying aluminium cast and mould locations

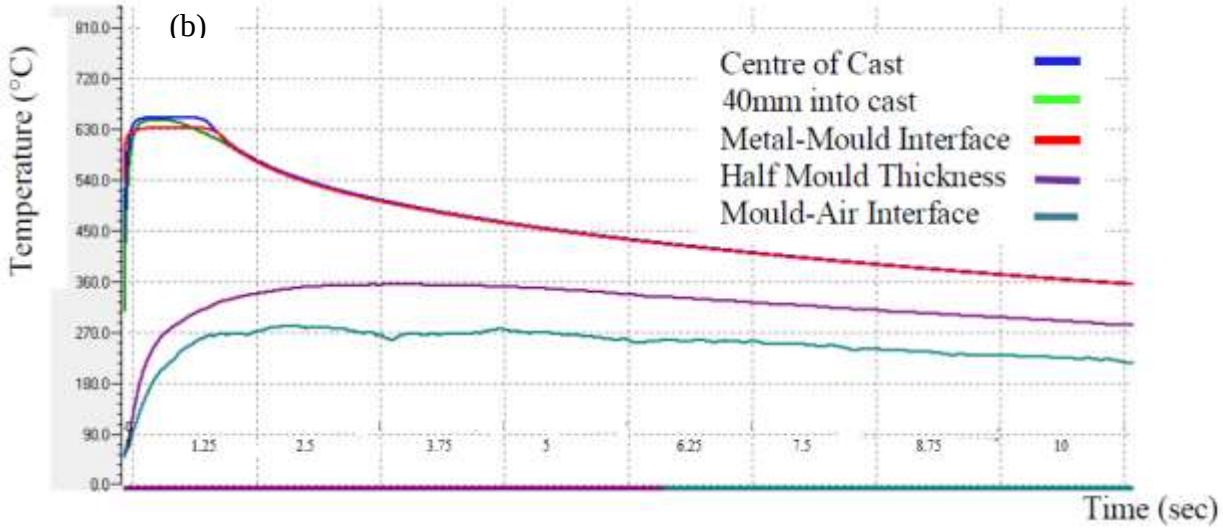

From the results above graph 6.22 (a b), the mould were kept at an initial temperature of 47°C and the molten aluminium alloy at 680°C. The solidification time for each thickness was obtained from the plot of graphs from the thermocouple temperature recorder at the point when the solidified aluminium cast started reducing in temperature from the constant value of fusion temperature. The mould heating curves as obtained at the mould/air interface and half mould thickness are shown in Figure 6.22 (a, b). Temperature rises rapidly in the small thick mould of Figure 6.22 (a) from the beginning of solidification until it reached a maximum value, it then starts decreasing. Whereas a progressive rise in temperature is observed for the thicker mould of decrease to increase as. Temperature plots for casting region obtained by simulations (Figure 6.21) and for experiment simulation (Figure 6.22) prove that they are in accordance with each other after t=10 sec. Figure 6.20 (a, b) shows that the temperature plots within the mould area obtained with simulation.

The figure 6.22 (c) indicates the temperature solidification between on point (13.197 ^{o}c to 22.093^{o}c) of cooling temperature produce part process. A close examination of the cooling curves shows that at the metal/mould interface the temperatures continue to fall rapidly for several degrees

and thereafter relatively slowly. At the center of the aluminium cast, the liquid aluminium metal cools quickly to the freezing temperature of the approximately constant temperature of 22.093°C for the metal and mould cast. There is a measurable thermal arrest at this location indicating the solidification time of the aluminium cast.

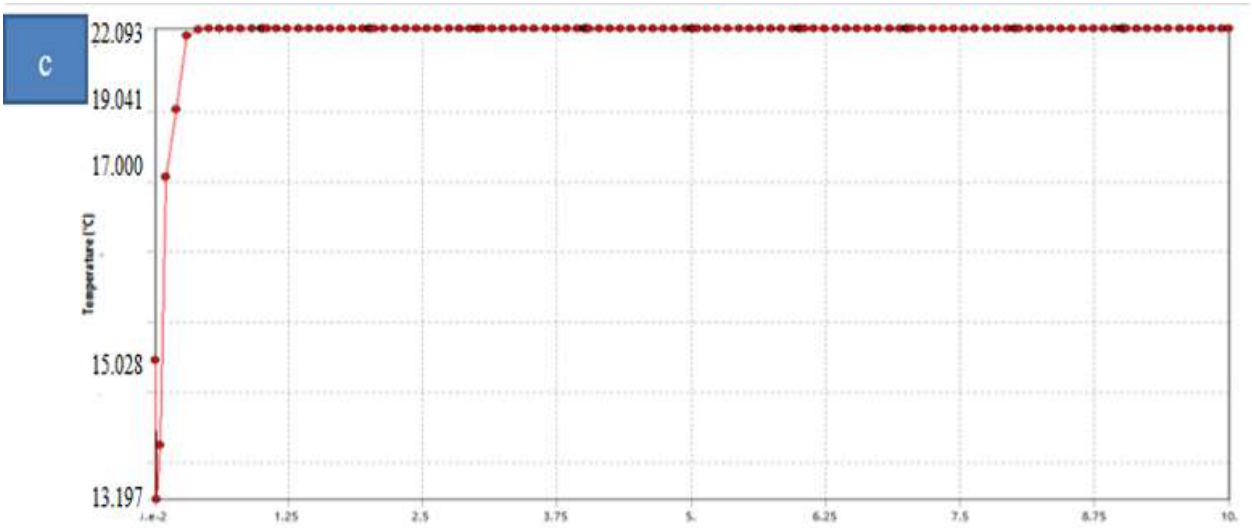

Figure 6. 20(a-c) Cooling and heating temperature variation with respect to time during solidification process.

This figure 6.22 result estimated that solidification period of the metal was considered fast cooling by taken the aluminium alloy thermo-physical properties into consideration and ignored the mould material properties. Hence, the actual solidification period of the metal in the cavity considered longer than from the result shown by simulation. Finally, the simulation results predict that the overall solidification process of the cast part production and can be considered as fast cooling/freezing of metal has occurred and this caused to lack of molten metal compensation/or metal feeding in the outer thin section of the part and produced volumetric solidification shrinkage. This intern leads to misrun and also difficult gas bubbles to out which are the causes of porosity formation in the production casting.

6.10 Effect of Pouring Temperature and Solidification result

The high of pouring temperatures of potential for metal casting shrinkage, it is helpful to work within a delineated temperature range. The range of materials temperatures Aluminum used between (630^{o}c-750^{o}c).at the pouring temperature 630^{o}c potential of metal melting low, 680^{o}c pouring temperatures optimal and at 750^{o}c above flow point. Metal should be heated to achieve

appropriate molten characteristics, but without reaching its full liquid state. This usually entails heating the material to slightly above its flow point, but well below its melting point. Preventing overheating can be just as important to effective casting as cultivating a molten flow.

However, the program deals with liquid and solidification contractions clearly by considering the density variations with temperature. It can be noticed that beyond 750°C, there is a dramatic increase in volumetric shrinkage.

Figure 6.23(b) indicate to be successful, a metal must flow into all regions of the mould, most importantly the main cavity, before solidifying. Figure 6.23 (a, b) The directional solidification to minimize damaging effects of shrinkage defect, it is desirable for regions of the casting most distant from the liquid metal supply to freeze first and for solidification to progress from these remote regions toward the riser(s), thus, molten metal is continually available from risers to prevent shrinkage defect minimized and the term directional solidification describes this aspect of freezing and methods by which it is controlled. The liquids castings can cool at a rate of up to 100 degrees per minute once molten pouring is complete. The phenomenon will result in a difference between short freezing and long freezing solidification which could greatly influence the prediction of defects such as hot tearing and shrinkage defect. Optimum location of riser based on software has helped in minimizing the solidification related defects, thereby providing a defect-free casting. The pouring time (Solidification time) of solidifying solidification between (10min.-25min. At this the Solidification time solidifying potential low 10min., 15min. Optimal Solidification time and 25min. above point (it known as short freezing and long freezing).

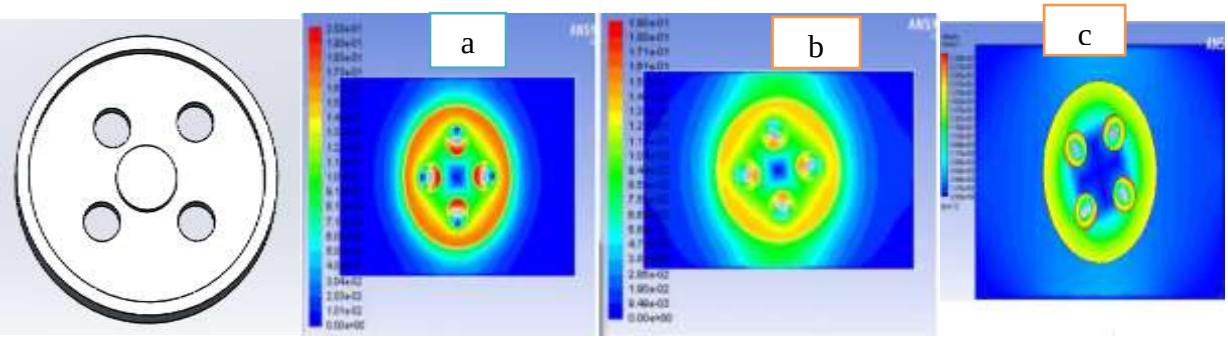

Figure 6.21 Local freezing time in seconds contours at a selected section

Desired directional solidification is achieved using according to Chvorinov's Rule to design the casting itself, its orientation in the mould, and the riser system that feeds it, locate sections of the casting with lower V/A ratios away from riser, so freezing occurs first in these regions, and the

liquid metal supply for the rest of the casting remains open and Chills internal or external heat sinks that cause rapid freezing in certain regions of the casting and Central portion was the point required for the best attachment of the main riser for minimized the shrinkage defect by considering the point of highest modulus within the casting, The effect can be seen in Figure 6.24 where the heat flux contours are plotted. The heat flux is greatest where the contact pressure is highest. Simulation results shown in Figure 6.24 indicated that temperature variation of the modelled flywheel during solidification in case of transient-thermal modes of heat transfer analysis carried out using ANSYS 17.0 software.

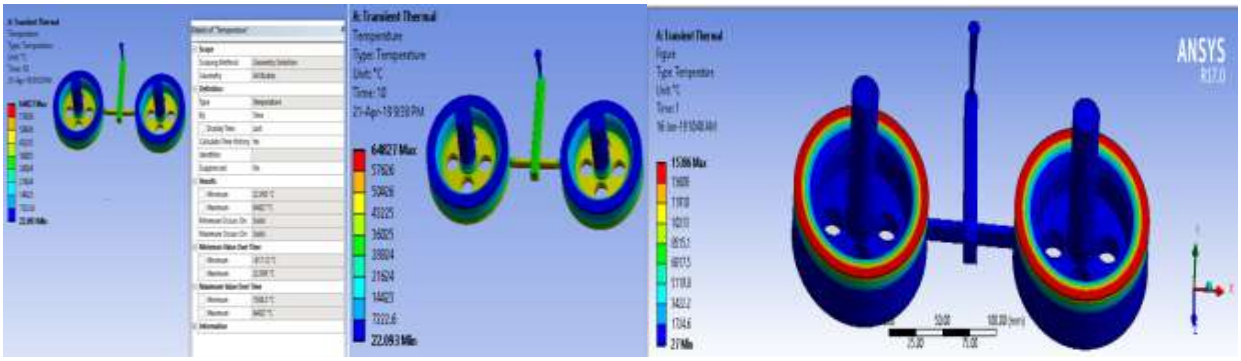

Figure 6 22 Temperature gradient during solidification

6.11 Shrinkage improvement of casting result

The liquidus-solidus interface evolutions of castings. Increasing the pressure and the pouring temperature of the molten alloys did not affect the reduction of shrinkage defect. The increases in the pressure of molten alloy and pouring temperature only cannot improve the shrinkage defects. Therefore, increasing the vertical *TG* during the solidification process may be a practical approach to reduce or eliminate shrinkage porosity. For this purpose, a mould-temperature-gradient method was applied. These temperature variations are an important factor in improving casting quality. With horizontal gating system, mould erosion was completely controlled as compared to the vertical one. increases the likelihood of shrinkage, especially if the sprue is too small for the volume of flow as show figure 6.25.

A properly sized sprue attached directly to the heavy section can fill the cavity and provide the feed material necessary to counteract shrinkage as cooling occurs. Also using a rounded, rather than an optimal gate on the sprue can further reduce the risk of forming defects. In general, the shrinkage porosity appeared in the late stage of solidification when the solid fraction of alloy was

large; therefore, the recommended temperature of ProCAST for the calculation of TG was: $T_G = T_{solidus} + 0.1\times (T_{Liquidus} - T_{solidus})$

Figure 6.25 indicate the effect of poor riser size causes shrinkage porosity defects formed in the casting. It can be using top risers neck small diameter riser size could not be reduced the shrinkage porosity defect in the casting. Shrinkage Porosity defects can be reducing when the neck of riser size adding and an optimum correct in-gate and correct solidification period from the producing sound casting as show fig 6.27 (a, b& c). They play an essential role in promoting directional solidification where the metal solidifies at the furthest point first before moving towards the riser.

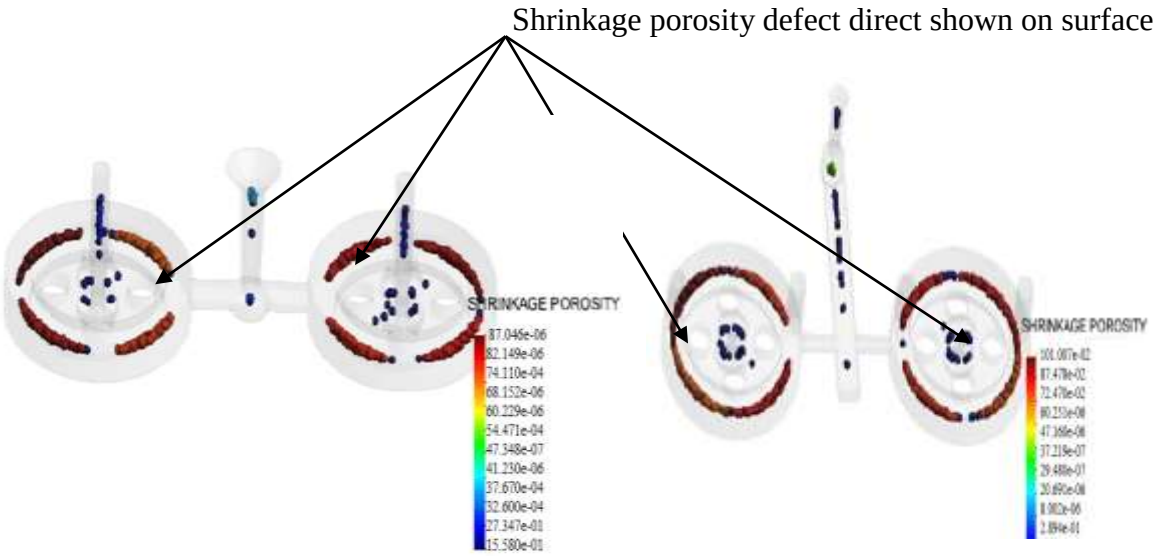

Figure 6.23 show simulation area defect

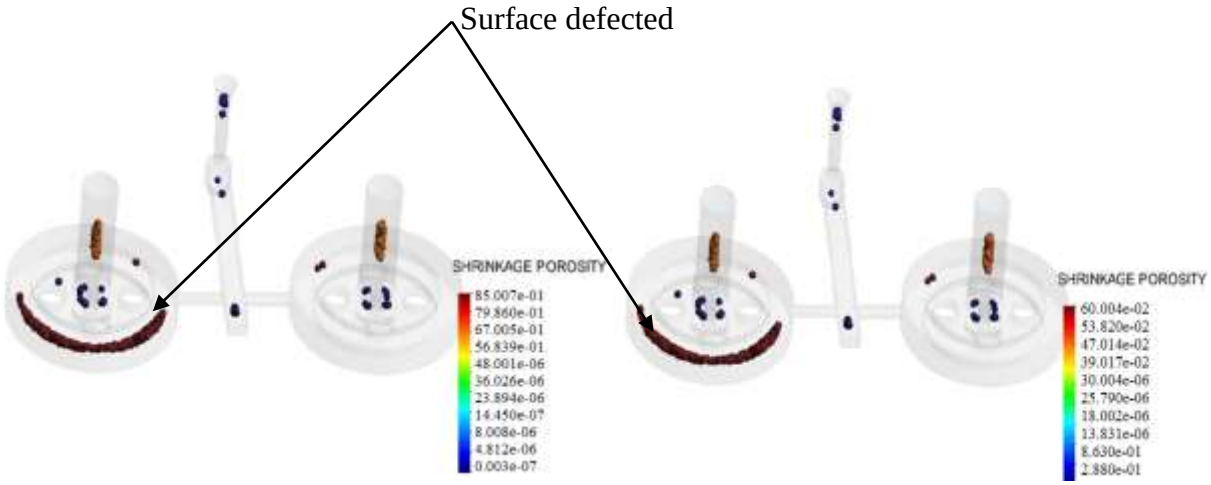

Figure 6.24 Casting simulation predict show defect surface defect

The gating and feeding system riser is solidified before the solidification of cast body so directional solidification is not achieved as shown figure 6.27 and figure 6.26. It is necessary to provide the directional solidification to achieve the free defect (sound) casting as show figure 6.28. The directional solidification starts from thinnest section to thickest section and which ends at the riser. The actual solidification of metal begins at liquidus temperature of 680°C. The solidification of metal ends at solidus temperature 750°C.

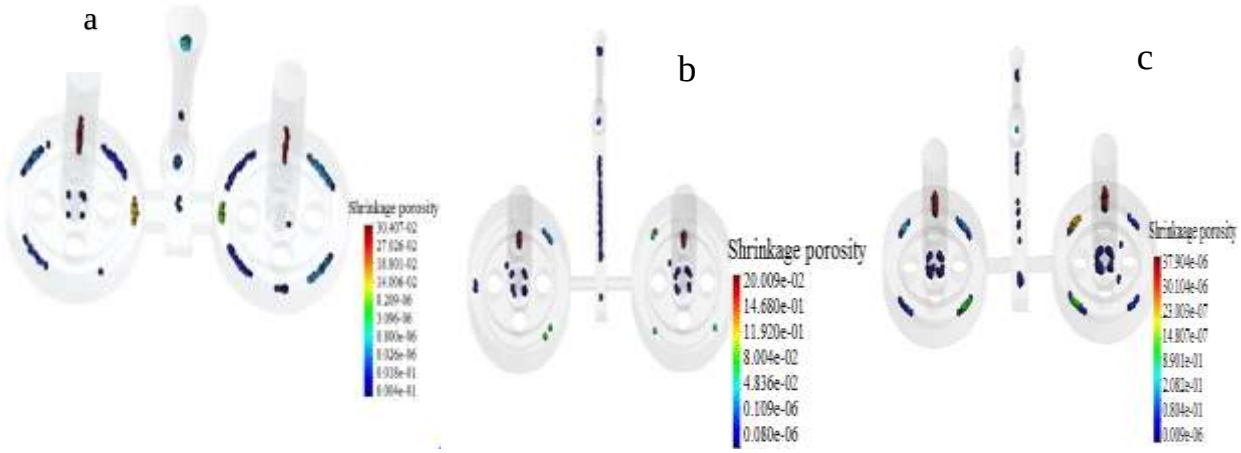

Figure.6.25Actual shrinkage porosity and the predicted results

The acquired results of shrinkage porosity (red coloured large area of top represent shrinkage defect) as show figure (6.28) model (a). All figure 6.27 as show minimized defect (sound casting) because after analysis (optimized) parameters (analyzed parameters caused defect).

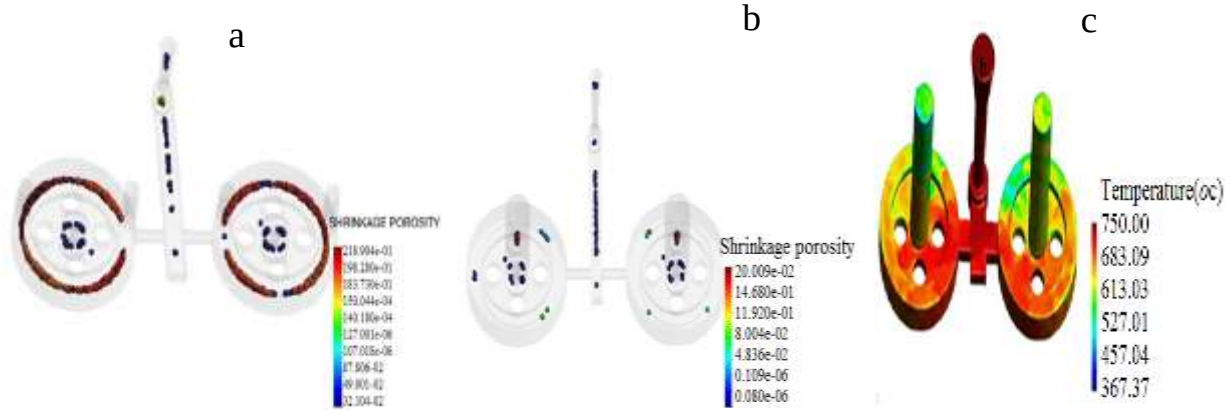

Figure 6.26 casting show Shrinkage defect and without defect

The obtained results of shrinkage defect (coloured dots represents shrinkage defect) in figure 6.28(b) also declares that the modified feeding, gating design is better than a conventional design.

Liquid to solid conversion plot shows that the size of riser neck is insufficient, due to which feeders are not properly feeding the casting during solidification through feeder sizes and locations are correct, as shown figure (6.27). In proposed one feeding and gating system is solidified before the solidification of cast body so directional solidification is not achieved. Therefore, it is necessary to make suitable changes the in-gating system to reduce or remove the level of shrinkage porosities or shrinkage defect.

6.12 Validate Experiment and Simulation Result

The methods used for shrinkage porosity defect prediction present in this study allows the numerical simulation of shrinkage porosity by considering the factor that contributes to shrinkage porosity defect information: (i)heat transfer and temperatures of melt (ii) cooling rate (iii) fluid flow which feeds the solidification shrinkage, etc. The simulation was software ProCAST and ANSYS. This software solves the conservation equation using the FEM. The mesh employed in the solution of the system is made of fine tetrahedral volume elements. The material of the castings was Aluminium alloy and resin sand was adopted as a material of mould. The primary parameters used in the simulation include specific heat, thermal conductivity, density, latent heat, solidus and liquidus temperatures. Most of these data were obtained by thermal analysis from real alloy. Regarding are the process conditions, the initial temperatures of the resin sand mould were assigned at 20^{o}c and the pouring temperatures were varying according to table2. Interface condition between melt and mould was set concerning the type of mould material and metal cooling curve.

Table 6.9 pouring Temperatures

Cast sample produce	Temperatures (^{o}c)
1	750
2	680
3	650
4	630

Figure 6.29 indicates compares the cooling curve monitored by the thermocouple with the ProCAST simulation. The calculated profile is in very good agreement with the experimental, what have achieved by gradual modifying heat transfer conditions and also mould properties. From the

graph can be also seen that the initial temperature which was set in Procast was slightly higher than the temperature from real thermocouple. The reason for the increase for was fact, that thermocouple wasn't preheated and during measurements thermocouple itself took a particular amount of heat from melt and it to consider this deviation.

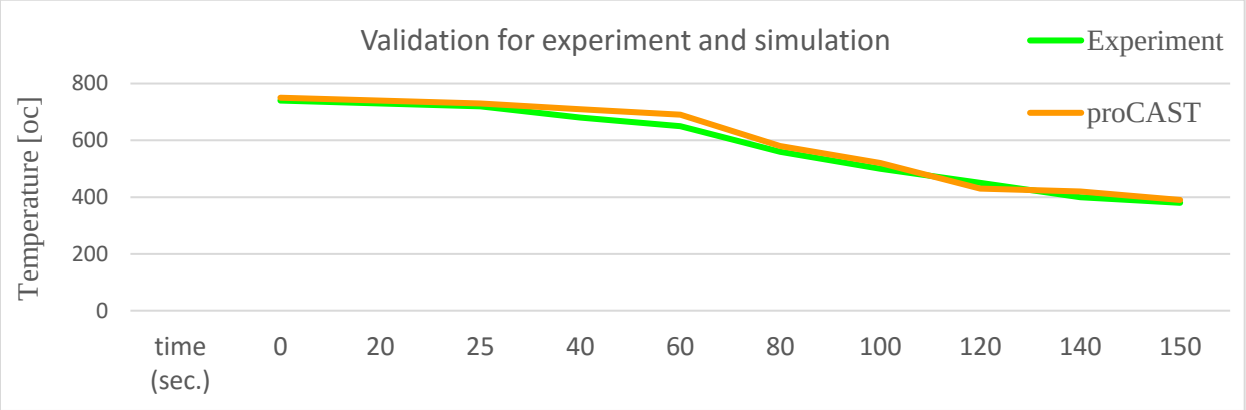

Figure 6.27 Validate empirical result comparison

and heat transfer coefficient is determined, simulation can proceed with calculations. For metallographic examination, all castings were section vertically across the centerline to observed the internal porosity. The percentage of shrinkage porosity was characterized with an area of the whole sample and compared with simulation results. As can be seen figure. 6.30, the red colors place (areas down) cluster which is assumed to be shrinkage porosity defect is found in the middle of the samples cast poured 680^{o}c and 630 ^{o}c (a, c). Less shrinkage defect in center areas can be observed at higher pouring temperature as shown in figure 6.30 (b, d). The correlation coefficient values for casting process simulation and experimental validation studies are indicating a positive relationship between them.

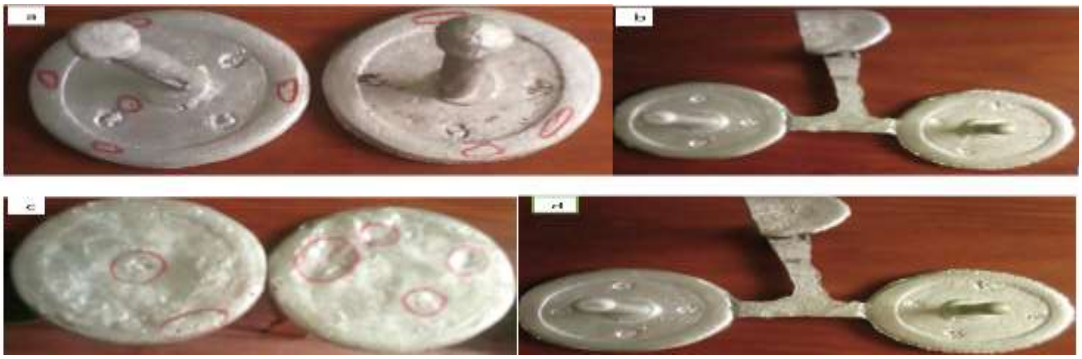

Figure 6.28 shrinkage defect cast test on sample

Solidification shrinkage is one of the casting defects which can be also identified in figure 6.32 (a, c), represents the dimensional reduction of metal changing from moulted to solid-state from the insufficient feeding ability. The colors at sample show at figure 6.30 (a, c) are fairly red circle put (into down) when compared with the other. This indicates that the porosity defect bigger and deep. At pouring temperature 730^{o}c & 680^{o}c external and internal solidification shrinkage is almost unnoticeable thanks to good feeding conditions. On figure 6.30 (a, b) is show the result after solidification focused on total shrinkage porosity analysis.

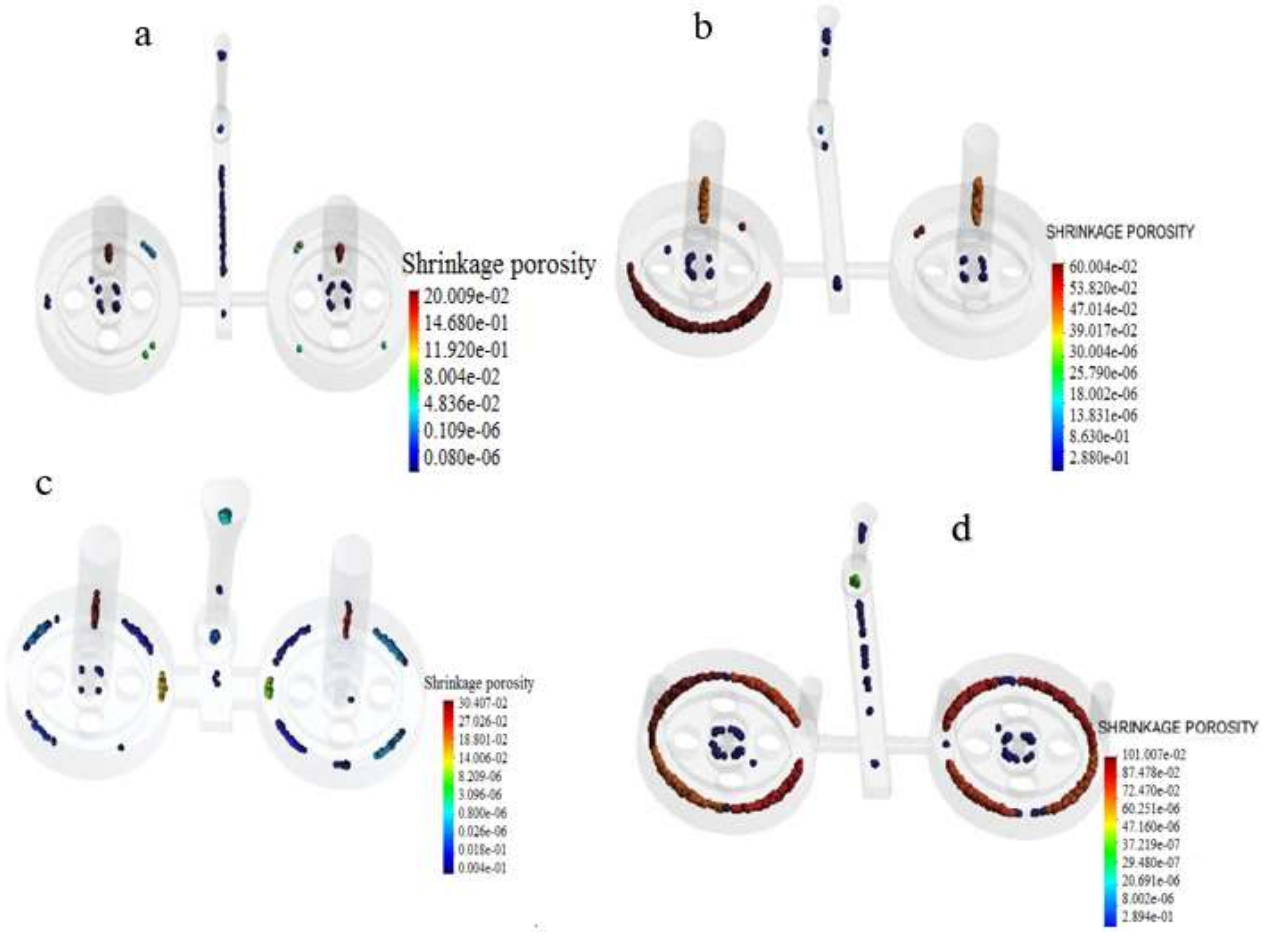

Figure 6.29 Shrinkage porosity defect ProCAST analysis

Colors represent the percentage amount of total shrinkage porosity predict in given areas. Spectrum was to all simulations on the estimation of the same value (specifications amount % of porosity), so the result may be compared and evaluation meaningful. Figure 6.30 Cast sample (a, c) shows a lower amount of total shrinkage defect in center areas, but cast sample (b, d) have shown direct of shrinkage porosity defect presence in upper areas as can be confirmed also at real

sample casting (figure 6 .31 a, c). from compassion of sample four real Vs simulation we can find to the top. For sample 4 the rules different, one big cluster of external shrinkage defect from insufficient feeding is near the narrow part and shrinkage porosity below is concentrated above the center. Similarly, Figure 6.31 simulation sample (a, c) shows a lower amount of total shrinkage defect in center areas, but simulation sample (b, d) have shown direct of shrinkage porosity defect presence in upper areas as can be confirmed also at real sample casting (figure 6 .30 (a, c)). from compassion of sample four real Vs simulation we can find to the top.

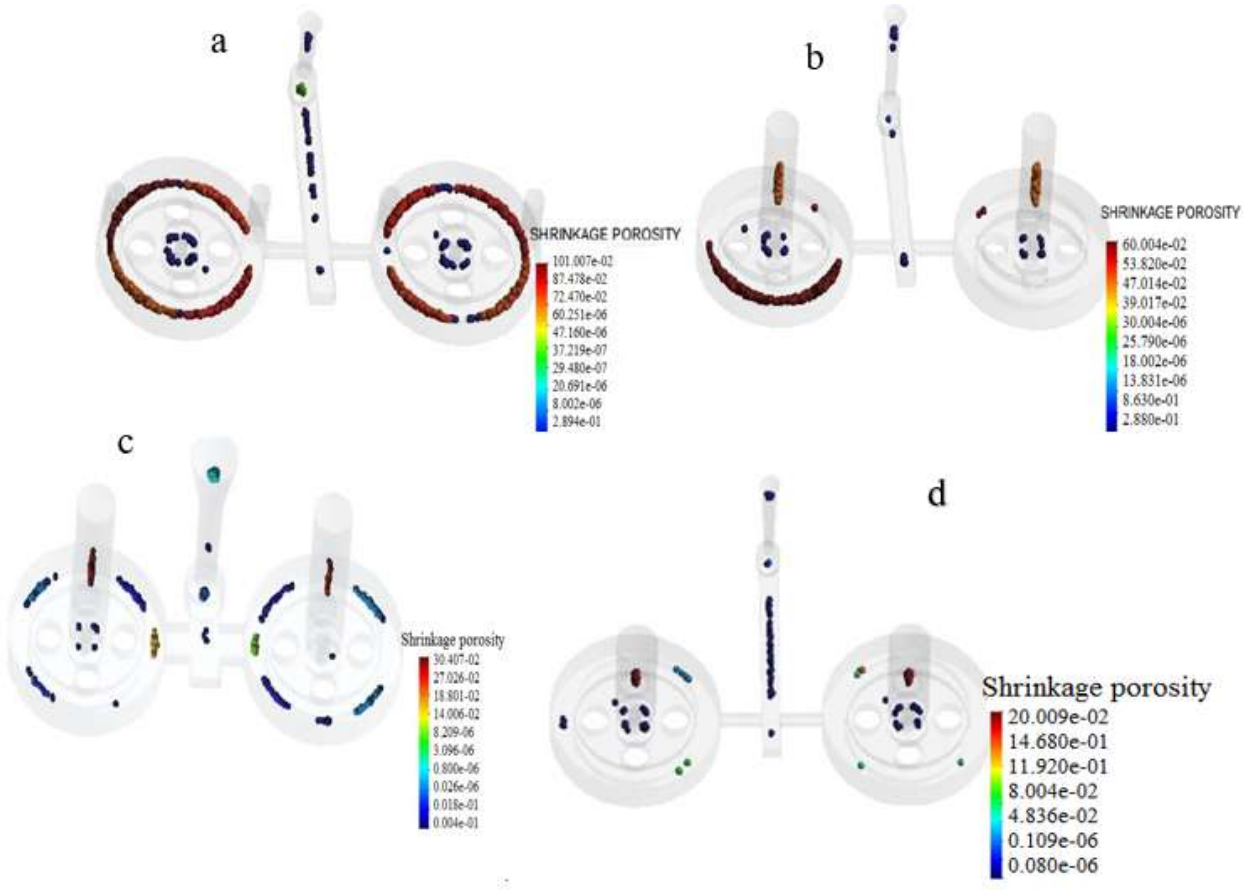

Figure 6.30 Results in experimental casting and in simulation model

Figures 6.30 and figure 6.32 are the simulation result and the experiment result the same procedure respectively. It is indicating the experimental result and simulation result of shrinkage defect distribution and figure 6.30 image in simulation result under gravity casting sectioning by the center line of the two risers. These indicators show the simulation result of the shrinkage defect in the optimum riser, long freezing is in good agreement with the actual test results. The simulation results have similar results with the experiment results. Placement of the pour riser/feeder at the

last solidifying regions did not shift the hot spot completely into the feeder. Hence, an exothermic sleeve was attached to the feeder, which has completely shifted the hot spot in the feeder and thereby eliminated shrinkage defect problem. This facilitated the optimized placement and design of feeders with improvement in yield by 88.9 % while ensuring casting soundness without expensive and time-consuming trial runs. This approach has helped in minimizing the solidification related defects, thereby providing a defect free casting. This study shows that simulation can be of great use in optimizing the feeder dimensions and increasing the feeding efficiency of the casting.

Overall the experimental and simulated results show good with an agreement, so the model has an acceptable reacting to the pouring temperature, pouring riser size & pouring time change. By these improved parameters in reducing the shrinkages defect in component cast product and the defect associated with the cast is eliminated and the free cast is achieved.

Finally, the outcome of the study is (i) minimizing flywheel casting defects (ii) produced defect free casting and (iii) selecting suitable process parameters. The products obtained by the improved parameters settings show that better improvement in misrun defect (length variation) but sand sintering problem (minor), rough surface and shrinkage defect (major) still appear on the produce part (flywheel) castings. Also, it can be estimated that the model improves the quality characteristics/ minimized shrinkage defects of produce part (flywheel) castings by 50%.

7 CHAPTER

7. CONCLUSION, RECOMMENDATION AND FUTURE WORK

7.1 Conclusion

The study covered effects of sand casting process parameters that used in flywheel castings produced from aluminum alloy through numerical, simulation and experimental methods. The results have shown that the applied methods for determination of the casting defects and the analysis (optimum) settings of factors were achieved successfully and the following conclusions can be summarized as follows: The numerical calculated results have shown that the misrun, and volumetric solidification shrinkage defects occurred in the part produced castings were due to the improper utilization of patterns of the gating system elements that resulted from less (2%) shrinkage allowance used for the aluminum alloy.

The simulation results have shown that volumetric solidification shrinkage, misrun and porosity defects occurred in the component produce castings were due to the long and short solidification

The experimental results have shown that the most significant factors that affected on the length variations were respectively the pouring temperature which accounted as 35.57% of the total effect, the riser size accounted as 24.93% and pouring time was the less which accounted as 7.14%. The optimum settings of the factors have shown that the pouring time as 120 seconds, riser size as 50 cm^2 and pouring temperature as $750^{O}c$.

The significant improvements in product quality, component performance, and design reliability can be achieved if shrinkage defect in castings can be predicted, controlled or eliminated. Casting yield improve up to some percentage, which indicates the new method design weight is less as compared to the initial method and also shrinkage defect is reduced to a minimum level. Proper design of feeding system helps to reduce the casting defect and give the sound casting. This study detail focused on improving the quality casting by controlling the various casting parameters such as process parameters and application of cooling aids.

Solidification has been performed in ProCAST and ANSYS software according to the design dimensions obtained for a pattern with allowances, gating system and feeder. A Simulation study of castings has provided the temperature contours which has helped in identifying the shrinkage defect locations, solidification time etc. The casting simulation should be used quality

enhancement by predicting and reducing surface defects like shrinkage porosity defect. The shrinkage defect and hotspot has got completely shifted in the riser/feeder.

Confirmation experiments were conducted based on optimum values and it was observed that the defects were minimized appreciably. The reducing percentage of part produce (flywheel) body castings was reduced from 88.9 to 11.1. The optimized levels of selected process parameters obtained by Taguchi method are: pouring temperature (A): (630^{o}c,680^{o}cand 750 ^{o}c.), pouring riser size(B): (50cm, 60cm and 70 cm) and pouring time (solidification time) (C):(90, 120 and 150 min.). Yield improvement by reducing the volume of feeders and gating channels for casting and hot spots in the part suggest the proper location of feeder resulting in reduced defects. From experimental observed Additional pouring temperature or superheat increases the fluidity and considers the allowance for heat losses before they are in their final position in the mould, thereby decreasing the shrinkage. The minimization of defects was done by optimizing the parameters control variables or factors affecting the output. Taguchi method was the best available method to analyzed (optimize) the factors and together with the help of analysis of variance the optimum parameters control factors were found out. The percentage minimization of the cast produce part can be the minimum reduced to 3.01 % which is a significant improvement in this case. Taguchi method is thus a cost effective method which can be used in industry to reduce the wastage of cast parts. By applying the optimal values for the production an Experiments is conducted and it has been found that the shrinkage defect is reduced from 45% to 50%.

7.2 Recommendation

As per the results indicated for the overall casting process of the casting production, the following recommendations may be for the foundry industry of casting:

- Macro shrinkage is a concentrated zone of shrinkage holes or single shrinkage porosity defect in cast products that can be detected through non-destructive tests such as radiography, ultrasound, and magnetic particle method.
- Should prepared and used patterns of gating system with actual sizes for the ordered parts' specifications because it may be produced sound casting with minimum defects.
- The samples were there after examined using optical metallurgical microscope.
- It is important to take the actual chemical composition of alloying elements for the ordered grade type that can be kept the quality, effectiveness life the and service casting product.

7.3 Future Scope

Some issues that are not the researched in this work and would be beneficial to perform further studies on are the mentioned.

- Casting samples in a simple shape geometry and provokes shrinkage porosity defects would be too beneficial for shrinkage defect characterization.
- It would be beneficial to investigate the amount of elements **H2, N2** and **Si** present in the liquid, if they can reach a critical level, close to the solubility limit.
- Implement the developed micro-shrinkage model into the stochastic mesoscopic models for prediction of microstructure evolution of dendritic alloys. This will improve significantly the predictions of the location and shape and size of the micro-shrinkage that is forming in the interdendritic region or at the grain boundary.

Reference

A. Reis, Y. Houbaert, Z. Xu, R. Van Tol, A.D. Santos, J.F. Duarte, and A.B. Magalhaes, *J. Mater. Process. Tech.*, 2008, vol. 202, pp. 428-434.

A. Reis, Z et al,2012, 2017. A. Reis, Z. Xu, R.V. Tol, and R. Neto, J. Manuf. Process., 2012, vol. 14, pp. 1-7. 2, 15–19.

Beddoes, J., Bibby, M., 1999. Principles of metal manufacturing processes. Butterworth-Heinemann, PP127-135.

Beeley, P., 2001. Foundry technology, PP 67-89.

Behera, R., Kayal, S., Sutradhar, G., 2010. Solidification behavior and detection of Hotspots in Aluminium Alloy castings, Int. J. Appl. Eng. Res. PP57-62.

C. Nadiah J. Ahmad 2015, Riser feeding evaluation method, pp89 -110.

Campbell, J., T.S. Piwonka and M.C. Flemings: Trans. AIME, 1966, vol. 236, pp. 1157–65, 2003. Castings. Elsevier.

C. Pequet, M. Gremaud, and M. Rappaz: *Metall. Mater. Trans.*, 2002, vol. 33A, pp. 2095–2016.

Choudhari, C., Narkhede, B., Mahajan, S., 2014a. Casting design and simulation of cover plate using AutoCAST-X software for defect minimization with experimental validation. Procedia Mater. Sci. 6, 786–797.

Çetinel, M., and Aygün, H., 2001. "Investigation and Development of the Quality Control of Al-Wheeln Rim Production Process," Doctoral dissertation, İzmir Institute of Technology, İzmir.

Choudhari, C., Narkhede, B., Mahajan, S., 2014b. Methoding and simulation of LM 6 sand casting for defect minimization with its experimental validation, PP97, PP1145–1154.

Choudhari, C., Padalkar, K., Dhumal, K., Narkhede, B., Mahajan, S., 2013. Defect free casting by using simulation software, in: Applied Mechanics and Materials. Trans Tech Publ, pp. 1130–1134.

Das, S., Himte, R.L., 2013. Design &Analysis of Pure Iron Casting with Different Moulds. Int. J. Mod. Eng. Res. IJMER 3, 2875–2887.

Di Sabatino, M., 2005. Fluidity of aluminium foundry alloys, PP48.

Farrokhnejad, M., 2013. Numerical Modeling of Solidification Process and Prediction of Mechanical Properties in Magnesium Alloys PP67.

Gajbhiye, A., Choudhari, C., Raut, D., Narkhede, B., Bhandarkar, B., 2014. Minimization of Shrinkage Porosity in A Sand Casting Process By Simulation In AUTOCAST-X Software with Experimental Validation by Destructive testing. Int. J. Mod. Eng. Res. IJMER 4.

Heine, R.W., Loper, C.R., Rosenthal, P.C., 1976. Principles of metal casting, PP 97.

Ingle, V., Sorte, M., 2017. Defects, Root Causes in Casting Process and Their Remedies: Review. Int J. Eng. Res. Appl. 7, 47–54.

Jabur, A.S., Kadhim, Z.D., 2010. Prediction of Shrinkage cavities in Aluminium-Silicon sand casting. J. Thi-Qar Univ. 5.

Jain, P., 2003. Principles of foundry technology. Tata McGraw-Hill Education PP72-75.

John, O., Pamtoks, H., Omolayo, M.P., Adelana, R.A., 2013. Taguchi Optimization of Process Parameters on the Hardness and Impact Energy of Aluminium Alloy Sand Castings. Leonardo J. Sci., PP1–12.

K. Kubo and R.D. Pehlke: *Metall. Trans. B,* 1985, vol. 16, pp. 359-366.

Katz, S., 2012. Foundry Processes: Their Chemistry and Physics, PP118-127

K.D. Carlson, Z. Lin, R.A. Hardin, and C. Beckermann: *56th Steel Founders Society of America Technical and Operating Conference*, Paper No. 4.4, Steel Founders' Society of America, Chicago, IL, 2002, PP60-72

Lee, P., Chirazi, A., See, D., 2001. Modeling microporosity in aluminum–silicon alloys: a review. J. Light Met., PP15–30.

Masoumi, M., Hu, H., Hedjazi, J., Boutorabi, M., 2005. Effect of gating design on mold filling. Trans. Am. Foundry Soc. Vol 113 113, 185–196.

McGuinness, M., Roberts, A., 2001. Efficient design of tall tapered feeders.

Montgomery, D.C., 2017. Design and analysis of experiments. John wiley & sons.

Moore, D., MCCabe's, G., 2010. Minitab for Introduction to the Practice of Statistics pp10-25.

Prajapati, T., Sutaria, M., 2013. Geometry dependency of filling related defects. Int. J. Eng. Trends Technol. IJETT Mech. Eng. Dep. CSPIT Changa Gujarat India 4, 1320Y1324.

Pyzdek, T., Keller, P.A., 2003. Quality engineering handbook. CRC Press, PP32-38.

Rajput, R., 2008. Manufacturing technology Laxmi publications limite, New Delhi, India, PP67.

Ravi, B., Joshi, D., 2007. Feedability analysis and optimization driven by casting simulation. Indian Foundry J. 53, 71–78.

Roy, R.K., 2001. Design of experiments using the Taguchi approach: 16 steps to product and process improvement. John Wiley & Sons, PP42-46.

Ruddle, R.W., 1956. The Running and Gating of Sand Casting. Inst. Met. Monogr. Rep. Ser. 19.

Shafiee, M.R.M., Hashim, M.Y.B., Said, M.N.B., 2009. Effects of gating design on the mechanical strength of thin section castings. Proceeding MUCEET Pahang MUCEET,PP 1–4.

T.S. Piwonka and M.C. Flemings: *Trans. AIME,* 1966, vol. 236, pp. 1157–65

Tiryakioglu, M., Askeland, D., Ramsay, C., 1993. Relationship between metal fluidity and optimum pouring time: a literature review. Trans.-Am. foundrymens soc. 685–685.

Tomar, v.p.s., dwivedi, d., 2015, Ansys modelling and simulation of temperature distribution in sand casting development 2, PP 98-113.

Vanara, H., Shalediya, M.V., 2018. Simulation and Analysis to Reduce the Shrinkage Defect in Sand Casting for the Rotor: A Review. J. Prod. Res. Manag. 7, 23–26.

Vasava, V., Joshi, D., 2013. Simulation of shrinkage defect-A review. Int J Eng Trens Technol 4, 2361–2365.

Yu, K.-O., 2001. Modeling for casting and solidification processing. CRC Press. N.d, PP230-245.

APPENDIX

Appendix 7.1: Data related with yield of casting alloys(A. Reis, Z et al,2012, 2017; John et al ,2013)

item	steel	Aluminum	Green cast iron	Cast iron
Yield (%)	40-60	26-40	80-90	75-80
Density $kg\ m^3$	7860	2700	7870	7870

Appendix.7.2: Fluidity factors of aluminum castings related to gating type with relative pouring temperature (Choudhari et al., 2014b),

Material	Supply of molten metal in to mold cavity	Normal pouring temperature	Elevated temperature
Cast aluminum	For bottom gating or into heavy section of casting	1.2	1.3-1.4
Cast aluminum	For side gating(In the middle of casting height or by steps)	1.3	1.4-1.6
Cast aluminum	For top gating or uniformly in to thin wall of casting	1.4-1.6	1.6-1.7
Cast iron	Arbitrary	1.7	2.00

Appendix7.3: Relations between inlet size and length of runner and in-gate sections (Lee et al., 2001)

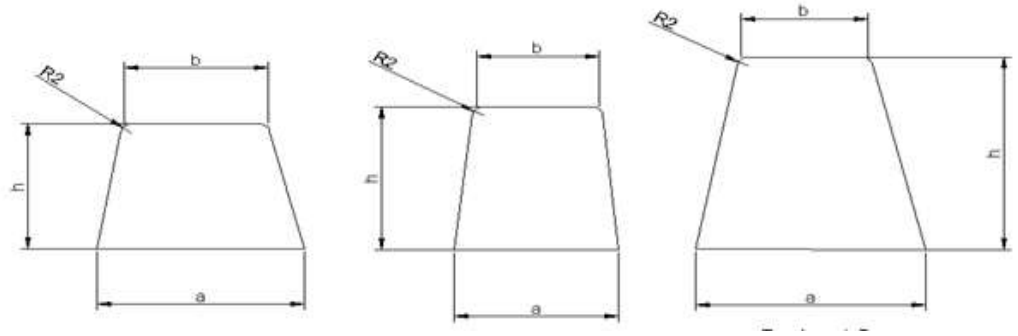

	For h = a			For h = 1.25a			For h = 1.5a		
A(cm^2)	a	b	H	a	b	h	a	b	h
1.0	11	8	11						
1.3	12	10	12	11	8	14			
1.6	14	10	14	12	9	15	11	7	17
2.0	15	12	15	14	10	17	12	8	20
2.5	16	13	17	15	11	19	14	1o	21
3.13	18	14	19	16	12	21	15	11	23
4.0	22	18	21	18	13	25	18	14	26
5.0	24	19	24	22	16	27	20	15	30

Appendix7.4: Thermo-physical properties of molten aluminum and heat transfer coefficients [(Choudhari et al., 2014b),]

Properties	**Values**
Density,ρ	2570 kg/m3
fluid density	2380
Thermal conductivity k	141.4 W/m K
Latent heat of fusion, $L.H.F$	311.0 kJ/kg
Specific heat capacity, C_p	1525.8 J/kg K
Solidus temperature, T_L	515 ^{o}c
Heat transfer coefficient at wall (mold-metal interface)	438.6 W/m^2 K
Liquids Temperature, T_s	731.1 ^{o}c
Volumetric Thermal expansion coefficient, β	3.26 x 10-4 /K
Dynamic viscosity, μ	4.5*10^{-7} kg/ m s

Appendix.7.5: Typical values of a, b and c for commonly used metals are given below (Beeley-2001)

Cast metals	a	b	c
Aluminum	0.10	0.06	1.00
Grey cast iron	0.33	0.33	1.00
Aluminum bronze	0.24	0.17	1.00

Appendix. 7.6: Thermal properties for casting materials (Beeley 2001)

Material	Specific heat, $c_p J/g$℃	Density ρ (Kg/m3)	Thermal conductivity K(W/m℃)
Sand	1.16		0.60
plaster	0.9	1.6 1.1	0.340
mullite	0.77	1.6	0.370
Iron	0.70	7 .9	73
aluminum	0.90	2.7	102
copper	0.39	9	385
magnesium	1.07	1.7	156

Appendix.7.7: Thermal properties of mold and chill materials at approximately (Choudhari et al., 2014b)

Material	Heat diffusivity, √(KρC) (J/m^{2}Ks$^{1/2)}$	Thermal deffusivility (K/ρC), (m^2/s)	Heat capacity per unit volume (ρC), (J/Km^3)
Silica sand	3.21 x10^3	3.60x10^{-9}	1.70 x10^6
Investment	2.12 x10^3	3.17 x10^{-9}	1.20 x10^6
Plaster	1.8 x10^3	3.79 x10^{-9}	0.90 x10^6
Iron (pure)	16.2 x10^3	20.3 x10^{-9}	3.94 x10^6
Graphite	22.1 x10^3	44.1 x10^{-9}	3.33 x10^6
Aluminum	24.3 x10^3	96.1 x10^{-9}	2.48x10^6
Copper	37.6 x10^3	114.8 x10^{-9}	3.60x10^6

Appendix.7.8: Thermal conductivities of selected materials at room temperature (Choudhari et al., 2014)

Material	Thermal conductivity, (W/m K)
Copper	401
Silver	429
Gold	317
Aluminum	237
steel	60.5
Limestone	2.15
Bakelite	1.4

Appendix .7.10: optimizing part design cast (Montgomery, 2017; Pyzdek and Keller, 2003)

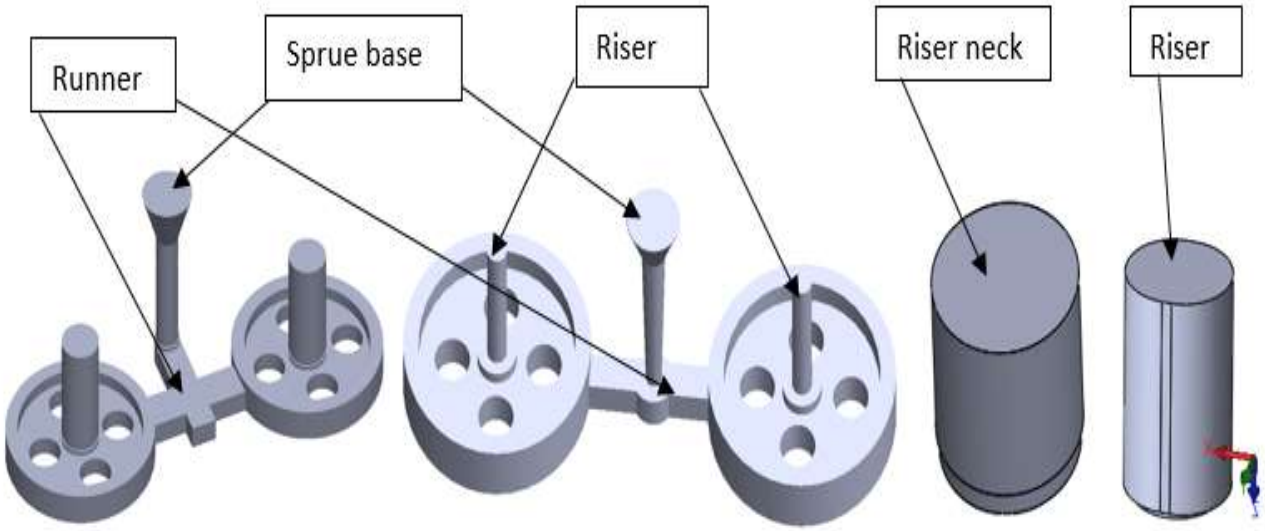
Runner
Sprue base
Riser
Riser neck
Riser

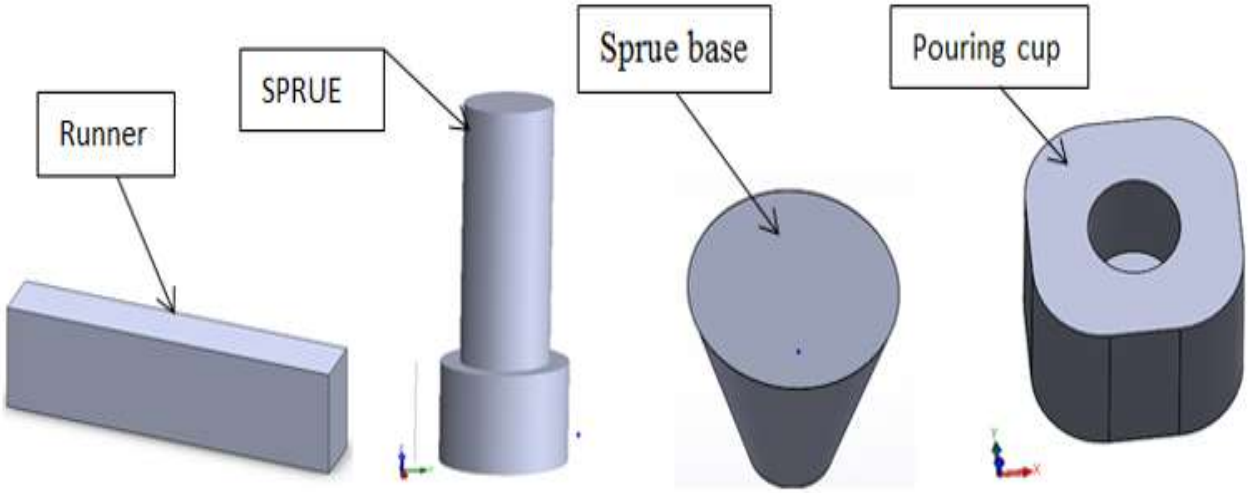
Runner
SPRUE
Sprue base
Pouring cup

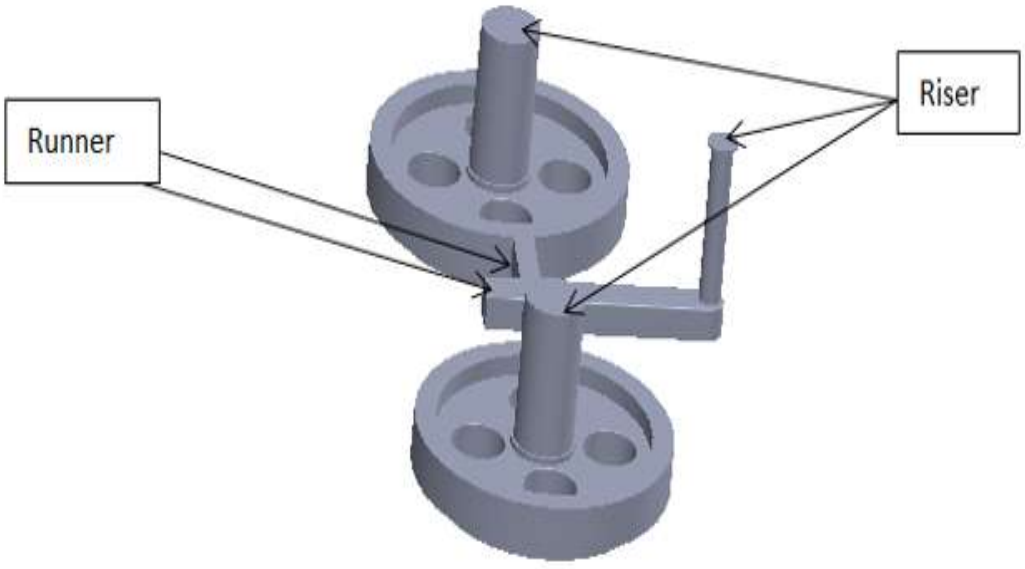
Runner
Riser